University of Trento

Center for Mind/Brain Sciences (CIMeC)

Doctoral School in Cognitive and Brain Sciences

Cycle XXXVII | 2021-2025

PhD Thesis

From Rest to Action: Functional Connectivity Architecture of the Human Hand Motor Network

Doctoral Student: **Enrica Pierotti**

Center for Mind/Brain Sciences, University of Trento, Italy

Advisor: **Dr. Luca Turella**

Center for Mind/Brain Sciences, University of Trento, Italy

Dedico questa tesi al mio caro Nonnino Achille, che mi è sempre stato vicino. Nonnino, vorrei tanto che fossi qui anche per questo traguardo, mi mancano tanto le nostre chiamate serali, mi manchi tanto tu. Lo so che forse saresti stato più contento nel veder arrivare un nipotino, ma il mio bambino è questo dottorato, una gestazione di 4 anni per poi arrivare a dire CE L'HO FATTA. Grazie per tutto quello che hai fatto e per tutti gli anni passati insieme, vi penso sempre e so che mi guardi da lassù con la nonna.

Enrica

Contents

1 Chapter 1: Introduction

1.1 Hand motor network in the non-human primate and the human brain

The human hand is probably the most powerful tool to interact with the world. Despite its highly complex anatomy, we can effortlessly use our hands daily to perform sophisticated interactions with the environment (Bernstein, 1966). Most of our knowledge of the hand motor system's functioning comes from decades of studies on non-human primates adopting invasive electrophysiological recordings (i.e., single-cell recordings) and lesion studies (for a review, see Jeannerod et al., 1995; Rizzolatti & Luppino, 2001; Turella & Lingnau, 2014).

The first theoretical model describing how the brain translates hand movements to interact with the world identified two different pathways one employed for perception, the other for action: the Ventral and the Dorsal streams, as proposed in the Dual-Streams Theory (Goodale & Milner, 1992). The Ventral and Dorsal streams have been described as two (relatively) independent pathways of visual processing. Both streams receive similar input from the primary visual cortex (V1), but sensory information is processed for distinct purposes. The Ventral stream processes visual information to support object identification and recognition, while the Dorsal stream transforms visual input into spatial and motor-relevant coordinates to guide appropriate motor actions (Goodale et al., 2005; Goodale & Milner, 1992). The Ventral pathway is primarily responsible for object recognition (the "what" pathway), whereas the Dorsal stream translates information into the appropriate motor commands (the "how" pathway - Goodale, 2005; Goodale et al., 2005; Goodale & Milner, 1992). The Ventral Stream (Figure 1.1, Green arrow) encodes object identity, shape, texture, size, and category information about objects and includes the Lateral Occipital Complex (LOC) and the Occipitotemporal cortex (OTC). Notably, the LOC plays a crucial role in object recognition by extracting semantic features and object properties, and it exhibits similar brain activity during both grasping and reaching movements (Culham et al., 2003). In contrast, the Dorsal Stream, which mainly comprises the Parietal cortex, is essential for the sensorimotor processes underlying the planning and the online control of reaching, grasping, and eye movements (Andersen & Buneo, 2002; Rizzolatti et al., 1998). Further investigation of the brain activity in the parietal and the premotor cortices (Rizzolatti et al., 2014; Rizzolatti & Matelli, 2003; Tanné-Gariépy et al., 2002) led to the identification of distinct cortico-cortical pathways connecting parietal and frontal areas with similar response patterns. Based on these findings, a further subdivision of the Dorsal Stream has been proposed: the Dorsomedial (or Dorsodorsal) Pathway (Figure 1.1. Yellow arrow), located on the medial surface, is mainly involved in

reaching movements towards peripherical targets, controlling arm position during the transport phase, and visuomotor transformations for the online control of hand and arm movements (Rizzolatti et al., 2014; Rizzolatti & Matelli, 2003). The Dorsolateral (or Ventrodorsal) Pathway (Figure 1.1. Orange arrow), located on the lateral surface, is predominantly involved in grasping actions (Culham et al., 2006; Culham & Valyear, 2006; Filimon, 2010; Rizzolatti et al., 2014).

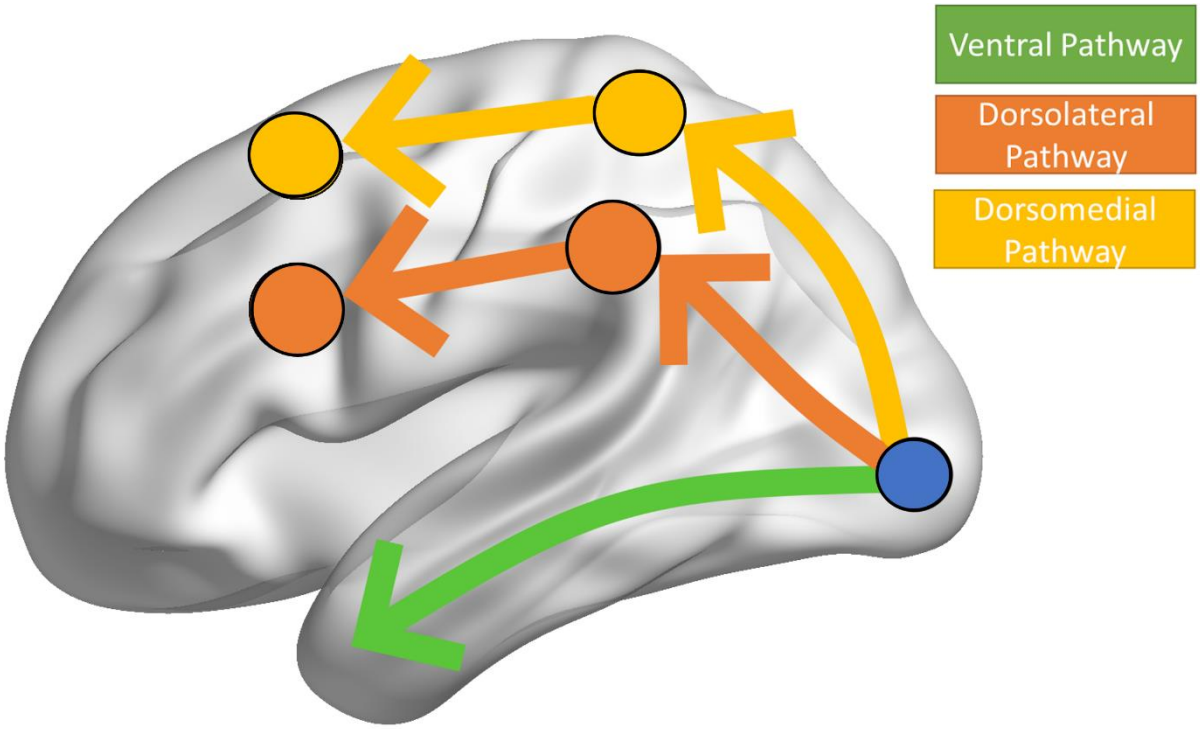

Figure 1.1. Graphical representation of the three motor pathways in the human brain (Gallivan & Goodale, 2018; Rizzolatti et al., 2014; Rizzolatti & Matelli, 2003). From the Early Visual Cortex (EVC) we have: 1) green: the Ventral pathways that passes toward the occipital and the temporal cortices and projects toward the Inferior Frontal Gyrus (IFG); 2) orange: the Dorsolateral pathways, that passes towards the inferior parietal lobe and projects toward the ventral Premotor cortex (vPM); 3) yellow: the Dorsomedial pathway that passes throughout the superior parietal lobe and projects toward the dorsal Premotor cortex (dPM).

1.2 Univariate fMRI studies on the human hand motor network

The advent of non-invasive neuroimaging techniques has opened new possibilities for studying the human motor network in vivo. In particular, functional magnetic resonance imaging (fMRI) allowed the recording of brain activity during the execution of various motor tasks. fMRI measures changes in Blood Oxygenation Level (BOLD) signals in the brain associated with neuronal activity. While investigating the neural underpinning of hand movements, univariate results have consistently revealed a sustained activation pattern within the motor network, encompassing temporal, parietal and frontal areas (Errante et al., 2021; Sartin et al., 2023). These findings align with prior theoretical frameworks, as illustrated in Figure 1.1. Moreover, recent reviews and metanalysis have provided a comprehensive description and discussion of these univariate studies (Errante et al., 2021; Ranzini et al., 2022; Rizzolatti et al., 2014; Rizzolatti & Matelli, 2003; Sartin et al., 2023; Turella & Lingnau, 2014; van Polanen & Davare, 2015; Vingerhoets, 2014). Figure 1.2 presents a summary of the brain regions included in the hand motor network (from Errante et al., 2021).

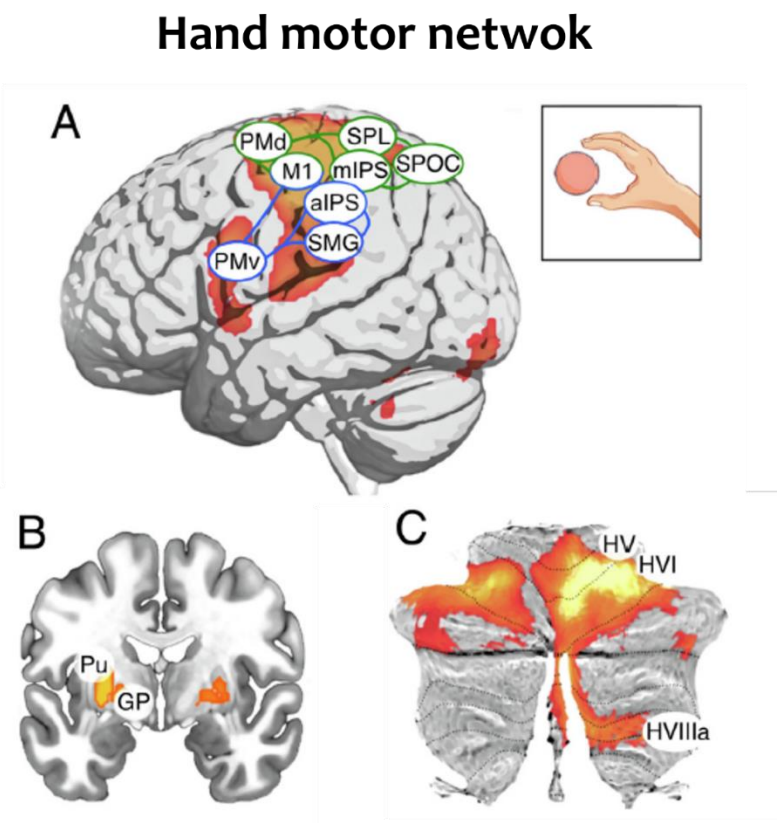

Figure 1.2. Neural Bases of Hand Movements. The image shows the brain areas consistently activated during the execution of grasping actions, with a cortical overlay into a standard 3D MNI template. Abbreviations: dPM – dorsal premotor cortex; vPM – ventral premotor cortex; M1- primary motor area; SPL – superior parietal lobe; mIPS – medial intraparietal sulcus; aIPS – anterior intraparietal sulcus; SMG – supramarginal gyrus; SPOC – superior parietal occipital cortex; Pu - putamen; GP – globus pallidus**, adapted from** (Errante et al., 2021).

As illustrated in Figure 1.2, the network underlying hand actions primarily comprises regions associated with the dorsolateral and the dorsomedial pathways. The Dorsolateral pathway includes key regions such as the anterior portion of the intraparietal sulcus (aIPS), the supramarginal gyrus (SMG), and the ventral premotor cortex (vPM), which are predominantly involved in visually-guided grasping (Jeannerod et al., 1995). The Dorsomedial pathway consists of the medial Intraparietal Sulcus (mIPS - Fattori et al., 2017; Filimon et al., 2009; Prado et al., 2005), the Dorsal Premotor Cortex (dPM - Filimon et al., 2007, 2009), the Superior Parietal Lobe (SPL - Cavina-Pratesi et al., 2010), the Superior Parieto-Occipital cortex (SPOC), and the Precuneus (PCu) (Cavina-Pratesi et al., 2010; Fattori et al., 2017; Filimon et al., 2009; Medendorp et al., 2005; Pitzalis et al., 2013; Prado et al., 2005). Although this body of univariate studies has provided fundamental insights into the neural bases of hand movements, univariate approaches present two key limitations in advancing our understanding of the hand motor network. First, univariate methods do not allow for the precise determination of what specific information is represented within different regions of the motor system (specificity of encoding). This limitation can be addressed by employing Multivariate Voxel Pattern Analysis (MVPA) approaches, which enable the examination of how distributed patterns of BOLD activation across multiple voxels encode distinct motor-related features (Kriegeskorte & Bandettini, 2007). Indeed, MVPA allows researchers to investigate both the location and the mechanisms by which different motor features are represented and integrated in the brain. Second, even when using advanced techniques such as MVPA, fMRI data remain inherently correlational, meaning they cannot establish a causal relationship between brain activity and behavior. Determining causality requires complementary approaches, such as neurostimulation techniques (e.g., transcranial magnetic stimulation, TMS), which allow researchers to directly perturb neural activity and assess its impact on behavior.

This introduction begins with an overview of how the Dorsal stream supports hand motor control, first focusing on reaching and then on grasping actions, integrating findings from both multivariate fMRI (MVPA) and TMS studies. We will then examine the contribution of the Ventral stream, again considering evidence from both MVPA and TMS. Finally, we will discuss how these two visual-motor pathways interact functionally, highlighting studies that reveal cross-stream integration during action planning and execution. This structure was chosen to allow a direct comparison of MVPA and TMS findings within each functional pathway, helping to clarify how correlational and causal evidence converge—or diverge—in characterizing the neural mechanisms underlying hand motor control.

To support this integrative review, we systematically extracted the stereotactic coordinates reported in each study (when available) and generated visual summaries to illustrate the current state of the literature. These figures focus on the left hemisphere, due to the limited number of investigations and reported results involving right-hemisphere regions.

1.3 Dorsal Stream involvement in motor control

Understanding how the brain plans and controls goal-directed actions requires examining both the spatial characteristics of movements and the specific effectors involved. Reaching and pointing tasks provide an ideal experimental framework for this investigation, offering precise control over low-level motor parameters such as movement direction, target location, and adopted effector. These tasks are widely used in both human and non-human primate studies and are uniquely positioned to bridge findings from invasive electrophysiological recordings with non-invasive neuroimaging and brain stimulation techniques.

To explore the neural representation of movement direction and effector identity, we divided our investigation into two parts. The first section examines how directional information is encoded within a single effector system—specifically, the right hand—during visually and non-visually guided pointing or reaching movements. This line of research allows us to isolate the spatial coding of movement trajectories and to test whether such representations rely on visual feedback or intrinsic motor planning.

In the second section, we extend this inquiry to investigate how direction encoding interacts with effector identity—comparing movements performed with different hands or with the eyes. This allows us to test whether the neural encoding of direction is effector-specific or reflects more abstract, effector-independent representations of action goals.

Together, these two lines of inquiry provide complementary insights into the neural mechanisms underlying goal-directed movements. By integrating findings from neuroimaging, brain stimulation, and cross-effector comparisons, we aim to build a more unified understanding of how the brain transforms spatial goals into motor commands across different sensory and motor contexts.

1.3.1 Decoding the direction of a movement (Reaching and pointing tasks)

We begin by examining how direction information is represented within a single effector system—specifically, the right hand—during pointing and reaching movements performed with and without visual feedback. This line of research provides a way to isolate the spatial encoding of movement trajectories and to determine whether these representations depend on visual input or arise from intrinsic motor planning mechanisms. The studies that have explored this question are summarized in Figure 1.3, which highlights the key regions implicated in encoding movement direction with the right-hand effector system. As illustrated in Figure 1.3, TMS studies (blue ROIs) have predominantly targeted the intraparietal sulcus (IPS), whereas MVPA studies (green ROIs) have identified distributed activations across the superior parietal lobule (SPL), frontal, and occipital regions. It is important to note that not all studies reported precise stereotaxic coordinates (for a full list, see: Paragraph 5.2-Supplementary materials: chapter 1); therefore, the spatial representations in the image are intended to provide a general overview rather than an exhaustive mapping.

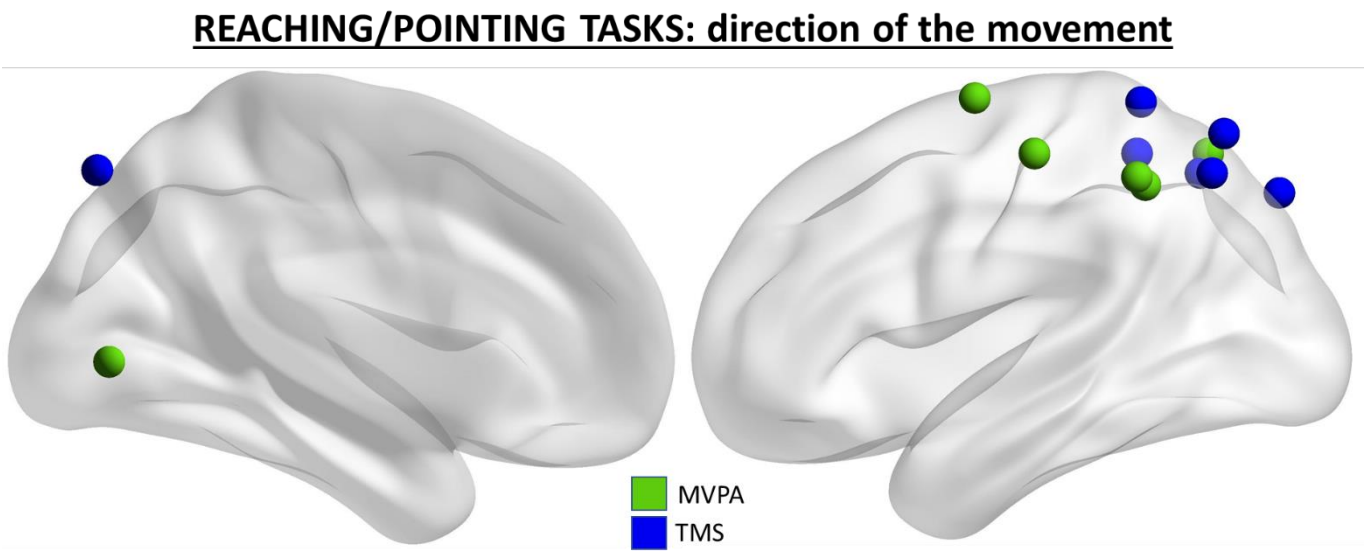

Figure 1.3. Spatial distribution of brain regions implicated in encoding movement direction, as identified by MVPA (green) and TMS (blue) studies. Each sphere represents a stereotactic coordinate extracted from the literature (left hemisphere only). A full list of the included studies and corresponding coordinates is provided in the Appendix (Paragraph 5.2-Supplementary materials: chapter 1).

In this section, we focus on studies investigating pointing and reaching actions. MVPA studies reveal how movement direction is represented across the brain, while TMS studies provide causal evidence by identifying which of these representations are essential for accurate behavior. Notably, the two

techniques examine different temporal aspects of motor processing: MVPA primarily captures planning-related activity patterns, reflecting the representational content of a region. In contrast, TMS allows for temporally precise interference of neural activity, as stimulation can be applied at different time points relative to the experimental conditions. This enables researchers to distinguish whether a brain region contributes to early planning, movement initiation, or online control, depending on the timing of stimulation.

Because most TMS studies have targeted the parietal cortex, we begin by examining findings in this region. Converging evidence from both MVPA and TMS studies supports a central role of the SPL in encoding movement direction, complementing earlier univariate findings (Pitzalis et al., 2013; Sartin et al., 2023). MVPA studies first established the involvement of the SPL in spatial aspects of motor planning. Krasovsky et al. (2014), for example, employed MVPA to dissociate neural encoding of movement direction (actual movement) from intended visual outcomes (e.g., observing a moving cursor). They found that the SPL reliably encoded the actual reach direction, reinforcing its role in motor planning. A subsequent MVPA study (Barany et al., 2014) further refined this picture, showing that the anterior portion of SPL encoded both target location and movement direction. Finally, Gallivan et al. (2011) have shown that the superior parieto-occipital cortex (SPOC) - a subregion of the SPL – could predict the upcoming reaching direction. These findings align with prior univariate studies suggesting that the SPOC transforms spatial information into appropriate motor commands for the hand (Pitzalis et al., 2013). Additionally, Ciavarro et al. (2013) and Vesia et al. (2010) implicated SPOC in goal representation and online adjustment during reaching, even in the presence of visual feedback.

Crucially, these MVPA results are causally supported by TMS findings. Striemer et al. (2011) showed that TMS over the SPL during the planning phase increased endpoint errors, particularly when the visual feedback was absent— confirming the SPL's involvement in trajectory specification. Notably, the same stimulation over the IPL had no effect, underscoring the SPL's specificity for direction encoding (Striemer et al., 2011). This absence of IPL involvement aligns with classical univariate evidence, which associates IPL primarily with grasp-related processing rather than reaching actions (Sartin et al., 2023).

Additional TMS studies provide complementary insights into the broader role of the parietal cortex, particularly during movement execution. Busan et al. (2009) showed that single-pulse online TMS over the parietal cortex during movement planning elicits a facilitatory effect, reducing reaction times

for reaching, regardless of direction. This suggests a more general role of the parietal cortex in initiating goal-directed actions. Complementing this, a landmark study by Desmurget et al. (1999) demonstrated that TMS over the PPC selectively impaired online correction of movement trajectories without affecting unperturbed reaches. In line with this, Della-Maggiore et al. (2004) showed that TMS over the PPC affects the learning of arm-reaching movements that require adaptation. Specifically, when TMS was applied 40 ms after movement onset during an adaptation task, it disrupted participants' ability to adjust their motor output across trials. These findings suggest that the PPC plays a role not only in immediate online corrections but also in motor adaptation during the later stages of movement learning. While previous univariate studies have already reported PPC involvement during action execution (Fattori et al., 2017; Pitzalis et al., 2013), the presented findings (Della-Maggiore et al., 2004; Desmurget et al., 1999) provide direct causal evidence linking PPC activity to real-time error correction and motor adaptation. Unlike univariate or MVPA approaches — which can only infer involvement based on correlated activity — these TMS studies show that disrupting PPC function impairs the brain's ability to update motor output in response to changing sensory conditions. Crucially, the selective disruption of feedback-based correction, without affecting unperturbed movements, suggests that the PPC is not broadly involved in generic motor execution, but is specifically engaged in sensorimotor recalibration and learning (Della-Maggiore et al., 2004; Desmurget et al., 1999). This dissociation underscores the importance of combining correlational and causal approaches: while fMRI and MVPA can identify where and what is represented in the brain, TMS reveals whether a region is functionally necessary for specific computations. Together, these converging methods offer a more complete and dynamic understanding of how parietal regions contribute to different stages of motor control—from planning and initiation to online adjustment and learning.

Going beyond parietal regions, other studies have jointly investigated the contribution of premotor and parietal regions to movement planning. In the same MVPA study by Krasovsky et al. (2014), anterior premotor clusters exhibited greater sensitivity to movement intention than parietal regions, suggesting a functional differentiation within the frontoparietal network. Supporting this distinction, Barany et al. (2014) showed that hand posture during reaching was encoded across M1, premotor, and parietal regions, indicating an integrated network that jointly represents sensory inputs and motor goals. These findings are consistent with prior work implicating the anterior SPOC and dPM in transforming visual information into appropriate motor commands (Fattori et al., 2010; Gallivan, McLean, & Culham, 2011; Gallivan et al., 2014; Monaco et al., 2011, 2014).

TMS investigations further support this distributed and overlapping functional organization. Busan et al. (2009) found that perturbing activity in the parietal cortex selectively impaired reaching performance, whereas stimulation of the dPM - a region traditionally associated with grasping - affected both reaching and non-reach control tasks. These results directly challenge the revised Dual-Stream model (Rizzolatti & Matelli, 2003), which posits a clear functional segregation between a dorsomedial pathway dedicated to reaching and a dorsolateral pathway specialized for grasping. Instead, those results (Busan et al., 2009) suggest that dPM, despite being anatomically part of the dorsolateral stream, contributes broadly to motor planning, including for reach-related actions. Taken together, these findings argue for a more flexible, task-dependent recruitment of frontoparietal regions, rather than a rigid, anatomically constrained functional dichotomy.

Finally, temporal specificity in motor encoding has also been demonstrated using TMS. Davare et al. (2012) showed that stimulation of the medial intraparietal sulcus (mIPS) during visually guided reaching led to increased trajectory deviations, implicating this region in the refinement of motor output during planning. In a follow-up study (Davare et al., 2015), the authors delivered TMS at different time windows before movement onset and found that the stimulation of the dPM altered movement amplitude when applied 40-100 ms before movement onset, whereas stimulation of mIPS interfered with movement direction only when applied 100–160 ms before onset. These findings suggest a temporally organized flow of processing, with dPM initiating the motor plan and mIPS subsequently fine-tuning its spatial parameters—highlighting a dynamic fronto-parietal interaction during action preparation. Supporting this view, Marigold et al. (2019) found no behavioral effects when mIPS was stimulated during movement execution, reinforcing the idea that mIPS is specifically involved in the planning phase rather than in execution. Taken together, these findings illustrate how a multimodal approach can disentangle the complex dynamics of motor planning and execution. Univariate fMRI studies established that both dPM and mIPS are reliably engaged during action preparation (Errante et al., 2021; Fattori et al., 2017; Pitzalis et al., 2013; Sartin et al., 2023; Turella & Lingnau, 2014). TMS then revealed that these areas contribute at distinct time points, with dPM influencing movement amplitude early in the planning phase and mIPS modulating directional parameters slightly later (Davare et al., 2012, 2015; Marigold et al., 2019). Crucially, MVPA studies added a representational layer, showing that these same regions encode specific features of planned movements—such as effector identity, direction, and posture (Barany et al., 2014; Gallivan, McLean, & Culham, 2011)—thereby clarifying the nature of the information processed within each node of the motor network.

1.3.2 *Decoding the adopted effector of a movement (Reaching and pointing tasks)*

Having explored how directional information is encoded in the brain, we now turn to studies investigating the encoding of effector identity — that is, how the brain represents actions performed with different effectors such as the eyes, hands, or tools. The central question here is whether neural activity patterns reflect effector-specific representations, tied to the biomechanics of a given effector, or instead support effector-independent, abstract representations of action goals. This line of research provides critical insight into the flexibility of the motor system and its capacity to generalize across different effectors to achieve similar behavioral outcomes. MVPA offers a unique advantage in this domain by revealing abstract, effector-independent neural codes – that is, representation of action goals that generalize across different effectors. In contrast, TMS provides causal evidence regarding whether regions are necessary for task performance.

Figure 1.4 illustrates only MVPA findings, as TMS studies typically do not report stereotactic coordinates (for a full list of papers, please see Paragraph 5.2- Supplementary materials: chapter 1). Nevertheless, we will discuss relevant TMS results throughout the text.

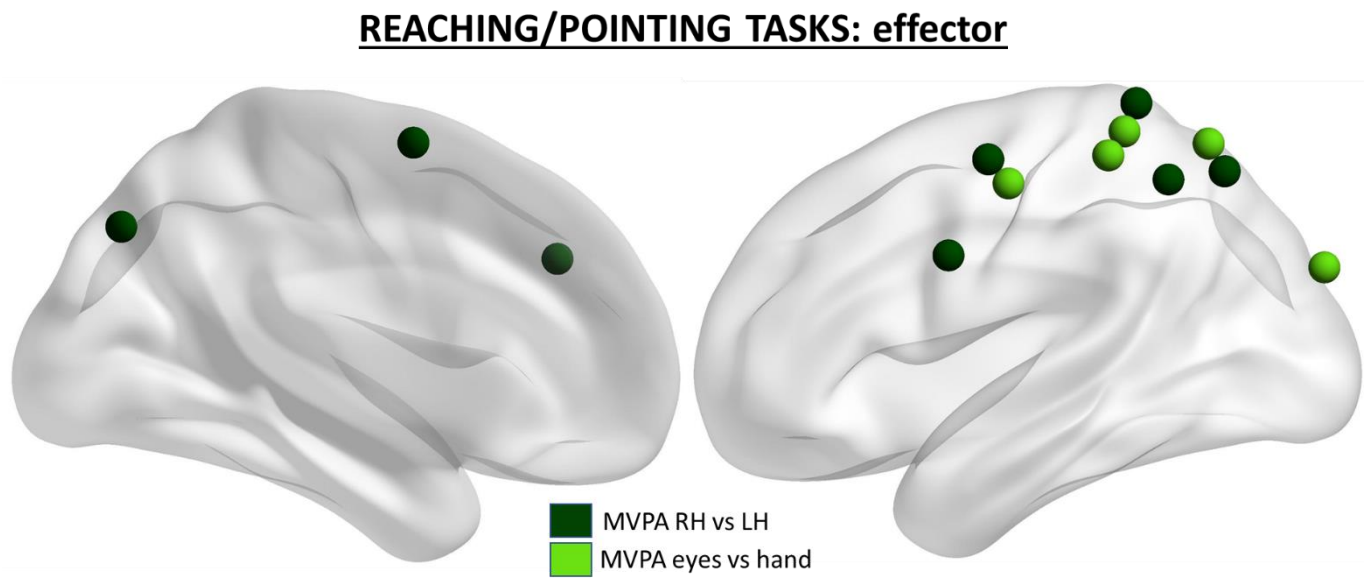

Figure 1.4. Spatial distribution of brain regions involved in effector-related action coding, as identified by MVPA studies. Dark green spheres represent studies decoding right-hand vs. left-hand movements, while light green spheres reflect decoding of hand vs. eye movements. TMS studies investigating effector specificity were excluded from the figure due to their limited number and lack of reported stereotactic coordinates. A complete list of included studies and coordinates is available in the Appendix (Paragraph 5.2- Supplementary materials: chapter 1).

Much of the MVPA literature has focused on parietal cortex involvement in encoding spatial goals independent of the effector used. Gallivan et al. (2011) demonstrated that subregions of the parietal cortex, particularly mIPS and pIPS, encode target location in an effector-independent fashion (hand or eye). These findings were confirmed through cross-decoding analyses showing stable representations across hand and eye movements. Although earlier invasive studies in non-human primates had hinted at similar coding (Battaglia-Mayer et al., 2013), this was the first demonstration of such abstract representations in humans. Univariate fMRI studies had previously shown that regions like mIPS and aIPS are activated by both hand and eye movements, though with stronger responses for hand actions (Filimon, 2010; Medendorp et al., 2005). However, univariate analyses cannot disambiguate whether overlapping activity reflects shared goal representations or simply spatial proximity of distinct effector-specific populations. MVPA helps resolve this ambiguity by demonstrating that the underlying patterns support cross-effector decoding – indicating a more abstract, goal-oriented representation in the parietal areas.

Further support comes from Leoné et al. (2014), who found that the rostral portion of the PPC (specifically, the anterior SPL, the aIPS, and the mIPS) responds to actions performed with the hands, eyes, or feet. While univariate studies had similarly observed overlapping activations in the PPC with some anatomical segregation (Medendorp et al., 2005), MVPA results suggest that this region may not merely encode spatial goals, but could also participate in effector selection or decision-making processes related to action choice (Leoné et al., 2014). This interpretation opens new hypotheses about the functional role of PPC in higher-order motor control.

To date, however, no TMS studies have directly tested the causal role of parietal regions in encoding effector-general or abstract goal representations. As such, this remains an open question for future research, ideally addressed through paradigms that combine MVPA's representational specificity with the causal precision of neurostimulation.

In parallel with parietal findings, MVPA studies have shown that premotor regions also contribute to effector-independent action planning. Univariate results have consistently shown activation in the dPM for both eyes and hand movements, with stronger engagement for hand-directed reaching (Errante et al., 2021; Medendorp et al., 2005; Sartin et al., 2023). Building on this, Gallivan et al. (2011) found that the dPM decodes spatial target location for both saccades and reaching movements during the planning phase - suggesting a shared spatial representation that may facilitate eye–hand coordination. These results are in line with non-human primate findings showing that dPM

maintains common reference frames for relative target position across different effectors (Pesaran et al., 2010).

The "classical" view posits a functional segregation between the dPM and vPM, with the former specialized for reaching and the latter for grasping actions (Rizzolatti & Matelli, 2003). However, a recent meta-analysis of univariate studies challenges this strict dichotomy (Sartin et al., 2023). The authors found that vPM is also consistently recruited during reaching tasks, especially in the planning phase, suggesting a more integrated and flexible role for premotor regions in motor control. These insights have been confirmed and extended by MVPA and TMS findings. The causal involvement of dPM in spatial integration and sensorimotor updating has been substantiated through TMS studies. In a seminal experiment, Lee & Van Donkelaar (2002) applied TMS over dPM during coordinated pointing and saccadic movements. Stimulation impaired pointing accuracy in a manner that depended on saccade amplitude, but only when delivered 100–200 ms after cue onset—indicating a temporally specific role for dPM in integrating spatial information across effectors. Further supporting this view, Lee & Van Donkelaar (2006) used a prism adaptation paradigm and showed that TMS over the left dPM increased reaction times and delayed error correction. These results highlight dPM's involvement not only in early planning but also in sensorimotor remapping and the online updating of motor plans in response to changes in visual input.

Together, these findings offer a more nuanced view of premotor cortex organization than what was previously inferred from univariate studies alone. While univariate analyses reliably identified dPM and vPM activations during planning and execution of reaching and grasping actions, they could not determine whether these regions encode effector-specific or abstract representations. MVPA addressed this limitation by showing that both dPM and vPM contain fine-grained activity patterns that generalize across effectors, suggesting they contribute to higher-order action planning (Gallivan, Adam McLean, et al., 2011, 2013). TMS further demonstrated that dPM plays a causal and temporally specific role in integrating spatial information and updating motor plans in real time (Lee & Van Donkelaar, 2006; Lee & Van Donkelaar, 2002). Thus, by combining representational, spatial, and causal evidence, a more integrative picture emerges in which premotor regions flexibly support both effector-specific and effector-independent aspects of motor behavior (Gallivan, Adam McLean, et al., 2011, 2013).

1.3.3 Decoding action information (grasping tasks)

Grasping actions rely on the integration of multiple parameters – such as reach direction, grip type, and object features - coordinated across a distributed frontoparietal network. Representational Similarity Analysis (RSA) by Fabbri et al. (2016) provided compelling evidence for how object properties are encoded across this network. They found that specific features, particularly object elongation, are robustly represented in both dorsal and ventral streams, highlighting their role in shaping grip configuration. By dissociating perceptual and motor-related representations, this study advanced our understanding of how the brain transforms object features into action-relevant motor plans.

To better capture the dynamic nature of grasping, we now summarize previous investigations based on two key phases of action: planning and execution. Within each phase, we further distinguish the contributions of parietal and premotor regions. This structure allows us to examine how spatial, object-related, and motor parameters are processed over time and across brain systems involved in grasp control.

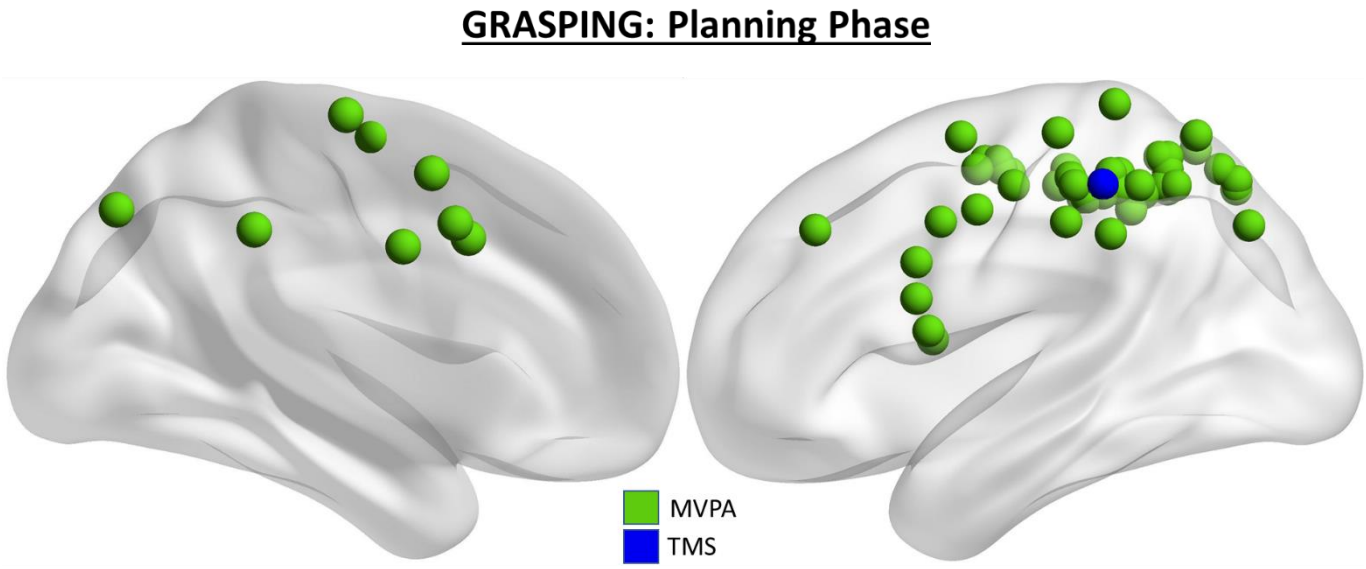

Figure 1.5. Spatial distribution of brain regions involved in grasping, as identified by MVPA (green) and TMS (blue) studies. Each sphere represents a stereotactic coordinate extracted from the literature (left hemisphere only). Due to the limited number of TMS studies reporting precise coordinates, this figure is predominantly based on MVPA data. A detailed list of the included studies and coordinates is provided in the Appendix (Paragraph 5.2- Supplementary materials: chapter 1).

We begin with the planning phase of grasping. As illustrated in Figure 1.5, the majority of available data comes from MVPA studies, although a limited number of TMS studies also provide causal insight. In what follows, we compare the findings from both approaches to better characterize the spatial and functional organization of parietal regions during grasp planning.

Univariate results have shown that the SPL is more strongly active during grasping rather than reaching, particularly when the visual feedback is available (Filimon, 2010). This has been interpreted as reflecting SPL involvement in feedback-dependent movement adjustments (Filimon, 2010; Sartin et al., 2023) and in the goal-directed shaping of the hand (Pitzalis et al., 2013). However, MVPA results have provided a more fine-grained view of the functional roles of these regions. Fabbri et al. (2014) showed that during grasping, the anterior SPL and the aIPS represent information about both reach direction and grip type. Importantly, they also found that anterior SPL and aIPS exhibit integrated coding of transport and grip components, suggesting that although these features may be initially processed in separate channels, they are combined in higher-level parietal areas to support coherent motor planning. These findings indicate that the parietal cortex not only integrates spatial and motor parameters but also contributes to the coordination of grasp components into unified action plans. However, successful motor behavior requires more than just integration—it demands flexibility.

Beyond coordinating multiple features, humans can execute the same action with subtle variations depending on context. For instance, grasping a coffee cup by its handle to drink involves a precision grip similar to that used to throw a dart, yet the motor goal and dynamics differ markedly. Such flexibility highlights the need for the motor system to generalize across similar actions, rather than relying on fixed, kinematic-specific templates for each instance. Rather than encoding every possible movement variation independently — a strategy that would be computationally costly and biologically inefficient — the brain likely supports more flexible and abstract motor representations that can be adapted across different contexts and effectors.

Supporting this idea, Kadmon Harpaz et al. (2014) showed that aIPS and M1 encode letter-drawing movements in a scale-invariant way. This interpretation refines conclusions from univariate studies, which consistently report M1 activation during execution, particularly for precision grip tasks (Errante et al., 2021). While univariate analyses emphasize M1's role in generating fine motor output and digit control, MVPA reveals that M1 may also participate in higher-order motor planning, encoding action structure in a more abstract and flexible format (Kadmon Harpaz et al., 2014).

Similarly, Gallivan et al. (2013) found that pIPS and mIPS encoded grasping actions independently of which limb was used, emphasizing effector-independent, goal-driven planning. Extending this line of work, Gallivan et al. (2013) showed that mIPS and pIPS generalized across hand and tool use, suggesting that these parietal regions represent goal-related information rather than specific motor patterns or commands. At the same time, anterior parietal areas (aIPS) and motor areas discriminated grasping hand versus tool actions in the planning phase. At a finer scale, Gallivan et al.

(2011) revealed that left SPOC, anterior precuneus, mIPS, and pIPS could decode grasping versus touch in the planning phase. Interestingly, they found a functional gradient within the aIPS: while the posterior portion (post-aIPS) was already selective for grasp type during the planning phase, the anterior portion (ant-aIPS) showed differentiation only during execution. This aligns with prior univariate findings suggesting that post-aIPS is involved in object feature processing, while anterior portions contribute to somatosensory integration and grip control (Culham, 2004; Ehrsson et al., 2003; Valyear et al., 2007). MVPA extended these findings by revealing that different subregions within aIPS not only show differential activation, but also encode distinct grasp parameters with varying temporal profiles. Specifically, it demonstrated that posterior aIPS carries grip-type information already during planning, while anterior portions become selectively tuned only during execution (Fabbri et al., 2014; Gallivan et al., 2013; Kadmon Harpaz et al., 2014) —evidence of a functional progression not detectable through univariate methods alone.

In line with this proposal, Freud et al. (2018) demonstrated that aIPS can discriminate between 3D and 2D objects during both reaching and grasping tasks involving real and imaged objects. During execution, aIPS was sensitive to object dimensionality for both types of actions. However, during planning, aIPS showed a dissociation only for grasping—differentiating between 2D and 3D objects before movement initiation. The authors suggest this reflects the added precision demands of grasping, which require the maintenance of detailed object representations in advance. Notably, these effects were found only in the left aIPS, supporting the idea of a hemispheric asymmetry in anticipatory motor coding.

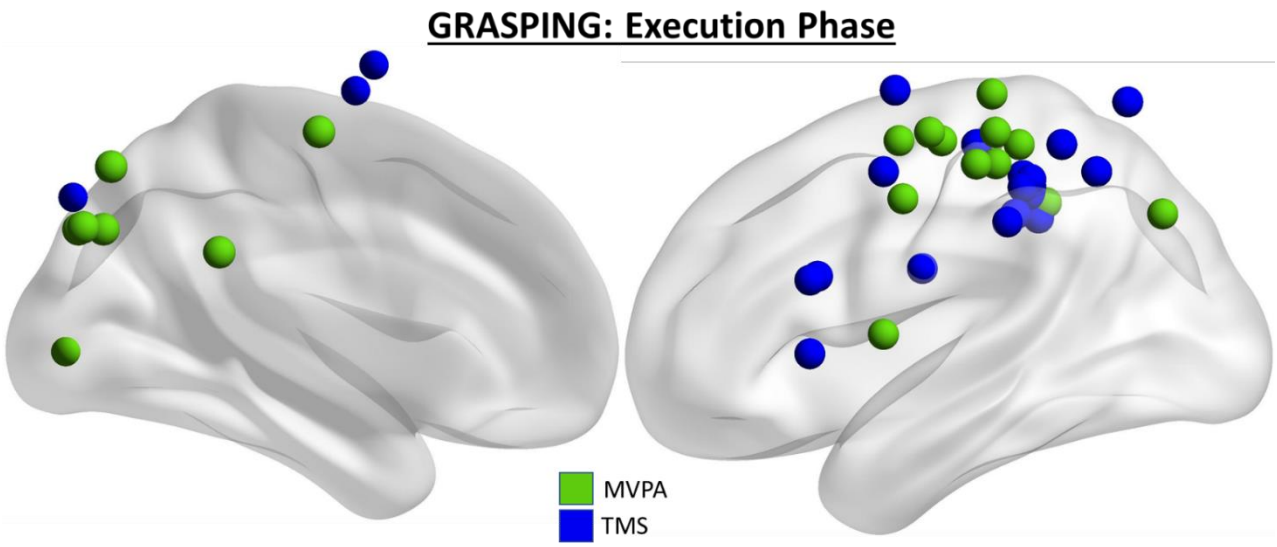

Figure 1.6. Spatial distribution of brain regions involved in the execution phase of grasping, as identified by MVPA (green) and TMS (blue) studies. Each sphere represents a stereotactic coordinate extracted from the literature (left hemisphere only). Compared to planning-related studies, a greater number of TMS investigations report coordinates for this phase, enabling a broader causal comparison. A full list of included studies and coordinates is provided in the Appendix (Paragraph 5.2- Supplementary materials: chapter 1).

Having examined the neural mechanisms involved in the planning phase of grasping, we now turn to the execution phase. As illustrated in Figure 1.6, a greater number of TMS studies report coordinates for this phase, providing a valuable opportunity to compare MVPA and causal evidence (for a full list, see Paragraph 5.2- Supplementary materials: chapter 1). This allows us to more directly assess the role of frontoparietal regions—particularly aIPS—in the fine-tuned control of grip force and hand shaping during action execution. These MVPA and TMS findings converge in the execution phase of grasping, where causal evidence has been particularly informative due to the higher number of TMS studies with precise temporal and spatial resolution. For example, Glover et al. (2005) showed that TMS over aIPS disrupted grip scaling in response to object size, but only when stimulation occurred during movement — not during planning — highlighting aIPS's role in online motor correction. Interestingly, this causal role of aIPS is not limited to the processing of object size but extends to force scaling as well. Davare et al. (2007) investigated the direct role of aIPS in precision grasping, showing that TMS delivered 270–200 ms before object contact disrupted hand shaping, while later stimulation (170–120 ms after contact) specifically affected grip force scaling. These findings suggest that aIPS contributes both to the initial configuration of the hand for precise object interaction and to the subsequent modulation of grip force. Notably, the study also showed that left aIPS stimulation impaired grip force scaling, while bilateral stimulation was required to disrupt hand shaping, suggesting that aIPS involvement in grasping is effector-independent. That is, each aIPS appears

capable of performing visuomotor transformations of object properties for both hands, with the left aIPS playing a dominant role in grip force scaling regardless of which hand is used (Davare, Andres, et al., 2007). Building on this, Dafotakis et al. (2008) investigated the effects of TMS on both predictive and reactive grip force adjustments. Stimulation was applied either at movement onset or at the peak of grasp aperture. They found that TMS over aIPS disrupted grip force scaling to novel object weights regardless of stimulation timing. The authors concluded that aIPS is crucial for detecting and correcting errors in grip force modulation, supporting its role in predictive force processing during grasping. Similarly, Van Polanen et al. (2020) found that TMS over aIPS impaired anticipatory force scaling during object lifting, reinforcing the idea that aIPS is involved in planning force output before object contact. In a follow-up study (van Polanen et al., 2022), the authors demonstrated that TMS over aIPS not only affected grip force scaling but also disrupted weight perception, suggesting that aIPS contributes to the integration of sensorimotor signals necessary for both motor and perceptual judgments.

Further extending this line of evidence on timing, Rice et al. (2006, 2007) further confirmed the temporal specificity of aIPS involvement by showing that TMS impaired grip adjustment under visual occlusion, but only when delivered during execution. Notably, the effects were lateralized, with each hemisphere's aIPS modulating contralateral hand shaping. While recent univariate studies have shown consistent activation of aIPS during both planning and execution phases (Errante et al., 2021; Sartin et al., 2023), TMS findings challenge the functional relevance of this early activation. Specifically, aIPS stimulation during the planning phase produces no behavioral disruption on grasping (Gutteling et al., 2013; Rice et al., 2006, 2007; Tunik et al., 2005a, 2008), suggesting that although aIPS is active during planning, it may not be causally necessary at that stage.

Other parietal and frontal regions also contribute to grasp control. Tunik et al. (2005, 2008) further demonstrated that aIPS is essential for integrating unexpected perturbations into ongoing motor plans, while the Supramarginal Gyrus (SMG) and the frontal operculum are more involved in the initial specification of spatial goals. TMS over SMG or the operculum delayed planning for goal-directed grasping, without affecting the execution of simpler control tasks. These results are supported by McDowell et al. (2018) and Potok et al. (2019), who showed that TMS over the SMG during execution impaired the online correction, while stimulation during planning yielded timing-dependent effects: early stimulation slowed response initiation, whereas later stimulation facilitated grasp execution. These findings indicate a temporally specific role for SMG in both anticipatory and online phases of

grasping, in line with univariate data identifying this region as critical for hand-object interaction (Errante et al., 2021; Sartin et al., 2023).

Expanding on these insights, Taubert et al. (2010) found that online TMS over the aIPS during cue presentation delayed wrist rotations, suggesting that aIPS is crucial for the rapid integration of sensory cues into motor plans. More recently, Breveglieri et al. (2023) demonstrated functional differentiation within the parietal grasping network: phAIP (putative human aIPS) was more involved in wrist orientation, while hV6A contributed to grip aperture control. Both regions were essential for real-time reprogramming of grasp parameters. Similarly, Cattaneo et al. (2015) showed that the parietal operculum supports haptic memory for blind grasping, and Goldenkoff et al. (2023) revealed that the PPC can exert a facilitatory influence on grasping behavior via Intermittent Continuous Theta-Burst Stimulation (iTBS), possibly reflecting long-term changes in cortical excitability. To conclude, TMS results provide the functional necessity of these regions, showing how few regions (e.g., aIPS, SMG) are essential to online correction or late-phase integration. These temporally precise disruptions validate the functional alignments proposed by MVPA and univariate studies, while also challenging some assumptions (e.g., planning role of aIPS).

MVPA studies have also revealed the role of premotor and motor areas in grasping. Fabbri et al. (2014) showed that the SMA and the dPM encoded reach direction during grasping actions, while the M1, the SS, and the vPM encoded both reach direction and grip type. Notably, the vPM and the M1 showed an interaction between transport and grip components, suggesting that although low-level motor features may be processed in a segregated manner, they are integrated in higher-level motor regions. In subsequent studies (Gallivan, McLean, Valyear, et al., 2011; Gallivan, McLean, et al., 2013), the authors showed that vPM, dPM, pre-SMA, and the dlPFC encoded grasping actions independently of the effector used for the action. Extending this line of work, Gallivan et al. (2013) demonstrated that vPM and dPM encoded grasping actions in a manner that generalized across both hand and tool use, suggesting that these premotor regions represent high-level action goals rather than effector-specific motor patterns. Interestingly, the joint involvement of both vPM and dPM (Gallivan, Adam McLean, et al., 2011) in distinguishing between grasp and reach actions during planning challenged the classic proximal-distal distinction (Rizzolatti & Matelli, 2003; Tanné-Gariépy et al., 2002), suggesting that premotor cortex supports a more flexible coordination of multiple grasp-related parameters. In addition, Gallivan et al. (2013) showed that both dPM and vPM can decode upcoming action types regardless of whether the task is executed with a hand or a tool—two effectors with

markedly different biomechanical profiles. This suggests that premotor areas encode high-level, abstract representations of intended actions, rather than merely specifying effector-specific motor commands.

These MVPA findings are further supported by causal TMS evidence, showing a gradient within the premotor cortex. First, Davare et al. (2006) investigated the role of premotor cortices in grasp-to-lift tasks performed with the right hand. They found that the left vPM is engaged at early stages—approximately 200 ms before object contact—playing a key role in visuomotor transformation and in generating the appropriate muscle activation pattern. Specifically, TMS over both the left and right vPM altered finger positioning on the object, while stimulation of the left vPM alone disrupted the sequential recruitment of intrinsic hand muscles, confirming its contribution to motor program elaboration. Notably, about 100 ms after vPM activation, dPM becomes involved, primarily in controlling the timing of the lifting phase relative to grasping. Importantly, dPM was not implicated in the magnitude of proximal muscle contraction, but rather in ensuring correct temporal coordination between phases.

This early-late division within premotor areas is consistent with other TMS findings. On one hand, Taubert et al. (2010) applied TMS over dPM during a cue-based grasping task (matching color to action) and found that stimulation disrupted movement execution, likely due to the dPM's role in preparing complex actions based on internal goals and stored representations (Sartin et al., 2023). On the other hand, TMS over vPM has been shown to disrupt grasp aperture shortly after perturbation onset, supporting its role in rapid online adjustment (Schettino et al., 2015). In addition, (Schettino et al., 2015). In addition, Dafotakis et al., (2008) demonstrated that vPM is also engaged in predictive grip force scaling, indicating its role in adapting motor output based on internal models of object properties. Lega et al. (2020) expanded on this by identifying three premotor regions—two in vPM and one in dorsal SMA—whose stimulation affected grip aperture during object grasping, confirming a distributed premotor grasping network. Schramm et al. (2019) further demonstrated that SMA stimulation influences motor timing and coordination across different motor tasks, including grasping. In addition, White et al. (2013) investigated the role of the SMA in a grip-to-lift task performed with both the right and left hand. They found that TMS over the left SMA increased grip force and grip force rate for both hands, but only when stimulation was delivered 130–180 ms before object contact. Moreover, stimulation of either the left or right SMA selectively augmented the pre-load phase for the contralateral hand. Based on these findings, the authors concluded that

the left SMA likely plays a key role in scaling grip force appropriately for upcoming actions, and does so in an effector-independent manner.

Taken together, these results support a model in which vPM refines grasp execution (Dafotakis et al., 2008; Davare et al., 2006; Fabbri et al., 2014; Gallivan, Adam McLean, et al., 2013; Gallivan et al., 2011; Gallivan, McLean, et al., 2013; Schettino et al., 2015), dPM orchestrates timing and action selection (Davare et al., 2006; Fabbri et al., 2014; Gallivan, Adam McLean, et al., 2013; Gallivan et al., 2011; Gallivan, McLean, et al., 2013; Taubert et al., 2010), and SMA contributes to bilateral coordination and anticipatory force modulation (Lega et al., 2020; Schramm et al., 2019; White et al., 2013). This evidence underscores a broader functional hierarchy across premotor regions, integrating abstract planning with precise, time-sensitive motor output.

Finally, both M1 and SI have been implicated in the modulation of force and digit positioning, particularly under constrained grasp conditions. Davare et al. (2007) investigated the role of M1 in grasp-to-lift tasks and found that TMS over M1 altered the timing of muscle recruitment in both the lifting and control (step-tracking) tasks. More recently, Parikh et al. (2020) employed continuous Theta-Burst Stimulation (cTBS) to show that M1 is critical for force control when constraints are present, and that both M1 and SS support grasping performance when actions are less constrained—supporting their involvement in memory-based retrieval of grasp parameters (Sartin et al., 2023).

Altogether, these findings from MVPA and TMS converge to show that grasping is supported by a flexible, hierarchical network in which posterior parietal and premotor areas encode abstract and context-dependent action plans, while motor and somatosensory cortices ensure their precise execution and correction. A central role is played by the PPC—particularly the aIPS and pIPS—which acts as a key integration hub, representing actions at multiple levels of abstraction and translating them into specific motor commands via premotor output to M1 (Turella et al., 2020).

A recent study (Turella et al., 2020) directly tested this hierarchical model by examining three levels of grasp representation: concrete (grasp type with fixed effector and wrist orientation), effector-dependent (generalizing across wrist orientations), and effector-independent (abstract representations invariant to effector and posture). They found that although these representations were distributed across frontal, parietal, and temporal cortices, the PPC—especially bilateral aIPS and left pIPS—served as the main convergence point. The authors proposed that PPC enables flexible action remapping by maintaining the goal of the action and communicating effector-specific adjustments to premotor areas, which in turn generate revised motor plans for execution in M1.

This hierarchical organization may explain how the brain seamlessly adapts grasping strategies when faced with changing task demands or effector constraints. By integrating MVPA's insights on representational structure with TMS's causal evidence, a clearer picture emerges of how abstract motor intentions are transformed into concrete, goal-directed behavior in real time.

1.4 Ventral stream's involvement in motor control

The Dual-Stream Theory (Goodale & Milner, 1992) posited a clear separation between the Ventral stream ("what" pathway, for object identification) and the Dorsal stream ("how" pathway, for action execution). However, growing evidence challenges this rigid dichotomy, suggesting that the Ventral stream also plays a supportive role in motor control—particularly in situations requiring memory-based actions, perceptual inference, or delayed movement planning. As shown in Figure 1.7, although fewer studies have targeted the Ventral stream compared to the Dorsal stream, both MVPA and TMS results highlight its involvement in grasping and reaching tasks (for a full list of papers, see Paragraph 5.2- Supplementary materials: chapter 1). These findings indicate that the Ventral stream is not solely dedicated to perception but can contribute to action-related processing under specific contextual demands. The following section reviews the key MVPA and TMS studies contributing to this evidence, highlighting how Ventral stream regions participate in both perceptual and motor aspects of grasping and reaching.

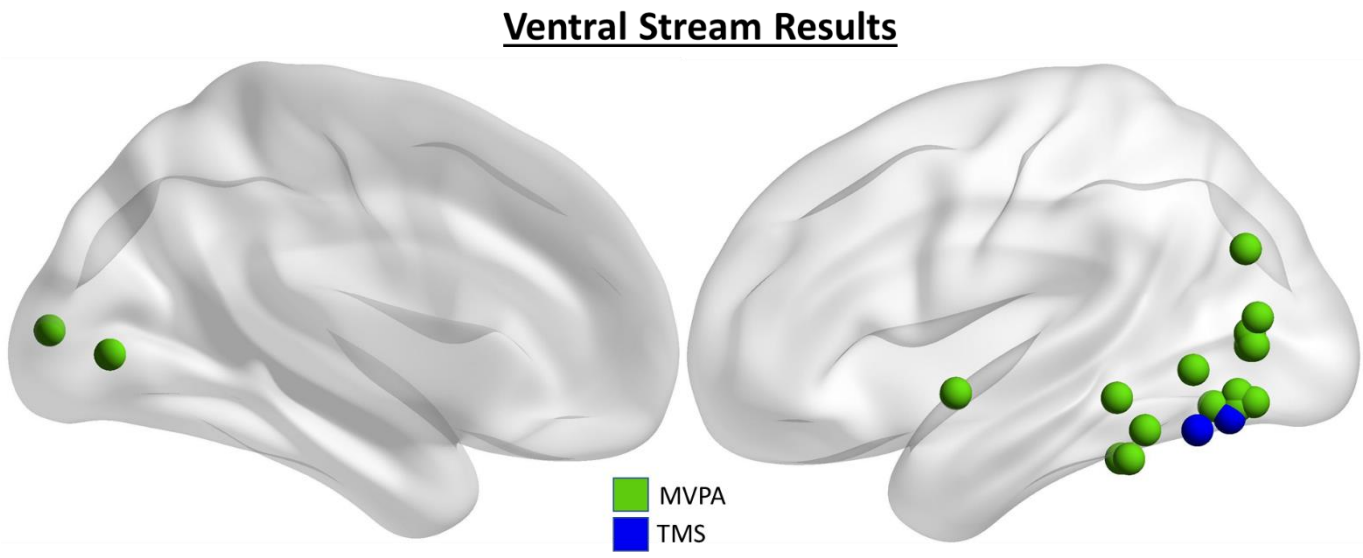

Figure 1.7. Spatial distribution of brain regions within the Ventral stream involved in grasping and reaching, as identified by MVPA (green) and TMS (blue) studies. Each sphere represents a stereotactic coordinate extracted from the literature (left hemisphere only). While fewer studies have targeted the ventral pathway compared to the dorsal stream, both correlational and causal approaches point to the involvement of occipitotemporal areas in visually guided and memory-based action planning. A detailed list of included studies and coordinates is provided in the Appendix (Paragraph 5.2- Supplementary materials: chapter 1).

Multivariate analyses have revealed that even early visual areas participate in motor coding. For example, Gutteling et al. (2015) showed that the early visual cortex (EVC) encodes upcoming hand movements during the action planning phase, prior to execution. Similarly, Gallivan et al. (2019) and Rens et al. (2023) demonstrated that EVC can distinguish between grasp types and intended object manipulations, even without visual feedback—suggesting top-down motor modulation of sensory cortices. A series of studies by Monaco et al. (2017, 2019, 2020) further support this view. They showed that visual and haptic object exploration modulates activity in EVC and category-selective Ventral stream areas (e.g., LOtv), and that these regions encode abstract action intentions—such as grasp versus reach—during motor imagery and planning, even without visual input. Notably, Monaco et al. (2020) found that parietal regions generalized across imagined and executed actions, whereas EVC did not. This supports the idea of a representational hierarchy, where abstraction increases along the sensorimotor pathway. In line with these findings, Freud et al. (2018) examined activity in ventral regions during reaching and grasping actions directed toward real versus imaged objects. They found that the lateral occipital cortex (LOC) distinguished between 2D and 3D objects across both tasks, reinforcing its role in encoding visual properties of target objects. Importantly, during the planning phase, LOC activity showed a preference for grasping actions—presumably because grasping requires processing of object structure for hand shaping, whereas reaching merely required contact. This grasp-selective modulation during planning suggests that LOC may be directly influenced by dorsal stream inputs (Sim et al., 2015), further supporting the notion of cross-stream interaction during goal-directed actions.

TMS studies provide causal validation of these representational gradients. Cohen et al. (2009), for instance, showed that online TMS over the LOC selectively impaired delayed grasping—actions reliant on memory—but not immediate visually guided actions. In contrast, TMS over aIPS disrupted both, suggesting that LOC contributes specifically to memory-based motor planning. Supporting this, Threethipthikoon et al. (2023) decoded grasp orientation in both visual (V1–V7) and parietal (IPS) regions during grasping without vision, highlighting the contribution of tactile and proprioceptive inputs to visual cortical representations. Similarly, Gallivan et al. (2013) showed that action planning modulates activity in the occipitotemporal cortex (OTC), including object- and category-selective regions such as the Lateral Occipitotemporal cortex (LOTC), the Fusiform Face Area (FFA), and the Parahippocampal Place Area (PPA). These regions encoded effector type (e.g., hand vs. tool) and action type (e.g., reach vs. grasp), suggesting that the Ventral stream contributes to both concrete and abstract motor representations.

Consistent with this view, van Polanen et al. (2022) applied TMS to LO during object lifting tasks, specifically during the static phase. TMS impaired weight estimation—especially for heavier objects—while stimulation during the dynamic phase increased grip force. These results support a direct role for LO in integrating object properties like weight into ongoing motor plans. Further evidences come from Adam et al. (2016), who employed cTBS over LOC and the Angular Gyrus (AG) to dissociate egocentric and allocentric reaching. Disruption of both regions impaired movement times for peripherally located targets, showing that both dorsal and ventral areas are necessary for spatially guided action.

Collectively, these findings challenge the classical boundaries of the Dual-Stream model. The Ventral stream — traditionally considered purely perceptual — clearly participates in motor prediction, memory-based action planning, and the integration of tactile and visual information. While the Dorsal stream remains crucial for immediate visuomotor transformations, the Ventral stream supports flexible, goal-directed behavior when visual cues are absent or incomplete. MVPA findings reveal how representational abstraction increases from posterior to anterior regions, while TMS studies identify causal roles that depend on task context and timing. Together, these methods support a dynamic, interactive model in which Ventral and Dorsal pathways cooperate to guide real-world action.

1.5 Ventral and Dorsal streams interactions

The findings reviewed here challenge the classical model of strictly segregated visual pathways. Rather than functioning independently, the Ventral and Dorsal streams exhibit extensive anatomical and functional integration, contributing to action planning and execution in a complementary manner. While the Dorsal stream has traditionally been linked to online movement control and the Ventral stream to object recognition, accumulating evidence demonstrates that both pathways encode concrete and abstract motor representations (Gallivan, McLean, et al., 2013; Gallivan et al., 2014; Gallivan & Culham, 2015; Hutchison et al., 2014).

This integration offers important advantages for sensorimotor control. The Ventral stream, specialized for processing object features such as identity, texture, and shape (Grill-Spector & Malach, 2004), is modulated not only by visual attention (Kastner & Ungerleider, 2000), but also by the action goal (Gallivan, McLean, et al., 2013; Gutteling et al., 2015; Monaco et al., 2020) and effector identity. Conversely, the Dorsal stream can enhance object-related processing through shared representations with Ventral regions, optimizing motor prediction and action planning (Gallivan & Culham, 2015). For example, anticipatory encoding of movement consequences within the Ventral stream may support distinctions between self-generated and external stimuli, as well as sensorimotor prediction and error monitoring (Culham et al., 2003; Hutchison & Gallivan, 2018). TMS studies provide causal evidence for this bidirectional interaction. In a study involving pointing movements influenced by the Ebbinghaus illusion, Lee & Van Donkelaar (2002) found that TMS over both dorsal (PPC, SMA) and ventral (inferotemporal) regions disrupted illusion effects. However, only dorsal stimulation interfered with pointing toward non-illusory targets, confirming the Dorsal stream's primary role in execution and the Ventral stream's contribution to perceptual modulation of action.

In the context of grasping, Culham et al. (2003) showed that the lateral occipital cortex (LO)—a Ventral stream area—is activated during both grasping and reaching, while aIPS exhibits grasp-specific tuning. These results suggest that grasp parameters emerge from functional integration between aIPS and ventral visual areas. Supporting this, Hutchison & Gallivan (2018) observed increased functional connectivity between occipitotemporal regions (e.g., OTG, EBA, MTG) and parietal cortex during action planning. Such dynamic coupling supports the idea that motor planning can influence perceptual representations, even before movement onset (Gallivan, McLean, et al., 2013).

Further evidence for functional convergence comes from tool-use studies. Bracci et al. (2012) and Bracci & Peelen (2013) found that hand- and tool-selective regions in the LOTC show functional connectivity with aIPS and premotor cortex, reflecting how tools are neurally represented as body extensions. Representational similarity analyses (RSA) in the LOTC revealed selective encoding of both tool- and body-related actions, indicating that visual areas integrate sensorimotor signals. This is further supported by topographic maps in LOTC aligning body parts with the tools they manipulate (Orlov et al., 2010). Complementing these findings, Sim et al. (2015) investigated object identification during action observation by presenting participants with videos of tool use. In line with the classical dorsal/ventral framework, they found activation not only in dorsal stream regions (left S1, premotor, and parietal cortices) associated with action representation, but also in ventral stream regions, including the middle and inferior occipital gyri and the inferior temporal gyrus. Crucially, effective connectivity analyses revealed a temporal progression: dorsal areas (frontal and parietal cortices) became active approximately 120 ms after object presentation, followed by activation in occipitotemporal and anterior temporal areas around 380 ms. These findings suggest that object-related action representations are first encoded within the dorsal stream and then modulate processing in the ventral stream. In particular, SPL appeared to influence activity in ventral regions, supporting a model of dorsal-to-ventral information flow during goal-directed object recognition.

Anatomical studies corroborate these functional findings. In both humans and non-human primates, direct temporo-parietal connections link aIPS with Ventral stream areas (Borra et al., 2008, 2010; Bracci et al., 2012). These pathways likely convey efference copies of motor plans to visual areas such as LOTC, enabling the prediction of action outcomes and contributing to anticipatory adjustments such as hand pre-shaping (Cavina-Pratesi et al., 2010; Murata et al., 2000). Nonetheless, while co-activation of aIPS and OTC is frequently observed, the precise computational roles of these regions remain an open question.

Together, these findings call for a reconceptualization of the dual-stream framework. The Ventral stream, once thought to be solely perceptual, clearly participates in action prediction, memory-guided planning, and perceptual-motor integration. While the Dorsal stream remains central for real-time visuomotor transformations, the Ventral stream complements it by integrating visual and semantic object information—particularly when visual input is incomplete or delayed. This reconceptualization is driven in part by methodological advances: MVPA has revealed representational gradients across ventral and dorsal areas, while TMS has provided causal,

temporally specific evidence of their contributions to behavior. Together, these approaches reveal a distributed, hierarchical sensorimotor network in which the Ventral and Dorsal pathways interact dynamically to support flexible, goal-directed action.

1.6 Open questions and thesis rationale

Over the past two decades, univariate fMRI, MVPA, and TMS have significantly advanced our understanding of the functional roles of individual brain areas involved in hand motor control. These techniques have helped delineate the specific contributions of regions such as aIPS, SPL, dPM, and M1 to various components of reaching and grasping, from planning and execution to online correction. Yet, while the functional profiles of these individual areas are now increasingly well characterized, our understanding of the network-level organization — particularly the connectivity architecture of the frontoparietal system — remains limited.

A major open question in motor neuroscience concerns the dynamic interactions among these regions: How do they coordinate during goal-directed hand movements? Which areas are responsible for integrating sensory input, generating abstract motor plans, and transmitting commands to motor effectors? And crucially, how are representational properties distributed across the network rather than localized within isolated nodes?

To date, most research has examined either correlational methods (e.g., fMRI, MVPA) or causal approaches (e.g., TMS) in isolation. Although each provides important insights, they are fundamentally complementary, offering different perspectives on the same underlying neural mechanisms. Only a few studies have attempted to combine them directly (Boudrias et al., 2012; de Vries et al., 2009; Foltys et al., 2003; Handwerker et al., 2020; Johnen et al., 2015; Reichenbach et al., 2011; Shitara et al., 2011), and these have primarily focused on clinical populations or examined localized, task-evoked activity.

We argue that this fragmented approach limits progress in understanding how the motor system functions as a distributed and interactive network. To move beyond region-specific interpretations, it is essential to integrate data across methods and across spatial and temporal scales. For example, neurostimulation techniques' targeting can be guided not only by anatomical landmarks but also by functionally defined and multivariate activation profiles, allowing for more individualized and precise stimulation. While this strategy has been adopted in clinical settings (Fornia et al., 2018; Grefkes et al., 2010), its use in healthy populations remains limited (Johnen et al., 2015).

In line with this integrative perspective, the first experiment presented in this thesis aims to investigate changes in functional connectivity before and after TMS stimulation, using resting-state fMRI. Resting-state activity, typically recorded in the absence of an explicit task, has been shown to reflect the underlying organization of functional networks — and to change as a consequence of

motor learning (Livne et al., 2022; Zhang et al., 2023, 2025). Given that motor activity can reshape the connectivity of the entire motor network, resting-state measures offer a valuable window into how TMS may modulate intrinsic network dynamics. A further advantage of this approach is its simplicity and versatility: if effective, resting-state acquisition could offer a more accessible alternative to task-based protocols, particularly when participants are unable to perform specific motor tasks or when a standardized task design is not feasible.

To this end, we used TMS to perturb the human Anterior Intraparietal area (hAIP)—a key hub in the dorsolateral pathway known to be involved in visuomotor transformations and grasping (Jeannerod et al., 1995; Rizzolatti et al., 1998; Rizzolatti & Luppino, 2001; Rizzolatti & Matelli, 2003). Evidence from non-human primates suggests that hAIP has widespread connectivity with both dorsolateral and dorsomedial pathways, as well as with the ventral stream (Borra et al., 2008, 2017; Borra & Luppino, 2019; Greulich et al., 2020; Howells et al., 2020; Lanzilotto et al., 2019; Rizzolatti et al., 2014; Rozzi et al., 2006). While its functional role in humans has been well documented (Culham et al., 2006; Culham & Valyear, 2006; Gallivan, Adam McLean, et al., 2011; Gallivan, McLean, et al., 2013; Gallivan & Culham, 2015; Grefkes & Fink, 2005; Monaco et al., 2019, 2020; Turella et al., 2020), its connectivity profile remains poorly understood. To address this gap, we adopted a dual analysis strategy: (1) a univariate ROI-to-ROI connectivity analysis, based on a predefined set of regions of interest, and (2) a multivariate searchlight analysis, examining how connectivity patterns from the stimulated site extend across the whole brain. By combining causal perturbation and functional connectivity mapping within a unified framework, this experiment seeks to move beyond isolated activation profiles—offering new insights into how motor functions are supported by coordinated, distributed network dynamics.

Building on this network-level perspective, our second experiment explored a related but distinct question: Can brain connectivity predict individual differences in motor behavior? While it is well known that motor control shapes behavioral output, few studies have directly linked resting-state functional connectivity (rs-FC) to motor performance. To address this, we adopted Connectome-Based Predictive Modeling (CPM) — a data-driven approach that has been successfully used to predict cognitive traits such as fluid intelligence and reading ability from rs-FC patterns in both healthy individuals (Rosenberg et al., 2016; Shen et al., 2017, p. 201; Wu et al., 2021, 2022, 2023; Yoo et al., 2022) and clinical populations (J. Kim et al., 2023; Lake et al., 2019; Rabini et al., 2023). In our second study, we employed CPM to identify functional connections that predict variability in hand motor behavior, revealing a reproducible set of connections we defined as the “Core Hand Motor

Network." This network reliably predicted performance across multiple behavioral variables, including measures of both dexterity and strength, for the left and right hands. To further characterize its generalizability, we tested whether its predictive power reflected task-specific features or more general aspects of motor function, using cross-decoding analyses and validating the model on an independent dataset (Study 1).

A key advantage of this approach lies in its feasibility: resting-state fMRI offers a simple, task-free method to investigate the intrinsic organization of the motor system. If successful, this framework could provide a valuable tool to study motor function even in populations unable to perform specific tasks. Importantly, we leveraged this advantage to evaluate the functional relevance of the identified network by examining whether TMS-induced perturbation of motor-relevant areas would alter prediction accuracy. To our knowledge, this represents the first attempt to combine resting-state functional connectivity with TMS in a predictive modeling framework—allowing us to assess not only the correlational structure of the hand motor network but also its causal role in supporting flexible motor behavior.

2 Chapter 2: Investigating resting-state functional connectivity of the human hand motor system: an offline TMS-fMRI study

This chapter has been published. Pierotti, E., Speranza, C., Cattaneo, L., & Turella, L. (2025). Investigating resting-state functional connectivity of the human hand motor system: an offline TMS-fMRI study. NeuroImage, 121254. https://doi.org/10.1016/j.neuroimage.2025.121254

2.1 Abstract

Skillful hand motor control engages complex interactions within a widespread brain network. Previous studies in non-human primates provided a precise picture of its connectivity profiles. Yet, whether the human hand motor network shows a similar connectivity fingerprint is still unclear. Our aim was to better characterize its functional connectivity profiles.

We combined offline Transcranial Magnetic Stimulation (TMS) with resting-state functional magnetic resonance imaging (RS-fMRI) to map the changes in functional connectivity following the stimulation of a key node in this network, the human Anterior Intraparietal area (hAIP). Participants underwent two sessions of RS-fMRI before and after offline TMS, applied with a Continuous Theta-Burst Stimulation (cTBS) protocol.

Univariate and multivariate analyses of RS-fMRI connectivity were performed. Univariate results showed that RS connectivity profiles within the hand motor network changed after cTBS to hAIP. Namely, we found increased functional connectivity between hAIP and SMA, and between SMA and M1. In multivariate analysis, we adopted a classifier to distinguish between RS-connectivity before and after cTBS. We showed significant decoding within a wide brain network comprising regions of the fronto-parietal motor pathways, of the ventral stream and within the cerebellum.

Overall, our data provided novel insights on the connectivity patterns of the human hand motor network which compared favorably to the brain architecture described in monkeys, but with some species-specific features, advocating a similar crucial role of this network for hand action processing also in our species.

2.2 Introduction

Skillful hand motor control engages complex interactions within an extensive network of brain regions spanning frontal, parietal and temporal cortices. Most of our knowledge on the connections between these regions derived from previous non-human primate anatomical research. Still, much less is known regarding the connectivity fingerprints of the human hand motor system. Our aim was to better characterize these connectivity profiles. We applied focal TMS to the human Anterior Intraparietal area (hAIP) to induce a transient change in neural activity of the stimulated region, with the hypothesis that brain regions functionally-connected to this parietal hub would show activity changes. This "perturb and measure" approach (Paus, 2005) is commonly used in the definition of brain networks, seeding from the stimulation site (Arfeller et al., 2013; Siebner et al., 2009). To this end, we adopted a multimodal approach, combining resting state functional Magnetic Resonance Imaging (RS-fMRI) with offline Transcranial Magnetic Stimulation (TMS). We stimulated a central region within this network – the hAIP – and described the associated modifications in RS functional connectivity within this network.

Extensive research on non-human primates provided evidence for the existence of - at least - two parieto-frontal pathways within the dorsal stream associated with upper-limb motor control (Binkofski & Buxbaum, 2013; Galletti & Fattori, 2018; Rizzolatti et al., 1998; Rizzolatti & Matelli, 2003; Turella & Lingnau, 2014): the dorsomedial and the dorsolateral pathway.

The dorsomedial pathway has been traditionally associated with sensorimotor transformations for space-oriented arm behavior, such as visuomotor control of reaching movements towards objects in the environment (Rizzolatti et al., 2014; Rizzolatti & Matelli, 2003; Tanné-Gariépy et al., 2002; Turella & Lingnau, 2014). This pathway connects regions within the superior parietal lobe (SPL) with the dorsal premotor cortex (dPM or F2 in monkeys).

The dorsolateral pathway has been associated with the transformation of visual information of object properties into an appropriate hand configuration for interacting with the environment, such as during grasping and dexterous manipulation of objects (Jeannerod et al., 1995; Rizzolatti et al., 1998, 2014; Rizzolatti & Matelli, 2003; Tanné-Gariépy et al., 2002). This pathway comprises regions of the anterior inferior parietal lobe (IPL) – anterior intraparietal (AIP) area and area PFG - which project toward the ventral premotor cortex (vPM or area F5 in macaque monkeys).

Research on non-human primates provided further evidence for the role of this inferior parietal hub - AIP and PFG - in a wider system for the control of hand actions, the so-called "lateral grasping

network" (Borra et al., 2017). As shown by anatomical tracer studies in non-human primates (for AIP see Borra et al., 2008; Lanzilotto et al., 2019; for PFG see Rozzi et al., 2006), this parietal hub has a much richer connectivity fingerprints, as it is not only connected with vPM (area F5), but also with regions of the ventral stream, of the ventrolateral prefrontal cortex and with the secondary somatosensory cortex (SII). Single cell recordings showed that all these regions are involved in the encoding of distinct aspects of skilled performance of hand actions (Borra et al., 2017; Borra & Luppino, 2019; Rizzolatti et al., 2014).

This parietal hub does not only represent a gateway for information transfer from the ventral stream to the dorsal stream (Borra et al., 2017; Rozzi et al., 2006), but its connections with parietal regions of the dorsomedial pathway (SPL–dPM circuit) suggest that it might also be a crucial communication hub across different pathways within the dorsal stream. The recent description of grasping-related activity also in the dorsomedial pathway (Fattori et al., 2017) support a revision of the role of this SPL–dPM circuit which might be particular important for the performance and online control of reach-to-grasp actions – particularly under temporal constraints (Fattori et al., 2017). The anatomical connections between the lateral grasping network and the dorsomedial pathway might provide the basis for the neural interactions between these two pathways which together might be flexibly adopted to coordinate complex hand interactions with the environment depending on behavioral goals, task requirements and external constraints (Galletti & Fattori, 2018).

Recent non-invasive neuroimaging evidence in non-human primates (Greulich et al., 2020; Howells et al., 2020) further showed that the organization of the anatomical connections of the "lateral grasping" network have also a functional significance, as hinted by tract-tracing studies. Indeed, RS-fMRI connectivity analysis showed a positive coupling between anatomically defined regions of this network. In particular, the two regions within this inferior parietal hub – AIP and PFG – showed a widespread patterns of connectivity with frontal, parietal and temporal cortices (Greulich et al., 2020; Howells et al., 2020). In agreement with previous anatomical studies, RS connectivity delineated a significant positive interplay with other regions of the premotor cortex, the dorsomedial pathway, the ventral stream, the lateral prefrontal cortex, the primary (SI) and secondary somatosensory cortex (SII). Overall, the functional connectivity profiles of these regions suggest that they are part of a functional network which shows a strong coupling even "at rest".

In human, a putative lateral grasping network - including an homologue parietal hub - has been proposed to exist (Borra et al., 2017; Errante et al., 2021; Jeannerod et al., 1995; Turella & Lingnau, 2014). Neuroimaging studies established a possible homology between regions of the macaque brain

- AIP, PFG - with human regions within the anterior intraparietal sulcus and of the supramarginal gyrus based on similar anatomical location and functional properties (Culham & Valyear, 2006; Gallivan & Culham, 2015; Grefkes & Fink, 2005). Our research focused on this hAIP.

Univariate fMRI studies showed the consistent engagement of this parietal hub during the performance of hand actions and particularly during grasping (Culham et al., 2006; Culham & Valyear, 2006; Grafton, 2010; Turella & Lingnau, 2014; Vesia & Crawford, 2012). More recently, MVPA studies showed the representation of different aspects of hand movements within this area (Gallivan & Culham, 2015), such as effector (Gallivan, McLean, et al., 2013), action type (Gallivan, McLean, Valyear, et al., 2011; Gallivan, McLean, et al., 2013; Malfatti & Turella, 2021; Monaco et al., 2019, 2020; Turella et al., 2020) and actions across effectors (Gallivan, McLean, et al., 2013; Turella et al., 2020) or tasks (Monaco et al., 2020).

Nevertheless, even if the functional specificity of the hAIP in the control of manual movement has been firmly established, its connectivity fingerprints have not yet been clearly described. With a multimodal approach, we aimed at investigating the functional connectivity fingerprints of the hAIP and at testing whether these connections are similar to the ones described in monkeys. To this end, we collected RS-fMRI before and after offline TMS on the human hAIP. Then, we employed univariate and multivariate analyses to characterize stimulation-induced modifications in RS functional connectivity.

As the hAIP is assumed to be the human homologue of the parietal hub of the lateral grasping network in non-human primates, we expect to describe connectivity fingerprints which are similar to those previously described with anatomical tracing (Borra et al., 2008, 2017; Borra & Luppino, 2019; Rozzi et al., 2006) and neuroimaging studies (Greulich et al., 2020; Howells et al., 2020; Premereur et al., 2015). Mirroring this connectivity architecture described in non-human primates, we expect that the stimulation of the human hAIP will produce effects in homologue areas of the hand motor network including: the lateral grasping network - comprising regions of the dorsolateral pathway, of the ventrolateral prefrontal cortex and of the ventral stream – and the dorsomedial pathway.

2.3 Material and methods

2.3.1 Participants

Thirty-two right-handed subjects participated in this study (21 females, average age = 24 years). Five out of 32 participants were excluded due to excessive motion (max motion between consecutive acquisition > 2 mm). The final sample of the study comprised 27 participants (18 females, average age: 25 years).

Participants had no contraindications for undergoing an MRI investigation and TMS (Rossi et al., 2009, 2011). They provided written informed consent to participate in the study and were reimbursed for their participation. The protocol of this study (N. 2018-015) was approved by the Ethics Committee of Human Research of the University of Trento.

2.3.2 TMS protocol

During the experimental session, we employed continuous theta-burst stimulation (cTBS) protocol (Huang et al., 2005), a repetitive TMS protocol consisting of three pulses at 50 Hz repeated at intervals of 200 milliseconds (600 pulses in total – 40 s). Before the experimental session, each participant underwent a preparatory session outside the MR scanner to define two parameters for the cTBS: the intensity and the site of stimulation.

To define the intensity of the cTBS, we measured the active motor threshold (aMT) for each participant through an electromyography system (EMG). The EMG responses were recorded with a gain of x1000 using Ag-AgCl surface electrodes over the right first dorsal interosseous (FDI) muscle (bipolar montage). Signals were amplified using a CED 1902 amplifier and digitized through a CED 1401 analog/digital converter, with data acquisition performed using CED Signal software (Cambridge Electronic Design, UK). The stimulation was given over the hand motor spot using a hand-held figure of eight coil (75 mm standard coil, MagPro MCF-B65) placed tangentially to the scalp with the handle pointing posteriorly (45° to the midline). The aMT was defined as the intensity required to elicit a motor-evoked potential (MEP) trials from the contralateral FDI while the subject was maintaining a voluntary contraction with an average amplitude of 200 μV across 10, rather than being based on a fixed number of successful responses (for e.g. 5 out of 10).For each participant, we set the intensity of the transcranial stimulation as 80% of the aMT (avg aMT = 28% of maximum stimulator output; average percentage of stimulation = 23% of maximum stimulator output, Huang et al., 2005).

2.3.3 *Site of stimulation*

The target area for each participant was the hAIP within the left hemisphere. This region has been referred to as human AIP or simply AIP in previous TMS studies (Breveglieri et al., 2023; Cohen et al., 2009; Glover et al., 2005; Gutteling et al., 2013; Rice et al., 2006; Taubert et al., 2010; Tunik et al., 2005a, 2008). For consistency, we adopt a similar nomenclature, even if it is difficult to assume that our TMS stimulation might be focused only on AIP as it was identified with neuroimaging (Culham et al., 2006), because it might also partially affect nearby regions. Nevertheless, it is well-accepted that stimulation of this parietal hub led to behavioral modifications associated with different aspects of hand actions (Breveglieri et al., 2023; Cohen et al., 2009; Glover et al., 2005; Gutteling et al., 2013; Rice et al., 2006; Taubert et al., 2010; Tunik et al., 2005a, 2008). Impairment in hand motor control has been also shown with invasive direct electrical stimulation of this parietal hub in patients undergoing awake surgery for tumor removal (Fornia et al., 2022). Moreover, this parietal hub probably comprises also the part of the anterior supramarginal gyrus which has been associated with tool use (Orban & Caruana, 2014).

All participants had individual anatomical images available from previous participation to other experiments. The site of stimulation was identified on individual brain images, guided by macroanataomical landmarks, i.e., the postcentral (PoCS) and the intraparietal (IPS) sulci. We looked for the intersection of the POCS with the IPS, moved 1 cm caudally from the intersection and targeted the lower lip of the IPS. The anatomical variants of the patterns formed by the PoCS and the horizontal segment of the IPS described in Zlatkina & Petrides, (2010) were all taken into consideration to identify the intersection of the two sulci.

Once the cortical target was determined, we used a neuronavigation system (SofTaxic system, software version 3.4, EMS, Italy) to localize the spot on the scalp that corresponded to the aIPS cortical target, which was indicated on the scalp by means of a permanent marker. This procedure was performed outside the MR facilities. The scalp mark was then used in the MR rooms to position the coil and perform cTBS. Post-hoc quantification of the cortical target localization at the group level indicated the mean coordinates in MNI space of: x= -52 ± 6, y= -43 ± 5, z= 57 ± 4. The coordinates of the stimulated sites for each participant are reported in Table 2.1 (for a graphical representation of their position see Figure 2.1).

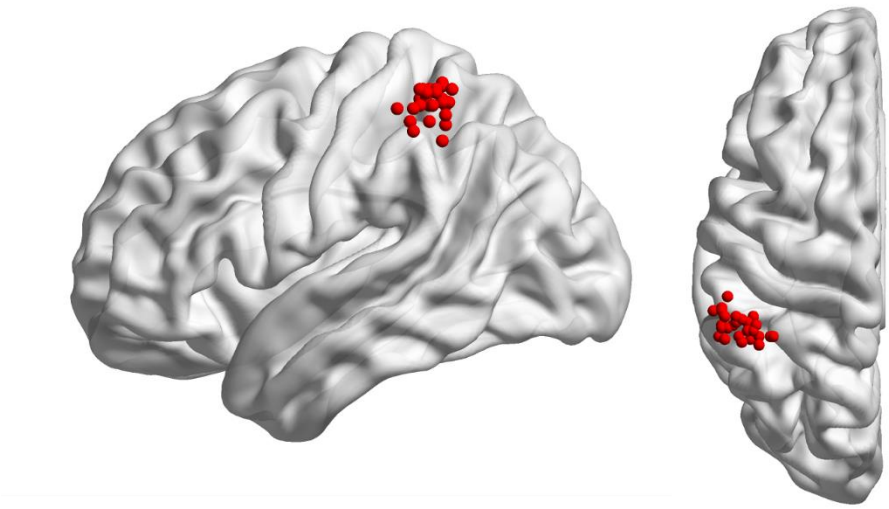

Figure 2.1. Position of the hAIP across participants. The image shows the graphical distribution of the MNI coordinates of the stimulated site, hAIP, for each individual participant included in the analysis (red spheres). The figure was created using BrainNet Viewer (Xia et al., 2013).

MNI COORDINATES	*X*	*Y*	*Z*
	-59	-46	45
	-46	-42	61
	-52	-46	57
	-47	-44	61
	-58	-36	51
	-46	-47	50
	-53	-41	60
	-56	*-43*	*56*
	-40	-46	63
	-45	-49	61
	-58	-42	51
	-53	-39	61
	-45	-46	58
	-49	-41	59
	-56	-32	55
	-47	-39	58
	-54	-42	56
	-48	-47	56
	-57	-47	53
	-58	-37	55
	-41	-46	62
	-49	-44	60
	-57	-39	56
	-58	-43	56
	-51	-40	61
	-51	-48	57
	-61	-37	48
MEAN	-52	-43	57
STANDARD DEVATION	± 6	± 5	±4

Table 2.1. MNI coordinates of the stimulation site, hAIP, for each participant

2.3.4 *Experimental procedure*

The experimental session was carried out on the same day and with a fixed order of stimulation for all the participants (for an overview of the timeline of the main experimental session, see Figure 2.2). For each participant, a total of four RS- fMRI acquisitions were performed (see Figure 2.2).

The experimental session started with a sham cTBS performed outside the scanner. Sham cTBS was delivered with a MagPro X100 stimulator (MagVenture Inc.) connected to a figure-of-eight "placebo" TMS coil (MagPro MCF-P-B65, 75 mm diameter). This placebo coil is visually identical to the "real" TMS coil (MagPro MCF-B65) and it can reproduce the same physical sensation and same noise but without producing any magnetic field stimulation. The cTBS was delivered with the coil positioned perpendicular to the left hAIP (orientation 60° to the midline) on the subject-specific scalp location identified during the preparatory session. The stimulation occurred with participants lying on an MRI-compatible stretcher, so that participant could be moved quickly within the MR scanner room with the stretcher.

Then, the participant was positioned within the MR scanner and underwent two RS-fMRI runs (post-SHAM in Figure 2.2). The average time between the end of the sham cTBS protocol and the start of the fMRI acquisition was 5:53 minutes. During the RS-fMRI runs, participants were requested to fixate a cross projected on a screen visible through a mirror while lying into the MR scanner. The duration of each RS-fMRI run was 10 minutes.

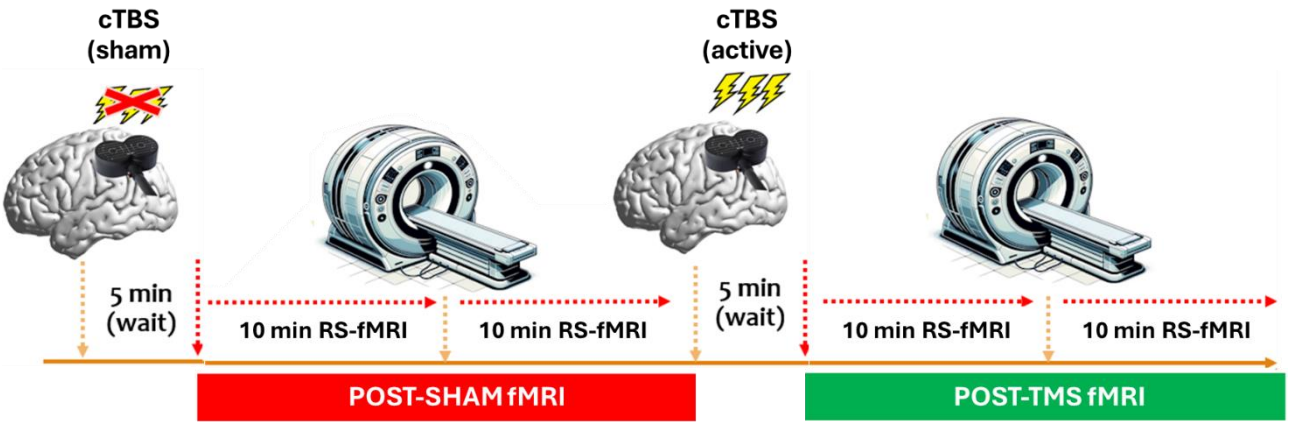

Figure 2.2. Timeline of the main experimental session. The experimental session was carried out on the same day and with a fixed order of stimulation for all the participants. Each session started with a sham stimulation. After around 5 minutes, the fMRI scanning session started. Participants underwent two 10-min session of RS-fMRI (post-SHAM fMRI – red panel). Then, the participant was moved outside the MR scanner and cTBS was delivered on the hAIP. Following cTBS stimulation, the subject was repositioned inside the MR scanner and underwent two runs of RS-fMRI (post-TMS fMRI – green panel).

After the two post-SHAM RS-fMRI runs (Figure 2.2), the participant was moved out of the MR scanner. Then, the "active" cTBS was delivered using a "real" TMS coil (MagPro MCF-B65, 75 mm diameter). The same procedure described for the sham cTBS was adopted here. After the "active" cTBS stimulation, participants were moved within the MR scanner room using the MR-compatible stretcher, repositioned inside the scanner and performed the two post-TMS RS-fMRI runs (duration 10 minutes each). The average time for the move after the stimulation was 5:09 minutes. As cTBS effect seems to be stable only after 5 minutes (Huang et al., 2005; 2007), we decided to have an approximate delay of 5 minutes for taking the participant inside the scanner with the stretcher after stimulation.

The original description of the effect of cTBS on human M1 showed that it lasts 1 hour (Huang et al., 2005; 2007) which is longer than the time we required to acquire our RS data. In addition, recent finding showed that the effect of cTBS on macaque monkey parietal cortex (area PFG) is evident at the single neuron level (Romero et al., 2022). This study showed long-lasting cTBS-induced changes in neuronal excitability already after 10 minutes, peaking around 30-40 minutes after stimulation and lasting even after 1 hour (Romero et al., 2022). This evidence suggest that the timeline of our experimental approach should be able to capture cTBS-induced modifications.

2.3.5 MRI data acquisition

MRI data were acquired with a 3 Tesla MR scanner (MAGNETOM Prisma, Siemens Healthcare, Erlangen, Germany) equipped with a 64-channel head-coil. We acquired a total of four RS-fMRI runs for each participant, two after SHAM and two after cTBS, with a full coverage of the brain and of the cerebellum (TR = 1 s, TE= 28 ms, FA = 59 degree; 66 slices; 3 mm isotropic voxels, 600 volumes, duration: 10 minutes). In addition, gradient echo fieldmap sequences (TR = 4810ms; TEs=4.92, 7.38 ms; 3 mm isotropic voxels) were acquired to control for geometric distortions during the preprocessing. Finally, a high quality structural T1-weighted multi-echo (TR=2.5 s; TEs=1.69, 3.55, 5.41, 7.27 ms, 1 mm isotropic voxels] was also acquired.

2.3.6 MRI data preprocessing

MRI data was preprocessed using SPM12 (https://www.fil.ion.ucl.ac.uk/spm/software/spm12/). We applied slice-timing correction and head motion correction to functional data. Then, we employed gradient echo fieldmap sequences to perform distortion correction and we realigned the functional

data. T1-weighted anatomical image was co-registered with the mean image of the functional data estimated after the realignment procedure. Segmentation of the anatomical image was performed with CAT12 toolbox (https://neuro-jena.github.io/cat/). With this procedure, we extracted individual grey, white matter, and cerebrospinal fluid (CSF) maps employed in the connectivity analysis and the forward deformation field adopted for the normalization of the anatomical image to MNI space. The resulting normalization parameters were also applied to the functional images.

Functional connectivity analysis was performed on preprocessed MRI images adopting the CONN Toolbox (Whitfield-Gabrieli & Nieto-Castanon, 2012). We applied the default denoising pipeline (CompCor function on CONN), performing bandpass filtering (0.008-0.09 Hz) and including white, grey matter, and CSF time series and the six-motion parameters as regressors of no interest.

2.3.7 Regions of interest (ROIs) selection and univariate RS functional connectivity analysis

RS-connectivity has been shown to be reliably adopted to identify motor networks (Kristo et al., 2014). We adopted univariate analysis to quantify changes in RS functional connectivity induced by offline cTBS on the hAIP. To this end, we focused on eight cortical regions which are known to be involved in representing different aspects of hand movements during planning and execution (Gallivan & Culham, 2015; Sakreida et al., 2016) in line with previous human fMRI studies (Gallivan, McLean, Valyear, et al., 2011; Gallivan, McLean, et al., 2013; Malfatti & Turella, 2021; Monaco et al., 2019, 2020; Turella et al., 2020). Figure 2.3 shows a representation of the position of the selected ROIs from different perspectives rendered on a template brain in MNI space.

In addition to the hAIP (red sphere in Figure 2.3), the selected ROIs were the following (blue spheres in Figure 2.3): the primary motor cortex (M1), the supplementary motor area (SMA), the dorsal premotor cortex (dPM), the ventral premotor cortex (vPM), the posterior superior parietal lobe (SPL), the superior parietal-occipital cortex (SPOC) and the posterior middle temporal gyrus (pMTG).

For all the selected ROIs, we considered a sphere with a radius of 9 mm. For the hAIP, the spherical ROI was centered on the average MNI coordinates of the stimulated point across all the participants (see Table 2.1).

To define the position of the other ROIs, we started from the MNI coordinates of previous fMRI studies on hand movements (Gallivan, McLean, Valyear, et al., 2011; Gallivan, McLean, et al., 2013; Malfatti & Turella, 2021; Monaco et al., 2019, 2020; Turella et al., 2020), which served as a starting point to anatomically and functionally localize these regions. Then, the final selection of coordinates

was based on a metanalytical map associated with studies involving “hand movements” obtained from the Neurosynth platform (https://neurosynth.org/analyses/terms/hand%20movements/). From our starting MNI coordinates, we selected the nearest local maxima from this metanalytical map for each of our ROI. In other words, we selected the anatomical position in each ROI which is more likely to be activated during hand movements as measured with fMRI. This point was the center of our spherical ROI. The MNI coordinates of each ROI are reported in Table 2.2.

We extracted functional connectivity measures calculated as the correlation coefficients (Fisher's z-transformed) between the time-courses of each pair of ROIs.

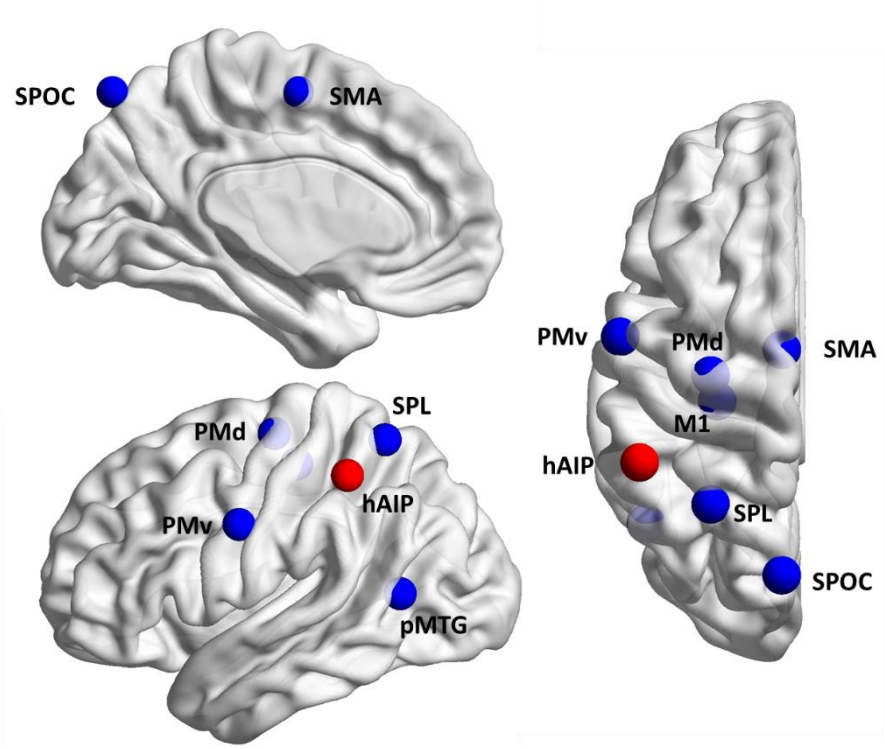

Figure 2.3. Position of the ROIs. Visual representation of the 8 ROIs considered for the univariate functional connectivity analysis. We presented the selected ROIs as blue spheres. The stimulated region, hAIP, is represented as a red sphere. We adopted transparency and three different perspectives to provide a clear overview of their position. The figure was created using BrainNet Viewer (Xia et al., 2013). Abbreviations: dPM = dorsal premotor cortex; vPM = ventral premotor cortex; SPL = superior parietal lobe; SPOC = superior parieto-occipital cortex; M1 = primary motor cortex; SMA = supplementary motor area; pMTG = posterior middle temporal gyrus; hAIP

ROI	*X*	*Y*	*Z*
M1	-28	-24	54
SMA	-8	-8	56
dPM	-30	-16	66
vPM	-58	4	40
SPL	-30	-56	64
SPOC	-8	-78	56
hAIP	-52	-43	57
pMTG	-50	-62	12

Table 2.2. MNI coordinates of the ROIs included in the univariate analysis. Abbreviations: dPM = dorsal premotor cortex; vPM = ventral premotor cortex; SPL = superior parietal lobe; SPOC = superior parieto-occipital cortex; M1 = primary motor cortex; SMA = supplementary motor area; pMTG = posterior middle temporal gyrus. hAIP was selected as the average stimulation site across participants.

To describe the functional connectivity associated with our network of ROIs at the group level, we extracted their connectivity separately for the post-SHAM runs (t-contrast: [post-SHAM run 1 + post-SHAM run 2]) and for the post-TMS runs (t-contrast: [post-TMS run 1 + post-TMS run 2]). This analysis provides a description of the possible interplay between the selected ROIs at rest.

To investigate TMS-induced functional connectivity modifications at the group level, we tested differences in RS functional connectivity comparing post-TMS against post-SHAM values for each connection between the ROIs. We focused on the main effect of TMS (t-contrast: [post-TMS run 1 + post-TMS run 2] – [post-SHAM run 1 + post-SHAM run 2]). All the reported p-values for the ROI analyses are corrected for multiple comparisons adopting false discovery rate (FDR) correction at the connection level (two tailed, $q<0.05$, Zalesky et al., 2010).

To further explore possible temporal effects, we also tested the comparison between the two post-TMS RS-fMRI runs (two tailed, $p<0.05$ uncorrected).

2.3.8 Functional connectivity MVPA

To further investigate the connectivity of the hAIP, we adapted the classical MVPA– which normally adopts activity patterns from task-based fMRI studies – so that it could be applied to RS-connectivity data. To perform MVPA, we adopted the CoSMoMVPA Toolbox (Oosterhof et al., 2016).

The general framework of our MVPA was the following. We started from the whole brain connectivity of the stimulated site (the left hAIP) and adopted a searchlight approach, i.e., for every voxel of the brain we tested the connectivity data extracted from a spherical ROI ("searchlight") centered on that voxel. Within each searchlight, we tested if a classifier could distinguish between post-SHAM and post-TMS using the pattern of connectivity of the searchlight (i.e., connectivity between this region and the hAIP) as features for the classifier.

The rationale for this analysis was to test whether TMS influences the connectivity between the hAIP and any other region within the brain. If this is the case, the connectivity pattern of this part of the brain should also be modified and this modification might be adopted to distinguish between connectivity before and after cTBS. We expect that this modification should be evident in regions anatomically and/or functionally connected to the hAIP.

In detail, our analytical approach is described below. During the experimental session, we acquired two functional runs before and after the "active" cTBS for each participant. To have a higher number of samples for our multivariate classification approach, we considered four "mini" runs (duration: 2.5 minutes) within each of our RS runs (duration: 10 minutes), obtaining a total of sixteen "mini" runs for each participant (eight after SHAM and eight after TMS). For each of the sixteen "mini" runs, we extracted the whole-brain connectivity maps from the stimulated point (left hAIP) to all the voxels in the brain. We did not apply any spatial smoothing to these connectivity maps.

For each participant, we employed a searchlight approach (radius 6 mm) on these whole brain connectivity maps. For each searchlight, we adopted a classifier (Support Vector Machine – SVM) to distinguish between post-SHAM and post-TMS data using a leave-one-out "mini" run cross-validation procedure, i.e., training the classifier on 14 connectivity datasets (7 post-SHAM and 7 post-TMS) and testing the classifier on the remaining 2 connectivity datasets (1 post-SHAM and 1 post-TMS) in each cross-validation fold. The decoding accuracy of the classifier was assigned at the central voxel of each searchlight. Then, we applied smoothing (3 mm FWHM) on the decoding accuracy maps. Finally, we tested for above-chance decoding (50 %) at the group level using a one-sample t-test ($p<0.001$ uncorrected at the voxel level and $p<0.05$ FWE-corrected at the cluster level).

2.4 Results

2.4.1 Univariate functional connectivity ROI analysis

The significant connectivity profiles of our network of ROIs for the post-SHAM and post-TMS runs are shown in Figure 2.4A and Figure 2.4B ($q < 0.05$ FDR-corrected). The general organization of the connectivity profiles was very similar between the two phases of our study. There was a strong positive coupling between most of the selected ROIs which support the idea that they are part of a functional network which is strongly correlated even at rest.

The significant functional connectivity differences between post-TMS versus post-SHAM are presented in Figure 2.4B ($q < 0.05$ FDR-corrected). There were two connections which showed a difference between the two phases of our experimental session and both connections showed an enhanced coupling after cTBS. The first effect was evident between the hAIP (i.e., the target site) and the left SMA ($t_{26} = 3.68$, $q < 0.05$ FDR-corrected). The second effect was evident between the left SMA and the left M1 ($t_{26} = 3.70$, $q < 0.05$ FDR-corrected).

We could find a significant effect comparing post-TMS run 2 vs post-TMS run 1 showing hyperconnectivity between hAIP and vPM, but the effect did not survive multiple comparison correction ($t_{26} = 2.40$, p=0.023 uncorrected). The direction of this effect suggests that the effect of cTBS on hAIP might take time to reach its maximal effect. This seems to be in line with the recent macaque monkey study (Romero et al., 2022) on the effect of cTBS on parietal cortex (area PFG) which showed that cTBS-induced changes in neuronal excitability evolves in time reaching the peak of the effect around 30-40 minutes after stimulation.

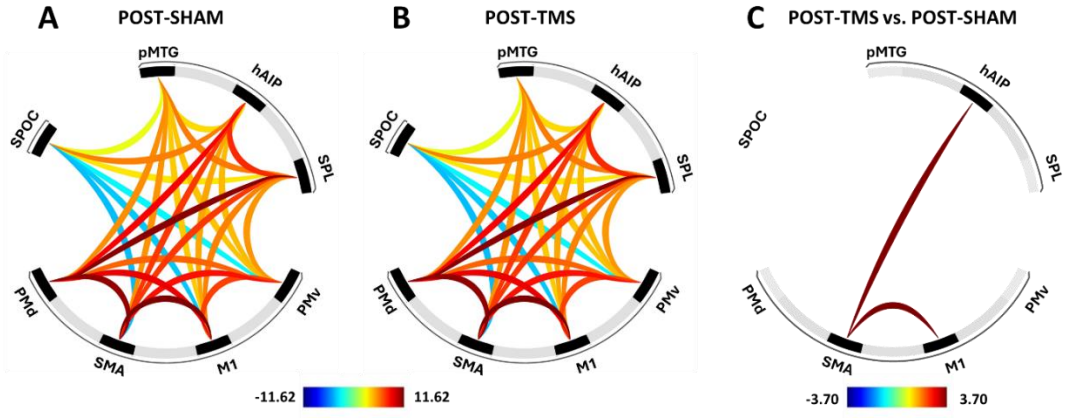

Figure 2.4. Univariate functional connectivity results. A. ROI analysis for post-SHAM effect. The significant connections with respect to baseline are represented in the circular plot (q< 0.05 FDR-corrected). **B. ROI analysis for post-TMS effect.** The significant connections with respect to baseline are represented in the circular plot (q< 0.05 FDR-corrected). **C. Differences in functional connectivity between post-TMS vs. post-SHAM.** The significant connections are represented in the circular plot (q< 0.05 FDR-corrected). The color of the lines represents the t-value for the significance of the connection tested at the group level. Abbreviations: dPM = dorsal premotor cortex; vPM = ventral premotor cortex; SPL = superior parietal lobe; SPOC = superior parieto-occipital cortex; M1 = primary motor cortex; SMA = supplementary motor area; pMTG = posterior middle temporal gyrus; hAIP = human Anterior Intraparietal area.

2.4.2 Functional connectivity MVPA

The results of our searchlight showed a widespread network of regions showing significant decoding when comparing their patterns of connectivity post-SHAM vs. post-TMS (Figure 2.5). In other words, MVPA allowed us to identify a network of regions which seems to be functionally connected with the hAIP, as they showed a modification in their connectivity with the left hAIP following cTBS. With respect to our original expectations, we identified a network of regions with MVPA comprised cortical areas which resemble the functional architecture of the connection of the possible homologue inferior parietal hub described in monkeys.

First, we could identify many functionally connected regions comprising a possible human homologue of the lateral grasping network - including the dorsolateral pathway (bilateral hAIP, IPL and left vPM), left SII, the ventral stream (the temporo-occipital cortex) and the ventrolateral prefrontal cortex - and the dorsomedial pathway (SPL, SPOC). In detail, the regions identified in this analysis were the following.

In the frontal cortex, significant decoding was evident bilaterally within the ventrolateral prefrontal cortex and the middle frontal gyrus. There were also significant clusters within the left medial prefrontal cortex, left precentral gyrus, left superior frontal gyrus.

In the parietal cortex, there was significant decoding bilaterally within the inferior parietal lobule and within the anterior intraparietal sulcus. In the left hemisphere there was also significant decoding within the superior parietal lobule, the parietal operculum and the postcentral gyrus.

In the temporal lobe there was significant decoding within the bilateral inferior temporal cortex and within several smaller clusters of the superior temporal gyrus.

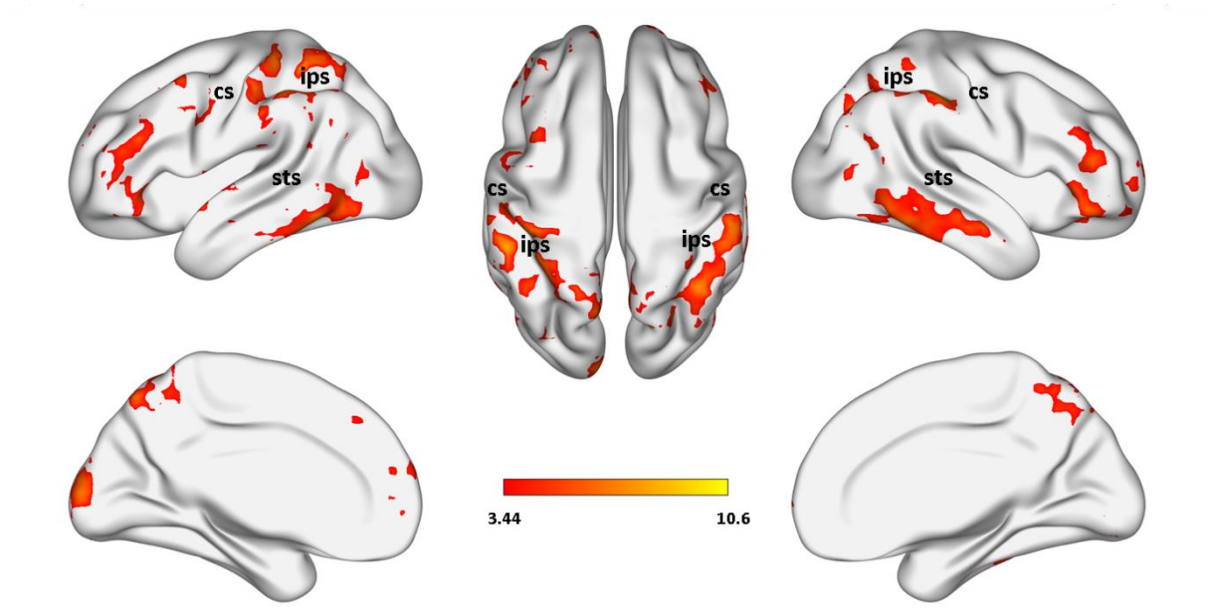

Figure 2.5. Functional connectivity MVPA searchlight results. MVPA searchlight (radius 6 mm) was performed on the unsmoothed accuracy maps. We tested if a classifier could distinguish between post-SHAM and post-TMS using the pattern of connectivity of the searchlight as features for the classifier. Then, we tested for significance on smoothed decoding accuracy maps (3 mm FWHM) at the group level (one-sample t-test against chance, 50 %). Significant decoding is presented on an MNI template ($p<0.001$ uncorrected at the voxel level and $p<0.05$ FWE-corrected at the cluster level). Colorbar represents the t-value for the one-sample t-test. The figure was created using BrainNet Viewer (Xia et al., 2013). Abbreviations: cs, central sulcus; ips, intraparietal sulcus; sts, superior temporal sulcus.

In addition to the effects in cortical regions, we showed also significant decoding in the cerebellum, with a greater extent in the right hemisphere. Indeed, we identified significant clusters within the right cerebellum (Lobule VI, VIIB, VIIIA, VIIIB) and bilaterally in Crus I and Crus II (see Figure 2.6A).

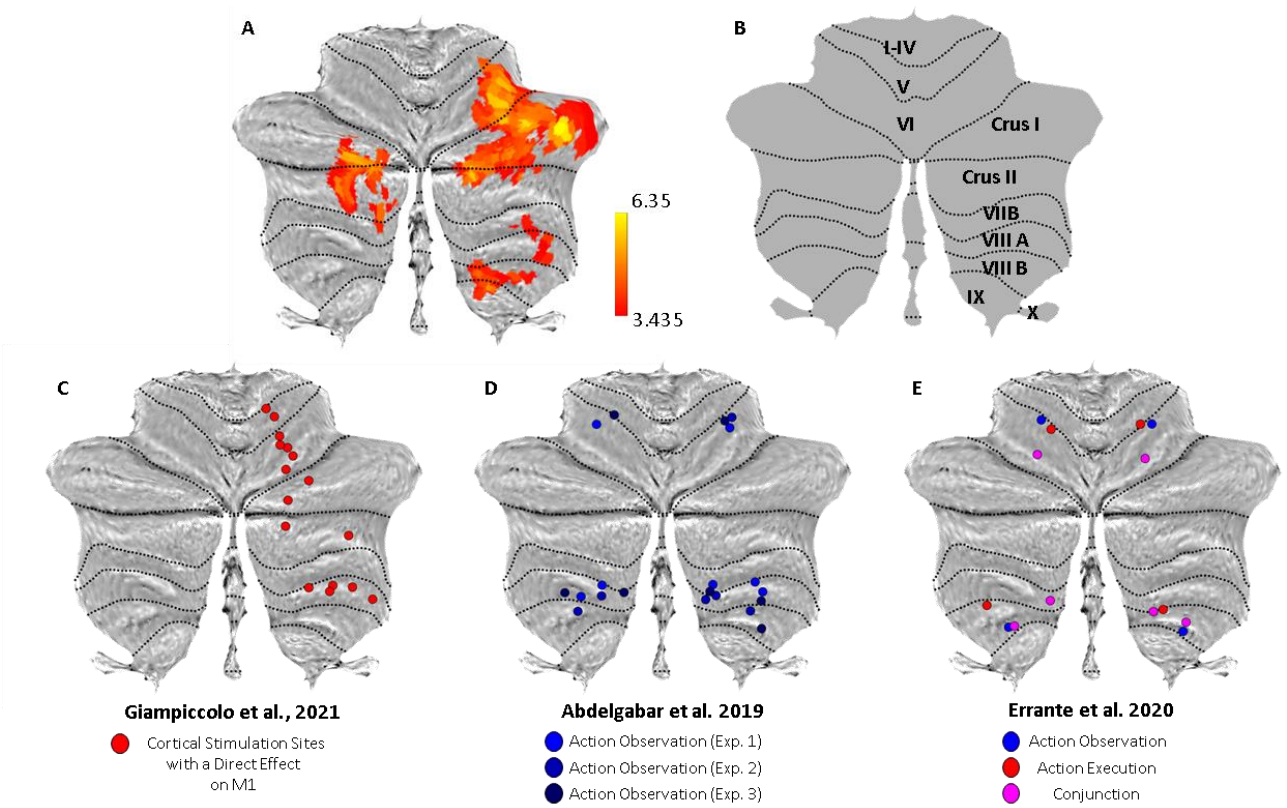

Figure 2.6. Cerebellar results. **A. MVPA connectivity**. MVPA searchlight (radius 6 mm) was performed on unsmoothed data. We performed smoothing (3 mm) on decoding accuracy maps before testing for significance (one-sample t-test against chance, 50 %). Significant decoding accuracy at the group level is presented on an MNI template using the SUIT toolbox (Diedrichsen, 2006; Diedrichsen & Zotow, 2015). **B. Anatomical position of the cerebellar lobules on the cerebellar flatmap. C. Stimulation sites within the cerebellum for the study by Giampiccolo et al., (2021). D. Peaks of activation within the cerebellum for the study by Abdelgabar et al., (2019). E. Peaks of activation within the cerebellum for the study by Errante & Fogassi, (2020).**

2.5 Discussion

We adopted a multimodal approach to describe the functional connectome of the human hand motor network. To this end, we combined RS-fMRI and offline TMS to map connectivity modulations following stimulation of a pivotal parietal hub within the network, i.e., the hAIP. Our findings provided two novel insights into the functional connectivity architecture of this network.

First, univariate approach showed that most of the selected ROIs showed a strong positive coupling even at rest. In addition, we demonstrated that cTBS over hAIP enhanced connectivity between the left hAIP and the left SMA, and between the left SMA and the left M1.

Second, MVPA showed a widespread network of areas functionally connected with the hAIP which included: inferior temporal regions, superior and inferior parietal areas, premotor and prefrontal cortices. This network of regions resembles the connectivity architecture described in anatomical studies in macaque monkeys. In addition, this analysis highlighted connectivity modifications also in the primary somatosensory cortex (SI) and the cerebellum.

In the next sections, we will discuss the implications of our description of the functional connectome of the human hand motor network.

2.5.1 Univariate analysis: functional connectivity modifications associated with TMS

The first finding stemming from our univariate ROI analysis was that most of the selected ROIs have a strong positive coupling even at rest. This description supports the existence of a large-scale brain network – comprising functionally connected frontal, parietal and temporal cortical areas - which emerge even if participants are not engaged in any explicit motor task. Similar positive interplay between putative homologue regions associated with skilled hand behavior was evident also in RS-fMRI in macaque monkeys (Greulich et al., 2020; Howells et al., 2020). Our data showed the feasibility of defining a similar hand motor network also in the human brain, supporting the possibility of adopting RS-fMRI to characterize homologies and differences of the hand motor networks between the two species using non-invasive neuroimaging data.

The second finding was that cTBS over the left hAIP produces an increase in RS-fMRI connectivity between: a) the stimulated point and the left SMA and b) between the left SMA and the left M1. Modifications in connectivity of the SMA were not completely expected as this was not in line with the anatomical tracer studies in non-human primates which represented the starting point of the predictions of this human investigation.

In macaque, direct connections between the arm-related area of SMA (F3) and the whole parietal cortex seems to be very limited, accounting for less than 5 % of the total connections of this region (Luppino et al., 1993). In addition, tract-tracing studies targeting the parietal regions of the lateral grasping network identified no connections (AIP) or very sparse connections (PFG) between these regions and the SMA (Borra et al., 2008; Lanzilotto et al., 2019; Rozzi et al., 2006).

How can we reconcile the modifications in functional connectivity induced by our stimulation of the hAIP with the known anatomical connectivity of the SMA?

Our predictions were based on tracer studies which characterized monosynaptic anatomical connectivity. Yet, functional connectivity measured with RS-fMRI is only partially associated with anatomical connectivity, as it can reflect both polysynaptic and monosynaptic connections.

A first interpretation might be that our analysis highlighted a uniquely human system, linking regions within the hand motor network with different functional roles, i.e., a stimulus-dependent hub (hAIP) with a volition-dependent region (i.e., SMA). This intriguing possibility should be further tested in future research. Another interpretation might be that this modification in connectivity might be mediated by other regions directly connected with the hAIP and SMA (e.g., SII), which we didn't include in our a priori ROIs. An alternative - or complementary - possibility might be that one or more ROIs (e.g. vPM) directly connected to hAIP and SMA might only – or also – mediate this effect (Volz et al., 2015). Classical univariate approach might not be sufficiently sensible to identify modifications in their connectivity due to the higher variability in the anatomical and functional position of these regions. Indeed, the results of our MVPA analysis could point towards regions (e.g., vPM) which might mediate these modifications (see next section). At this stage, it is difficult to directly compare classical univariate analysis and our novel MVPA, as they seem to capture different aspects of brain connectivity.

Nevertheless, irrespective of its origin, the increased connectivity of the SMA (with the hAIP and M1) is not surprising, as the SMA is an important node in the cortical network involved in skilled upper-limb motor control. In humans, many fMRI studies showed the recruitment of this region in motor tasks involving hand movements (Cavina-Pratesi et al., 2010; Fabbri et al., 2014; Filimon et al., 2007) and this consistent engagement has been shown also in a recent metanalysis on reaching and grasping movements (Sartin et al., 2023).

Overall, our data showed that hAIP stimulation-induced modifications in the connectivity of two crucial nodes of the hand motor network, i.e., SMA and M1. Still, the nature of this cTBS-induced enhancement in connectivity is not clear and additional research is needed to fully address its

functional meaning. In the next sections, we will focus on evidence stemming from our MVPA approach which seems to provide complementary insights on the connectivity architecture of the hand motor network.

2.5.2 MVPA of connectivity within the putative human lateral grasping network

The results of our MPVA searchlight showed a widespread network of regions where connectivity with the hAIP was modified after cTBS. Several of these effects were stronger - or only present - in the left hemisphere, as expected as the target site of TMS - hAIP - was in the same hemisphere.

Following our predictions based on anatomical tracer studies (Borra et al., 2017), we described modifications within a putative network of regions - hAIP, vPM, SII, temporal and ventrolateral prefrontal regions - in line with the known connectivity of the macaque "lateral grasping network".

The first expected result was the identification of modifications within the dorsolateral pathway, the parieto-frontal circuit connecting the anterior IPL with vPM. Indeed, significant decoding was evident within the bilateral hAIP - comprising the anterior part of the intraparietal sulcus and the adjacent convexity of the IPL - and the left vPM. These connections are possibly the homologous of the AIP/PFG-F5 circuit present within the macaque brain which has been demonstrated to mediate the visuomotor control and online correction of grasping actions (Borra et al., 2017; Rizzolatti & Matelli, 2003), but also engaged during hand action observation (Rizzolatti & Matelli, 2003).

The second expected finding was the description of significant decoding mainly within the inferior temporal cortex. Research on non-human primates proposed that this parietal hub represents a crucial region mediating the interactions between ventral and dorsal stream (Borra et al., 2008; Borra & Luppino, 2017; Premereur et al., 2015). Similarly, the connectivity between the hAIP and inferotemporal cortex might support the interplay between the hand motor system and areas of the ventral stream involved in object recognition (Borra et al., 2017; Premereur et al., 2015). Through these connections, the hAIP might integrate visual information about the geometry of an object into the appropriate motor command extracted in the dorsal stream with information about the semantic properties (e.g., weight) associated with the identity of the object computed in the ventral stream. In addition, during action planning and control, these connections might allow the dorsal stream to take advantage of the information coming from the ventral stream to anticipate the visual consequences of the movement (Gallivan & Culham, 2015).

Another region which was expected from monkey-tracing studies (Borra et al., 2017) was SII which was evident only within the left hemisphere. Neurophysiological recordings in monkey showed that

SII is engaged in orchestrating hand actions based on haptic information (Ishida et al., 2013, 2024). A similar role for human SII has been recently confirmed. TMS studies support the causal involvement of the SII region in haptic working memory, i.e. maintaining information of object intrinsic features and of hand grasping motor plan in the absence of visual feedback (Cattaneo et al., 2015; Maule et al., 2015).

Finally, we find significant decoding within the ventrolateral prefrontal cortex. This result is also in line with the proposal that AIP-PFG might integrate abstract information relevant to the task, such as behavioral goals, with pragmatic aspect of the actions extracted within this circuit (Borra et al., 2008). Indeed, it has been proposed that selection and implementation of the most suitable hand–object interaction based on environmental constraints cannot only rely on sensorimotor transformations implemented within these parieto-frontal pathways, but this selection might be modulated by top-down modulations from prefrontal regions (Simone et al., 2015).

Overall, our findings are strikingly in line with an extensive corpus of evidence coming from non-human primate data (Borra et al., 2017; Borra & Luppino, 2017, 2019). Our MVPA supports the existence of a putative human lateral grasping network encompassing regions with a similar anatomical position and connectivity profiles, which have been previously shown to be involved in sensorimotor transformations and control of hand actions, also in our species (Borra et al., 2017; Gallivan & Culham, 2015; Turella & Lingnau, 2014).

Besides having strong similarities with the proposed monkey “lateral grasping network”, our results largely mirrored a recent monkey study aiming at directly mapping the connectivity profiles of one of the regions of this parietal hub, i.e., monkey AIP. This study combined intracortical stimulation while simultaneously collecting fMRI data (Premereur et al., 2015). The main finding was that AIP can be divided in: 1) a more anterior part - connected with vPM, SII and other parietal regions (PFG, MIP) - and 2) a more posterior part - connected with different sectors of the posterior intraparietal sulcus (LIP, CIP, PIP), the ventral stream and ventrolateral prefrontal cortex (area 46 and 45B). When considering stimulation-induced modifications for both sectors of AIP in this study (Premereur et al., 2015), our MVPA showed a similar pattern of connectivity involving the recruitment of vPM (monkey F5), of the hAIP (monkey PFG, AIP), of SII together with cortical regions of the ventral stream and of the ventrolateral prefrontal cortex.

With respect to this study (Premereur et al., 2015), our data showed three additional regions which have been previously associated with hand motor behavior. First, even if there are known direct monosynaptic connections between AIP with a core region of the dorsomedial pathway, i.e. V6A

(Gamberini et al., 2009) - the putative homologue of human SPOC (Galletti et al., 2022), this region was not identified in this monkey fMRI study (Premereur et al., 2015). In addition, we could also find TMS-induced modifications in the primary somatosensory cortex (SI) and in the cerebellum. We will further discuss these three findings in the next sections.

2.5.3 MVPA of connectivity within the dorsomedial pathway

Our MVPA connectivity analysis identified significant modifications in connectivity between parietal regions of the dorsomedial pathway, i.e., the convexity of the SPL, the posterior intraparietal cortex and part of the medial SPL, possibly including SPOC. This effect was also expected as the hAIP has been proposed not only to be a crucial region within the "lateral grasping network", which mediate interactions with other regions within the dorsomedial pathway (Borra et al., 2017; Fattori et al., 2017; Galletti & Fattori, 2018).

The dorsomedial pathway (SPL-dPM) has been traditionally associated with visuomotor control of arm-reaching behavior (Turella & Lingnau, 2014), but the discovery of neurons modulated by grasping movements in this pathway (Fattori et al., 2012) has suggested a revision of its role which might encompass the visuomotor control of the whole components of prehension, i.e. reaching-to-grasp actions (Fattori et al., 2017; Galletti & Fattori, 2018). Indeed, neuroimaging showed a recruitment of the dorsomedial pathway for grasping (Gallivan, McLean, et al., 2013; Turella et al., 2020) and TMS studies showed a causal involvement not only for motor features associated with reaching (Breveglieri et al., 2020; Vesia et al., 2010), but also with grasping movements (Breveglieri et al., 2023).

Still, as both pathways encode grasping information, it is not completely clear which might be the specific contribution of these two networks in object-directed hand actions. Based on their functional properties and connectivity profiles, the dorsolateral pathway should be particularly relevant for computing the geometric features of the object and integrating this information with semantic information coming from the ventral stream, whereas the dorsomedial might be more involved in monitoring the ongoing visuomotor transformation necessary for accomplishing reach-to-grasp movements (Fattori et al., 2017; Galletti & Fattori, 2018). In this proposal, the interactions between parieto-frontal motor networks which orchestrates the accomplishment of complex everyday hand-object interactions might be strongly influenced by contextual constrains, so that the same region might be dynamically inhibited or recruited based task requirements (Galletti & Fattori, 2018). Our connectivity data supported the idea that hAIP might be a crucial actor in meditating these interactions given its reciprocal connections with key regions within both pathways.

2.5.4 MVPA of connectivity within the primary somatosensory cortex (SI)

Our MVPA identified significant modifications in connectivity within SI. In macaque monkeys, tracers studies showed that hand area of Brodmann Area (BA) 2 is mainly connected with other subregions in SI (BA 3a, 3b, 1), M1 and to SII (Gharbawie et al., 2011). There seems to be very few direct connections between SI with regions in the anterior posterior parietal cortex, whereas there seems to be stronger connections with regions within the SPL (Gharbawie et al., 2011).

We speculate that the effect in SI might be driven by the direct stimulation of these regions or indirectly through its connections with SPL, SII and/or M1. In any case, the causal role of SI during the manipulation of objects requiring fine finger movements is known. Reversible lesion (i.e. muscimol injection) of SI (BA 2 of hand/fingers) lead to impairment in grasping behavior (Hikosaka et al., 1985). This confirms that SI is directly involved in hand motor behavior.

This possibility has been further supported by recent single cell recordings in non-human primates which provided evidence for rethinking the role of SI (particularly BA 2) as a crucial "active" hub for upper limb motor. A recent neurophysiological study in non-human primates showed that the hand area of SI (BA 3a and 2) seems to encode hand postures during a grasping task, rather than kinematics (Goodman et al., 2019). This data seems to suggest that these neurons track the postures of multi-joint combinations spanning the entire hand across time. As in the same study, also M1 neurons were recorded showing a similar tuning, the authors proposed that this functional organizational similarity might favor the bidirectional communication between SI and M1.

Complementary neuroimaging evidence from human fMRI studies also support a more "active" role of SI in hand motor control. These recent investigations showed the encoding of hand actions (Gale et al., 2021) and also of finger movements (Ariani et al., 2022), not only during the execution of the action itself, but even before - during planning phase of the movement - suggesting that action-related information from other regions of the network might modulate SI activity.

Overall, our connectivity data complement this novel evidence suggesting that the active role of SI in motor control might be mediated by its interplay with other nodes within a wider hand motor network.

2.5.5 *MVPA of connectivity within the cerebellum*

Significant decoding for our MVPA connectivity analysis was localized mainly in the right cerebellum. As we stimulated the left inferior parietal cortex, this right lateralization of the effect could be expected, as it in line with the known cerebellar somatotopic organization which includes two ipsilateral upper-limb/hand representations in similar anatomical positions (Buckner, 2013; Giampiccolo et al., 2021; Manni & Petrosini, 2004). To directly compare our results with this known somatotopic organization, we considered a recent investigation that mapped the spatial organization of hand-related cerebellar regions using intracortical stimulation in patients with cerebellar tumors (Giampiccolo et al., 2021). The layout of the intraoperative stimulation of the cerebellum (in MNI space) showed a distribution compatible with our findings (Figure 2.6C).

Recent neuroimaging studies linked these two cerebellar clusters not only to hand motor functioning, but more in general in the processing of action-related information. For example, a recent investigation focusing on the cerebellum showed a consistent recruitment of similar cerebellar areas during action observation in three independent studies (Abdelgabar et al., 2019). Another study (Errante & Fogassi, 2020) also supports this idea, showing recruitment of similar cerebellar regions both during hand action execution and observation (Figure 2.6E). A conjunction analysis of the activations for these two tasks also showed a similar topographical distribution (Errante & Fogassi, 2020).

In general, our interpretation of MVPA connectivity data seem to also align with a recent characterization of the cerebellum based on functional clustering of fMRI activation patterns obtained in a series of multidomain tasks (King et al., 2019). Our pattern of results is also in line with the recruitment of areas associated with movement of the right hand and with action observation in this functional characterization (see Figure 1 and 5 of King et al., 2019; data accessible online at https://www.diedrichsenlab.org/imaging/AtlasViewer/).

To conclude, our connectivity pattern is consistent with the proposal of the possible recruitment of the cerebellum not only in motor task, but also in more cognitive processing (L. H. Kim et al., 2024; Schmahmann et al., 2019; Strick et al., 2009). Nevertheless, further task-related fMRI studies are required to better capture the complexity of cerebro-cerebellar interplay during action-related processing.

2.6 Conclusions

Our study provided a comprehensive overview of the connectome of the human hand motor network. Our TMS-fMRI framework provided converging evidence that its connectivity profile encompassed a widespread network of functionally connected regions which have been previously associated with the representation of upper-limb actions by neuroimaging and neurostimulation studies. This network closely mirrored the functional architecture previously described in non-human primates, providing evidence that the hAIP might act as a putative homologue parietal hub for hand actions also in our species.

3 Chapter 3:

Generalizable prediction of hand motor behaviour from spontaneous brain connectivity

3.1 Abstract

Dexterous hand motor behavior emerges from coordinated interactions within a distributed brain network. While task-related neural dynamics have been investigated, recent fMRI studies showed that also spontaneous - i.e. non-task related - brain connectivity can predict task-specific performance. Still, it remains unclear whether spontaneous functional connectivity reflects also the encoding of general aspects of hand motor control.

Here, we applied connectome-based predictive modelling (CPM) to resting-state functional connectivity (rs-FC) from the Human Connectome Project (HCP) to predict performance in hand motor tasks. We identified a "core" hand motor network whose intrinsic connectivity predicted not only task-specific measures (dexterity and strength) but generalized its prediction across different effectors and tasks.

This "core" model also generalized its predictions to an independent dataset (external validation), including different behavioral measures and rs-fMRI data. In addition, transcranial magnetic stimulation (TMS) over the inferior parietal cortex selectively impacted the core model's predictive power in a time-dependent manner, consistent with the known neurophysiological effects of the stimulation protocol.

Together, these findings demonstrate that spontaneous brain activity encodes behaviorally relevant information about hand motor control, spanning both low-level features and higher-order representations. By linking spontaneous brain activity to behavioural motor outcomes, our finding paves the way for a better understanding of how spontaneous connectivity alterations might underlie motor dysfunction in neurological disorders.

3.2 Introduction

Dexterous hand movements rely on the representation of action-related information within a widespread brain network. Traditionally, task-related functional connectivity has been used to study these networks. However, recent findings show that spontaneous connectivity can predict behavioral performance. For instance, whole-brain resting-state functional connectivity (rs-FC) has been shown to predict specific movement features, such as grip strength (e.g., Wu et al., 2021). However, it remains unclear whether rs-FC captures not only task-specific measures but also more general aspects of hand motor control - representations that are independent of the specific effector or task employed.

An extensive corpus of fMRI studies has shown the consistent recruitment of a wide network of cortical, subcortical, and cerebellar regions during the performance of hand actions (Culham et al., 2006; Culham & Valyear, 2006; Errante et al., 2021; Gallivan & Culham, 2015; Grafton, 2010; Sartin et al., 2023; Turella & Lingnau, 2014; Vesia & Crawford, 2012). Multivariate decoding approaches have further revealed the fine-grained specialization of these regions, showing decoding of information about specific aspects of hand actions (Gallivan & Culham, 2015), such as effector (Gallivan et al., 2013) or action type (Gallivan et al., 2011, 2013; Malfatti & Turella, 2021; Monaco et al., 2019, 2020; Turella et al., 2020). Recent MVPA studies also showed that it is possible to define regions hosting more “abstract” information, such as decoding action representations across effectors (Gallivan et al., 2013; Turella et al., 2020) or tasks (Monaco et al., 2020). This view aligns with the classical hierarchical organization of the motor system, where behavior is represented at multiple levels of abstraction. Whether similar abstract information about hand actions is also embedded in spontaneous brain connectivity, however, remains unknown.

To address this question, we employed Connectome-based Predictive Modeling (CPM), which is a data-driven approach that links brain connectivity with behavioral variables (Shen et al., 2017; Wu et al., 2023). This approach has been adopted to establish brain–behavior correlations across multiple cognitive domains. Previous studies have demonstrated that CPM can be employed to predict individual psychometric and behavioral variables from patterns of FC in both healthy participants (e.g., Rosenberg et al., 2016; Shen et al., 2017; Wu et al., 2022; Yoo et al., 2022) and clinical populations (Kim et al., 2023; Lake et al., 2019; Rabini et al., 2023). In healthy individuals, CPM has been employed to predict fluid intelligence (Finn et al., 2015; Wu et al., 2022; Yoo et al., 2019), attention (Rosenberg et al., 2016, 2018; Shen et al., 2017; Yoo et al., 2018, 2022), working memory (Avery et al., 2020; H. Zhang et al., 2020), creativity (Beaty et al., 2018) and personality traits (Cai et

al., 2020; Hsu et al., 2018; Jiang et al., 2018). In clinical populations, CPM has been applied to predict clinical scores for depression (Kim et al., 2023), severity of motor symptoms in Parkinson's disease (Rabini et al., 2023) and social abilities in Autism and Attention Deficit/Hyperactivity disorder (Lake et al., 2019). Crucially, CPM can also capture higher-order domain-general representations—for example, predicting attentional abilities across tasks, datasets and even months apart (Rosenberg et al., 2016, 2017, 2020; Yoo et al., 2022).

Building on this framework, we had three aims. First, using the Human Connectome Project (HCP) dataset, we sought to identify a brain network whose rs-FC could predict performance in two distinct tasks, measuring dexterity (Nine-Hole Peg Test) and strength (isometric grip force task), performed separately with the two hands. We anticipate that we could find a network of regions - a "core" hand motor network - which predicted three (out of four) specific motor tasks of the HCP dataset (right-hand dexterity, right-hand strength and left-hand strength). Second, we tested whether this core network generalized beyond specific task demands, predicting individual behavioural performance across different effectors and motor tasks. Third, we evaluated the generalizability of this core model to an independent dataset (external validation), assessing its predictive validity for novel behavioral measures of a different motor task. Finally, we probed its specificity by applying transcranial magnetic stimulation (TMS) to perturb a parietal region known to be involved in hand action processing, testing whether this intervention altered CPM's predictive performance.

3.3 Material and methods: datasets

3.3.1 HCP dataset: participants and behavioral tasks

Participants. We analyzed anatomical and rs-fMRI data from the HCP dataset (Van Essen et al., 2012, 2013). Although the full HCP sample includes 1,200 healthy young adults, we restricted our analysis to right-handed individuals, defined by an Edinburgh Handedness Inventory score greater than zero (Oldfield, 1971). This approach identified a total of 1,026 participants.

From this subset, we selected 969 participants (535 females; age range: 22–36 years) who met the following criteria: 1) completion of at least one rs-fMRI run with left-right phase encoding; 2) completion of the two behavioral motor tasks relevant to this study.

Behavioral tasks. The HCP includes a comprehensive battery of cognitive and motor assessments (Hodes et al., 2013). For the present study, we focused on two tasks measuring hand motor function. The first task was the Nine-Hole Peg Test (Mathiowetz et al., 1985), which assesses fine hand dexterity. Participants were instructed to insert and - then remove - nine pegs from a pegboard as

quickly as possible with one hand at a time. As a behavioral measure, we considered the time to complete the task (in seconds), recorded separately for the right and left hands.

The second task was the Grip Strength test (Hodes et al., 2013), which assesses upper limb strength. Participants used a hand-held dynamometer to exert maximal grip force, one hand at a time. The considered behavioral measure was the maximum exerted force (in pounds) measured separately for the right and left hands.

3.3.2 HCP dataset: MRI data acquisition and preprocessing

MRI data acquisition. Each participant completed two runs of rs-fMRI with opposite phase encoding directions: left-to-right (LR) and right-to-left (RL). For the present analysis, we used only the LR run. Each run consisted of 1,200 volumes acquired in 14.33 minutes (TR = 720 ms, TE = 33.1 ms, 72 slices, 2 mm isotropic voxels, Van Essen et al., 2012; Smith et al., 2013).

Preprocessing. We used the "minimally preprocessed" data provided by the HCP, which included motion correction and spatial normalization to MNI152 standard space (Glasser et al., 2013). Additional denoising was performed using ICA-FIX, which applies independent component analysis (ICA) to decompose the signal and a trained classifier (FIX) to automatically remove artifactual components (Griffanti et al., 2014; Salimi-Khorshidi et al., 2014; Smith et al., 2013).

3.3.3 Dataset for external validation: participants, kinematics and offline TMS-fMRI sessions

To validate the generalizability of our CPM, we employed an independent dataset comprising kinematic recordings and rs-fMRI data acquired before and after TMS. Part of this dataset has been previously published elsewhere (Pierotti et al., 2025).

Participants. Thirty-two right-handed participants participated in the study. Participants were excluded if they exhibited excessive head motion during fMRI acquisition (maximum displacement > 2 mm; $n = 5$) or experienced technical issues during kinematic data acquisition ($n = 1$). The final sample comprised 26 right-handed participants (16 females, average age: 24 years). Participants had no contraindications to MRI or TMS investigation. They provided written informed consent to participate in the study and were reimbursed for their participation. The protocol of this study was approved by the Ethics Committee of Human Research of the University of Trento (protocol 2018-015)

Kinematic session. On a separate day from the neuroimaging session, participants completed a motor task involving grasping and reaching actions toward a small spherical object (4 cm diameter, placed 30 cm from the starting point; see Budisavljevic et al., 2016 for a similar design). In the grasping

condition, participants used a precision grip (thumb and index finger) to grasp the object. In the reaching condition, they reached and touched the object with their knuckles. Each action was executed 15 times with each hand in separate blocks (one block per hand with block order counterbalanced across participants). In each block, an auditory cue indicated both the type of action (grasp or reach) and the go signal for movement initiation. This design allowed us to record not only movement kinematics but also the reaction times associated with each action.

Kinematics data were recorded using a Qualysis Track Manager System (Qualisys AB, https://www.qualisys.com/) including five infrared cameras (ProReflex MCU) sampling at 100 Hz. Five markers were applied to participants' hands: on the thumb distal phalange, on the index finger distal phalange, on the metacarpophalangeal joint of the middle finger, and two on the wrist (distal radius and ulna).

From this task, we extracted three behavioral measures per hand: 1) reaction time (RT) during grasping, 2) RT during reaching, 3) maximum grip aperture (MGA) during grasping, defined as the maximum distance between the thumb and index markers throughout the movement.

Offline TMS-fMRI session. Each participant underwent two rs-fMRI runs before and two rs-fMRI runs after offline continuous theta-burst stimulation (cTBS; Huang et al., 2005) applied to the human anterior intraparietal area (hAIP) - a key region involved in hand motor control (Grefkes & Fink, 2005). Each rs-fMRI run lasted 10 minutes. For more information on the TMS-fMRI session, please refer to the previous publication (Pierotti et al., 2025).

3.3.4 Dataset for external validation: MRI data acquisition and preprocessing

MRI data acquisition. The rs-fMRI data were collected using a 3T Siemens MAGNETOM Prisma scanner (Siemens Healthcare, Erlangen, Germany) equipped with a 64-channel head coil. Each rs-fMRI run lasted 10 minutes and consisted of 600 volumes (TR = 1 s, TE = 28 ms, 66 slices, voxel size = 3 mm isotropic). To correct geometric distortions, double-echo gradient echo field maps were acquired (TR = 4810 ms; TEs = 4.92 and 7.38 ms; voxel size = 3 mm isotropic Additionally, a high-resolution T1-weighted structural image was obtained using a multi-echo MPRAGE sequence (TR = 2500 ms; TEs = 1.69, 3.55, 5.41, 7.27 ms; voxel size = 1 mm isotropic).

Preprocessing. MRI data were preprocessed using SPM12 (https://www.fil.ion.ucl.ac.uk/spm/software/spm12/) with the following preprocessing steps: 1) slice-timing correction; 2) head motion correction; 3) distortion correction using the gradient echo-

sequences; 3) T1-weighted segmentation to obtain the deformation field for the MNI normalization; 4) normalization to the MNI space; 5) Bandpass filtering (0.1-0.01 Hz). Finally, we resampled voxel size to match the whole brain parcellation (2 mm isotropic voxels).

3.4 Material and methods: CPM models

3.4.1 Parcellation atlas and functional connectivity estimation

Parcellation atlas. To estimate whole-brain functional connectivity, we employed a parcellation approach that combined cortical, subcortical and cerebellar regions, resulting in comprehensive anatomical coverage (Figure 3.1). This composite atlas included 348 parcels distributed across nine functional networks.

Cortical regions were defined using the 300-parcel version of the Schaefer atlas (Schaefer et al., 2018), which is organized according to the seven canonical resting-state networks proposed by Yeo et al., (2011): 1) FrontoParietal, 2) Default Mode, 3) Dorsal Attention, 4) Limbic, 5) Ventral Attention, 6) Somatomotor, 7) Visual.

Subcortical regions were derived from an atlas based on previous work (Glasser et al., 2016; Gordon et al., 2016) comprising 16 parcels (bilateral: Hippocampus, Amygdala, Posterior and Anterior Thalamus, Nucleus Accumbens, Globus Pallidus, Putamen, and Caudate Nucleus) grouped into a single Subcortical network.

Cerebellar regions were extracted from a recent cerebellar atlas (Nettekoven et al., 2023), including 32 parcels that formed the Cerebellar network.

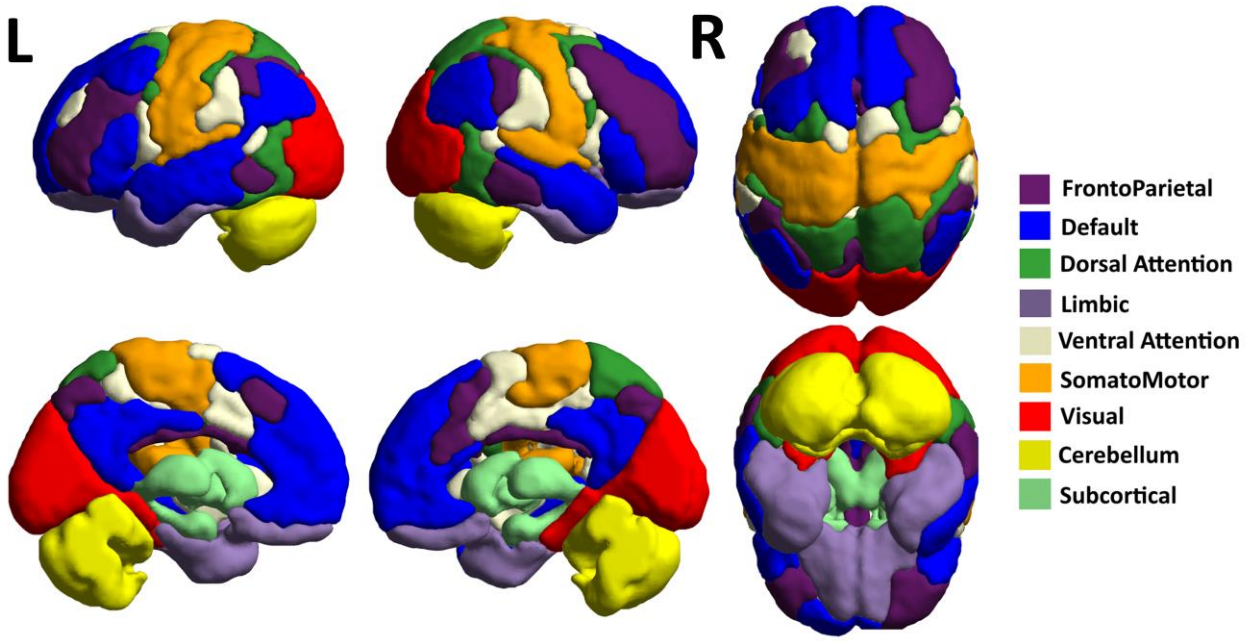

Figure 3.1. Customized whole-brain parcellation and functional network organization. The figure illustrates the parcellation scheme adopted in the present study, comprising 348 regions across nine functional networks. This composite atlas was created by integrating: 1) a cortical parcellation (Schaefer et al., 2018; Thomas Yeo et al., 2011); 2) a cerebellar parcellation (Glasser et al., 2016; Gordon et al., 2016), and a subcortical parcellation (Nettekoven et al., 2023). From left to right, the top row displays lateral views of the left and right hemispheres, and a coronal view. The bottom row presents medial views of the left and right hemispheres, along with an axial (bottom-up) view. The nine functional networks are color-coded as follows: fronto-parietal network (dark purple); default mode network (blue); dorsal attention network (dark green); limbic network (light purple); the ventral attention network (cream); somato-motor network (orange); visual network (red); the cerebellum(yellow); the subcortical network (light green).

Functional connectivity estimation. Using this customized parcellation, we extracted FC from both the HCP dataset and the external validation rs-fMRI dataset. The analysis was performed using custom MATLAB scripts (Version R2017b, The MathWorks Inc., https://www.mathworks.com). For each participant, we computed pairwise Pearson correlation coefficients between the mean time series of each parcel and every other parcel in the atlas. This procedure resulted in an individual 348 × 348 whole-brain FC matrix. All FC estimates were transformed using Fisher's z-transformation.

3.4.2 Whole-brain CPM for predicting hand motor behavior (HCP dataset)

Whole-brain CPMs. We started by testing if the CPM framework could be adopted to predict behavioral variables from whole-brain FC, i.e., to try to establish a link between rs-FC and hand motor functioning. To this aim, we applied Support Vector Regression (SVR) to the rs-FC matrices obtained from our 348-region parcellation, modelling each motor variable separately. Specifically, we constructed independent CPM models to predict the following four behavioral measures: 1) left-hand dexterity (Nine-Hole Peg test); 2) right-hand dexterity (Nine-Hole Peg test); 3) left-hand strength (Grip

Strength test); and 4) right-hand strength (Grip Strength test). All behavioral scores were z-scored before modeling.

We employed 10-fold cross-validation to evaluate each model. In each iteration, data from nine folds served as the training set, while the remaining fold was used for testing. To minimize data leakage, family members were kept within the same fold. Then, we computed the Pearson correlation coefficient between the predicted and observed behavioral scores in the test set, which served as an index of model accuracy. This entire procedure was repeated 1,000 times, and the resulting correlation coefficients were z-scored and averaged across repetitions.

To determine statistical significance, we adopted a non-parametric permutation approach. Specifically, we permuted the behavioral scores within each iteration of the cross-validation (1,000 repetitions), generating a null distribution of correlation values (1,000 values). We then compared the observed average correlation with this null distribution. False Discovery Rate (FDR) correction (Benjamini & Hochberg, 1995) was applied to correct for multiple comparisons.

Weights for Whole-brain CPMs. For each model, we also extracted and analysed the model weights, representing the functional connections (i.e. model features) contributing most to prediction. Direct interpretation of weights can be misleading, so we applied the Haufe transformation (Haufe et al., 2014), which converts the weights into interpretable values. After transformation, larger absolute values indicate greater relevance of specific connections in predicting the behavioral outcome (Haufe et al., 2014; Scheinost et al., 2019; Wu et al., 2023). We averaged these transformed weights across folds and repetitions to generate a final weight matrix for each behavioral model.

To assess the significance of individual connections, we again used a non-parametric approach. For each model, we generated null distributions by permuting behavioral values and recalculating the transformed weights (1,000 permutations). Observed average weights were then compared to these null distributions, and FDR correction (Benjamini & Hochberg, 1995) was applied to control for multiple comparisons across the matrix.

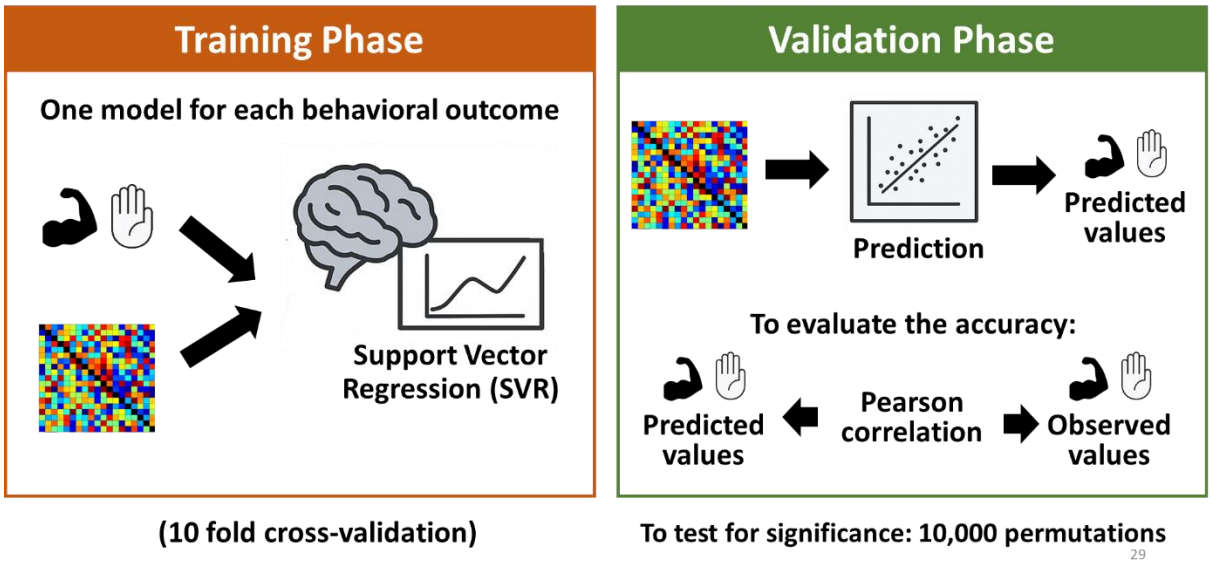

Figure 3.2. Schematic representations of the predictive modeling pipeline employed. During the Training Phase, behavioral performance measures and individual functional connectivity matrices were used to train the predictive model (support vector regression) and identify connectivity features associated with motor behavior. In the Validation Phase, the trained model was applied to an independent dataset to predict behavioral scores based on resting-state connectivity, providing an external test of model generalizability.

3.4.3 *Identification of a core hand motor network and test of its predictive power (HCP dataset)*

Our first objective was to determine whether a core hand motor network could be identified across multiple behavioral tasks and whether this network alone could predict motor performance.

As described in the Results section ("Whole-brain CPM, identification of the core hand motor network and test of its predictive power"), three out of four whole-brain CPM models yielded significant predictions: dexterity of the right hand, strength of the left hand and strength of the right hand.

To define the core hand motor network, we first extracted all the significantly predictive connections (based on FDR-corrected Haufe-transformed weights) from each of these three models. Then, we calculated the intersection of these connections across the three models. While each whole-brain model included 60,552 unique pairwise connections (based on the 348 × 348 symmetric matrix), the core network consisted of 1,833 connections.

We tested the predictive power of this core network by conducting the same CPM analyses using only these 1,833 connections. We followed the same SVR and cross-validation procedure described in the previous section. This allowed us to evaluate whether the core network CPM could predict each of the four behavioral motor variables: dexterity for the left hand, dexterity for the right hand, strength for the left hand, strength for the right hand.

3.4.4 *Generalization of the core hand motor network CPM to different motor variables (HCP dataset)*

The second aim of our study was to evaluate whether the core network captures more general aspects of hand motor control - beyond the specific motor variable used for training. In detail, we tested whether a CPM model trained to predict a specific motor variable (e.g., force) could also predict the same variable for the opposite hand and/or a different motor variable (e.g., dexterity). This analysis allowed us to investigate whether the core network encodes higher-order aspects of motor control and not only task-specific motor variables.

As in our previous analyses, we employed a 10-fold cross-validation scheme with 1,000 repetitions. To evaluate statistical significance, we generated null distributions by permuting behavioral values within each motor variable before computing the CPM (1,000 permutations). False Discovery Rate (FDR) correction (Benjamini & Hochberg, 1995) was applied to correct for multiple comparisons.

3.4.5 *External validation and network perturbation analysis of the hand motor network motor CPM (HCP dataset)*

Our final objective was to evaluate the generalizability of the core hand motor network CPM by testing its predictive performance on an independent dataset that included both new rs-fMRI data and different behavioral measures (external validation).

One of the primary challenges in the CPM framework is overfitting, where a model captures noise specific to the training dataset rather than the true signal. This risk can be mitigated through external validation, which evaluates model performance on a separate dataset that was not used in model training. Such a procedure enhances the robustness and reproducibility of the findings by ensuring that the test data cannot influence model optimization (Scheinost et al., 2019).

We leveraged the unique structure of our external validation dataset, in which each participant contributed four rs-fMRI runs and six behavioral kinematic measures: RTs (separately for reaching and grasping actions) and maximum grip aperture (MGA) for both hands.

This allowed us to evaluate model performance in two distinct external validations: 1) unperturbed external validation using the two rs-fMRI runs acquired before cTBS stimulation; 2) perturbed external validation using the two rs-fMRI runs acquired after cTBS stimulation over the left hAIP, a key region involved in hand motor control.

For the unperturbed external validation, we applied the core CPM model trained on the HCP dataset (N = 969) separately to the two pre-TMS runs from the external sample (N = 26), assessing whether the model could predict new motor behavior based on FC in a different population. Specifically, we tested the three CPM models that showed significant performance in the training dataset (left-hand dexterity, left-hand strength, right-hand strength), using them to predict RT and MGA values in the independent sample.

For the perturbed external validation, we repeated the analysis using the two post-TMS runs. This allowed us to examine whether offline cTBS to the left hAIP would alter the predictive performance of the core CPM.

In both analyses, we computed Pearson correlation coefficients between the predicted and actual behavioral values to quantify model performance. To assess statistical significance, we generated a null distribution for each model by permuting the behavioral labels (1,000 times) and compared the observed correlation coefficients to these null distributions. Statistical significance was determined by comparing the true correlation value against its corresponding null distribution. False Discovery Rate (FDR) correction (Benjamini & Hochberg, 1995) was applied to correct for multiple comparisons.

3.5 Results

3.5.1 *Prediction of Hand Motor Variables for Whole-brain Functional Connectivity (HCP dataset)*

We started by testing whether whole-brain rs-FC could predict performance in different motor tasks. Using CPM trained on the HCP dataset, we tested four separate models targeting different motor variables. Three of the four CPMs significantly predicted behavior: right-hand dexterity and strength for both hands ($p < 0.005$ FDR-corrected; see Figure 3.3).

In the whole-brain analyses, we adopted a conservative approach ($p < 0.005$ FDR-corrected), as the objective was to constrain as much as possible the number of possible connections included within the core hand motor network (see next section).

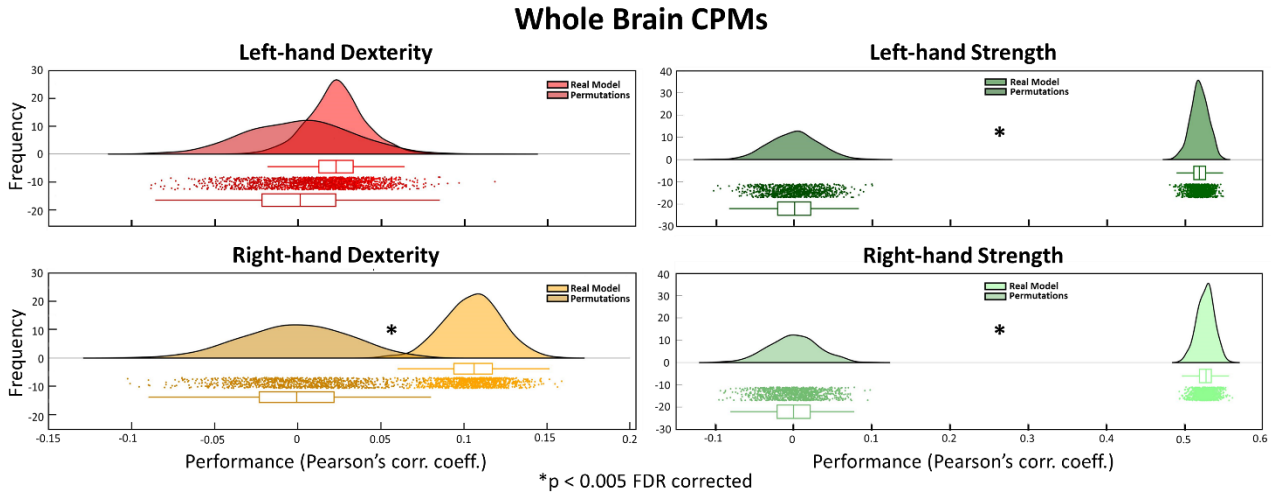

Figure 3.3. Prediction performance of whole-brain CPMs for hand motor variables (HCP dataset). Each panel displays the distribution of model performance (Pearson's correlation between predicted and actual behavioral scores) for the real CPM compared to the null distribution obtained via permutation testing. The top-left panel shows the non-significant model for left-hand dexterity. The bottom-left panel shows a significant model for right-hand dexterity. The top-right and bottom-right panels show significant models for left-hand and right-hand grip strength, respectively. All significant results passed false discovery rate correction ($p < 0.005$ FDR-corrected).

3.5.2 *Prediction of Hand Motor Variables from the Core Hand Motor Network Functional Connectivity (HCP dataset)*

Our first objective was to identify a core network, i.e. a subset of functional connections that consistently predicted performance in different hand motor tasks. To this end, we extracted the statistically significant connections from the three whole-brain CPMs that showed predictive power (right-hand dexterity, left-hand strength and right-hand strength) and computed their intersection. This procedure yielded a core network composed of 1,833 connections.

Figure 3.4A illustrates the distribution of these connections across the nine functional networks defined by our customized parcellation. Notably, the most frequent connections were between the Somatomotor and Default Mode networks, Default Mode and Fronto-Parietal networks, Somatomotor and Fronto-Parietal networks, Somatomotor and Visual networks, and between the Dorsal and Ventral Attention networks. Within-network connections were most prominently represented within the Default Mode Network.

As previously described (see Methods), we used a customized whole-brain parcellation combining cortical (Schaefer et al., 2018; Yeo et al., 2011), subcortical (Glasser et al., 2016; Gordon et al., 2016), and cerebellar (Nettekoven et al., 2023) atlases. The cortical large-scale networks were defined based on rs fMRI data, preserving their original naming conventions (Yeo et al., 2011) to facilitate comparison with previous studies. Still, it is important to note that there is not a consensus on the nomenclature and function of this networks (Biswal & Uddin, 2025). For this reason, Figure 3.4B shows the spatial distribution of parcels involved in the core network. The color code depicts the number of significant connections for each parcel.

We then tested whether the core network CPM alone could predict hand motor variables, applying the same procedure adopted with whole brain data, but limiting the features to the 1,833 core connections. As shown in Figure 3.4C, the core CPM successfully predicted the same three behavioral measures as the original whole-brain models: right-hand dexterity and left/right-hand strength ($p < 0.005$, FDR-corrected).

These results indicate that the identified core network - despite being much smaller than the whole-brain connectivity matrix (1,833 vs. 60,552 connections) - is functionally associated with upper-limb motor performance.

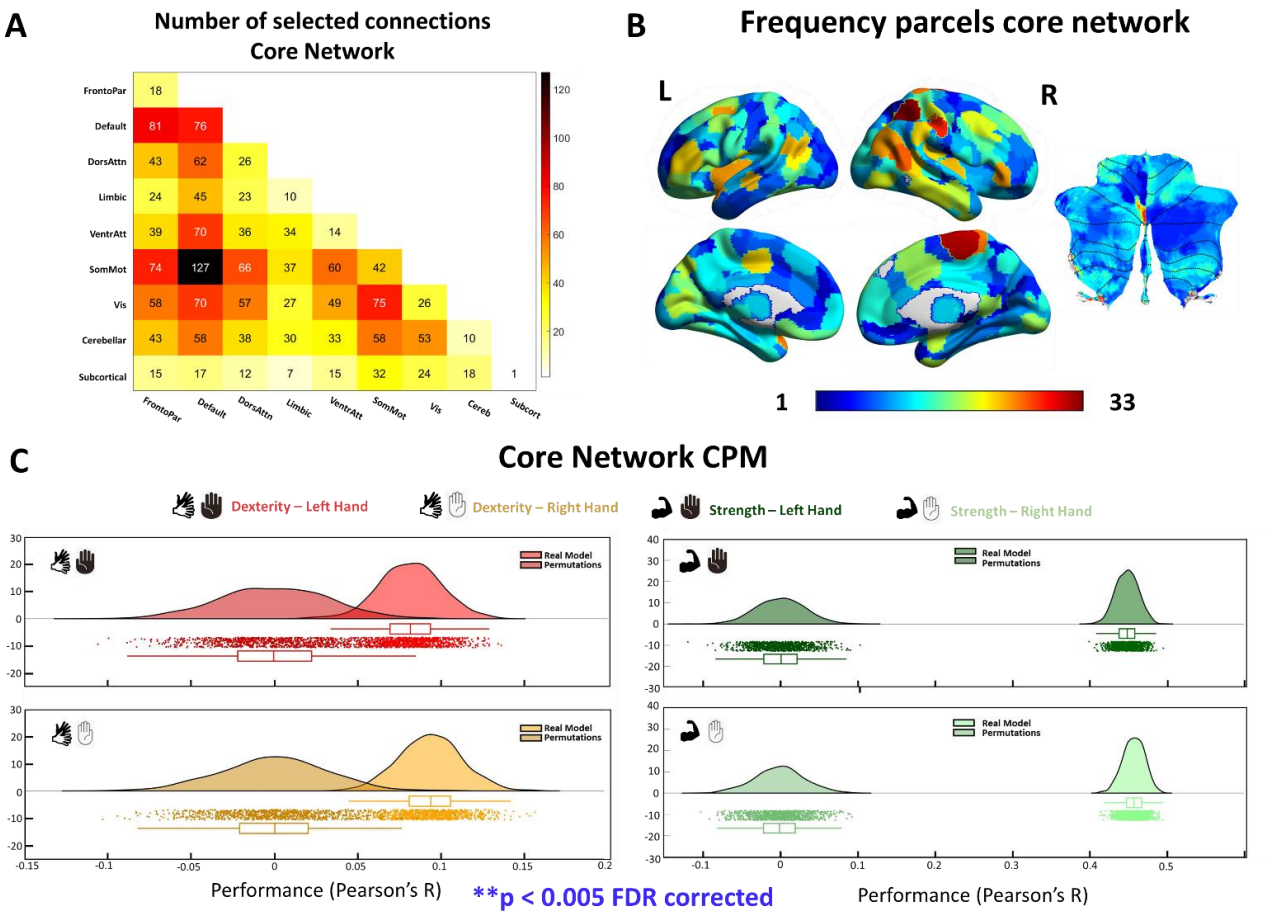

Figure 3.4. Core hand motor network and its predictive performance. **A. Distribution of connections across functional networks.** The heatmap shows the number of connections within and between functional networks that comprise the core hand motor network (1,833 connections). FrontoPar = fronto-parietal network; Default = default mode network; DorsAtt = dorsal attentional network; Limbic = limbic network; VentrAtt = ventral attentional network; SomMot = somatomotor network; Vis = visual network; Cerebellar = cerebellum; Subcortical = subcortical network. **B. Spatial distribution of parcels in the core network.** Brain surface maps show the frequency with which each parcel was involved in the core network. Frequencies reflect how often a parcel appeared across the significant connections shared by the three predictive whole-brain CPMs (right-hand dexterity, left-hand strength, and right-hand strength). **C. Predictive power of the core network.** Each panel displays the distribution of model performance (Pearson's correlation between predicted and actual behavioural scores) for the real CPM compared to the null distribution obtained via permutation testing. The model significantly predicted right-hand dexterity, left-hand strength, and right-hand strength ($p < 0.005$ FDR corrected, blue asterisks), but not left-hand dexterity.

3.5.3 *Generalization of the Predictive Performance of the Core Hand Motor Network CPM to Different Motor Variables (HCP Dataset)*

Our second aim was to evaluate whether the core CPM captures general features of hand motor functioning, beyond adopted effectors or specific task requirements. To address this, we employed a cross-generalization approach in which the CPM was trained on one motor variable and tested across tasks (dexterity vs. strength), across hands (right vs. left) or across both.

Several cross-generalization comparisons yielded significant results, indicating that core CPMs trained on a specific motor task can generalise their prediction to different motor tasks (see Figure 4). First, core CPM trained on right-hand strength significantly predicted dexterity of the same hand and vice versa (see Figure 3.5A). These results suggest that the core network captures task-independent information about motor performance, regardless of the specific requirement of the task (i.e., dexterity vs. strength).

Second, core CPM trained on strength for one hand (e.g., left) could significantly predict strength for the opposite hand (e.g., right) and vice versa (see Figure 3.5B). This result indicates that this network encodes effector-independent information, generalizing across the left and right hands for the same type of motor task.

Finally, core CPM trained on right-hand dexterity significantly predicted left-hand strength and vice versa (Figure 3.5C). These findings suggest that this network integrates broader action-related information that supports general motor performance across motor domains and effectors.

Taken together, these results highlight the generalizability of the core CPM across different motor domains, supporting the idea that it encodes higher-order neural representations of upper-limb motor control.

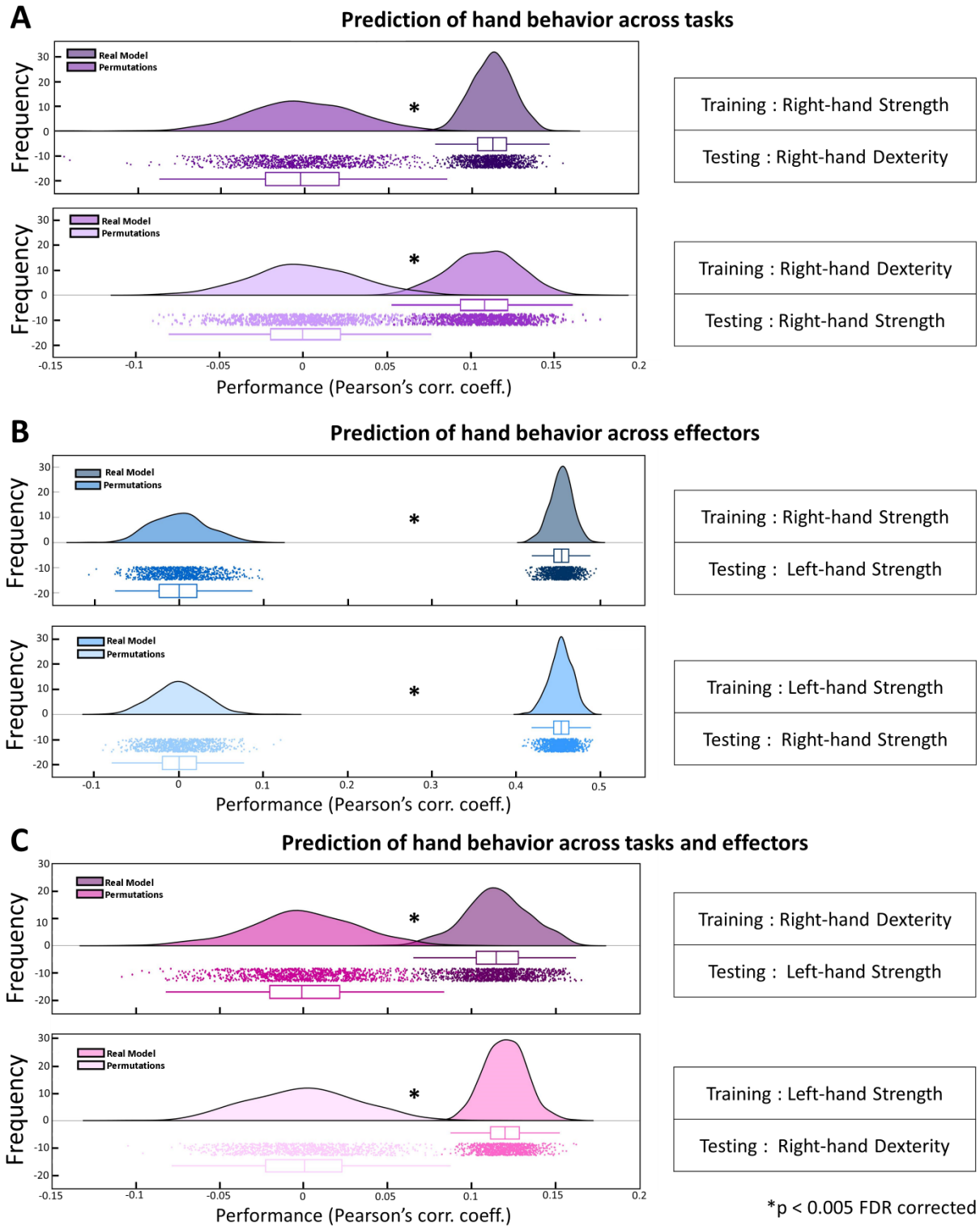

Figure 3.5. Cross-generalization results of the core CPM. A. Task-independent cross-generalization. Distributions of model performance compared against the null distribution obtained through permutations. The y-axis displays Pearson's correlation coefficients (prediction accuracy) and the x-axis shows the cross-generalization comparison. **B. Effector-independent cross-generalization.** Distributions of model performance compared against the null distribution obtained through permutations. The y-axis displays Pearson's correlation coefficients (prediction accuracy), and the x-axis shows the cross-generalization comparison. **C. Task- and effector-independent cross-generalization.** Distributions of model performance compared against the null distribution obtained through permutations. The y-axis displays Pearson's correlation coefficients (prediction accuracy), and the x-axis shows the cross-generalization comparison. All models showed significant predictive power ($p < 0.005$ FDR corrected), supporting the hypothesis that the core network captures action-related information that extend beyond specific tasks or effectors

3.5.4 *Generalization of the predictive performance of core network CPM to an independent dataset (external validation)*

To evaluate the generalizability of the core CPM beyond the original dataset, we tested its predictive performance on an independent sample comprising rs-fMRI and kinematic data. This external validation dataset included behavioral measures that differed from those of the HCP dataset: reaction times (RTs) for grasping and reaching tasks, and maximum grip aperture (MGA), a key kinematic parameter associated with skilled hand control. These measures were assessed for both hands separately. The inclusion of these novel motor variables allowed us to assess whether the core network CPM could generalize to different dimensions of motor behavior - ranging from a general index of action preparation (RTs) to more specific aspects associated with dexterous hand action execution (MGA).

Figure 5 summarizes the external validation results across four rs-fMRI runs. The different panels (A–D) represent a separate run presented in temporal order. The columns in each panel depict the HCP-trained CPMs (based on different motor tasks and hands), and rows represent the target behavioral variables from the independent dataset. Prediction significance is indicated by a red-colored correlation coefficient ($p < 0.05$ FDR corrected).

Figure 3.6A displays the prediction results for the first rs-fMRI run acquired prior to TMS, which represents an "unperturbed" FC state. Significant predictions were observed for MGA of the right hand when the model was trained on right-hand dexterity in the HCP dataset. Similarly, MGA for the left hand was significantly predicted across three HCP training models (right-hand dexterity and strength for both hands), suggesting that the core CPM can capture general aspects of dexterous hand behavior, even across datasets.

Figure 3.6B shows a similar pattern adopting the second "unperturbed" run of rs-fMRI (before TMS). Significant predictions were again found for MGA of the right hand (training on right-hand dexterity) and for MGA of the left hand when training on either left-hand dexterity or strength ($p < 0.05$ FDR corrected). The prediction accuracy for MGA left-hand when training on strength left hand was close to the significant level (p uncorrected = 0.08), suggesting a trend toward generalizability in this condition.

To assess the potential impact of perturbation on the predictive power of the network, we tested the model on two additional "perturbed" rs-fMRI runs acquired after continuous theta-burst stimulation (cTBS) over the left inferior parietal cortex.

Figure 3.6C shows the results from the rs-fMRI run acquired approximately 5 minutes after cTBS (the first post-TMS session). Despite the stimulation, prediction performance remained consistent with the pre-TMS state: MGA of the right hand was again significantly predicted from right-hand dexterity training, and MGA of the left hand was predicted from all three HCP models ($p < 0.05$ FDR corrected).

Figure 3.6D shows the results from the final rs-fMRI run (the second post-TMS session) which was acquired later in time (approximately 15 minutes after TMS). Here, all model predictions failed to reach significance (all uncorrected p-values > 0.12). This suggests that cTBS affected the FC in the core network only at this time point, suggesting that the effects of cTBS over the parietal area might take time to become evident. This is in line with a recent non-human primate investigation that demonstrated that the effects of cTBS on parietal cortex take from 20 to 30 minutes to reach its maximum effect (Romero et al., 2022).

All in all, these findings demonstrate that the core network CPM shows generalization to novel motor-related variables from an independent dataset - i.e. MGA, a measure of fine motor control - and that its predictive performance is sensitive to TMS-induced modulation of parietal connectivity.

External Validation

Run 1 before TMS: unperturbed FC

		TRAINING DATASET		
		RIGHT-HAND DEXTERITY	RIGHT-HAND STRENGHT	LEFT-HAND STRENGHT
RIGHT HAND	RT REACHING	0.08	-0.19	-0.12
	RT GRASPING	0.21	-0.15	-0.06
	MGA	**0.45**	0.19	0.22
LEFT HAND	RT REACHING	-0.02	0.05	-0.12
	RT GRASPING	-0.02	0.07	-0.10
	MGA	**0.43**	**0.45**	**0.37**

Run 2 before TMS: unperturbed FC

		TRAINING DATASET		
		RIGHT-HAND DEXTERITY	RIGHT-HAND STRENGHT	LEFT-HAND STRENGHT
RIGHT HAND	RT REACHING	0.28	-0.19	-0.14
	RT GRASPING	0.31	-0.15	-0.10
	MGA	**0.45**	0.08	0.17
LEFT HAND	RT REACHING	-0.05	0.19	-0.09
	RT GRASPING	-0.06	0.19	-0.09
	MGA	**0.37**	**0.45**	0.30

Run 1 after TMS: perturbed FC

		TRAINING DATASET		
		RIGHT-HAND DEXTERITY	RIGHT-HAND STRENGHT	LEFT-HAND STRENGHT
RIGHT HAND	RT REACHING	0.13	-0.29	-0.18
	RT GRASPING	0.18	-0.26	-0.14
	MGA	**0.46**	0.09	0.17
LEFT HAND	RT REACHING	-0.14	0.13	-0.24
	RT GRASPING	-0.13	0.10	-0.23
	MGA	**0.40**	**0.45**	**0.34**

Run 2 after TMS: perturbed FC

		TRAINING DATASET		
		RIGHT-HAND DEXTERITY	RIGHT-HAND STRENGHT	LEFT-HAND STRENGHT
RIGHT HAND	RT REACHING	0.09	-0.13	-0.12
	RT GRASPING	0.08	-0.07	-0.07
	MGA	0.08	0.17	0.13
LEFT HAND	RT REACHING	-0.01	0.08	-0.02
	RT GRASPING	0.00	0.06	-0.01
	MGA	0.24	0.08	0.23

p < 0.05 FDR corrected

Figure 3.6. External validation results across rs-fMRI runs in an independent dataset. Prediction accuracy of CPM models trained on HCP data (columns) when applied to behavioral data from the independent dataset (rows). Behavioral variables include reaction times for grasping (RT GR) and reaching (RT RE), and maximum grip aperture (MGA), for both hands (RH, LH). Red-highlighted cells mark significant predictions ($p < 0.05$, FDR corrected). **A. Results from the first rs-fMRI run acquired before TMS stimulation ("unperturbed" functional connectivity).** Significant predictions were observed for MGA of both hands, particularly when testing models trained on HCP dexterity and strength tasks. **B. Results from the second "unperturbed" pre-TMS rs-fMRI run.** The pattern largely replicates Panel A, with significant prediction for MGA of both hands, especially following training on dexterity and strength tasks for the corresponding hand. **C. Results from the first post-TMS rs-fMRI run.** Predictive performance remains comparable to pre-TMS runs, suggesting initial preservation of the network's functional architecture. **D. Results from the second post-TMS rs-fMRI run.** All prediction models failed to reach significance (all $p > 0.12$, uncorrected), suggesting a delayed effect of cTBS on the functional architecture of the core motor network..

3.6 Discussion

The aim of this study was to investigate whether the encoding of general aspects of hand motor control is embedded in spontaneous functional connectivity. To this end, we adopted CPM on rs-FC to predict individual performance across a range of motor tasks.

Our first finding was the identification of a core hand motor network, derived from the intersection of significant connections across whole-brain CPMs for three motor tasks of the HCP dataset (right-hand dexterity, right- and left-hand strength). The core CPM predicted behavioral performance in these tasks, demonstrating that rs-FC contains information associated with distinctive features of the behavioural output.

Our second finding was the generalization of the prediction of the core CPM across different effectors and/or tasks. This seems to suggest that the rs-FC in the core network also captures high-order aspects of hand functioning, not bound to specific motor outcomes.

Finally, we demonstrated that the core CPM generalized to an independent dataset featuring a different behavioural metric, i.e., MGA, further supporting the idea that the core network encodes task-independent information. Moreover, employing rs-FC acquired after TMS to hAIP, we could observe a time-dependent change in predictive power compatible with the effect of cTBS. This suggests that perturbed rs-FC affects the generalization of our core CPM.

In the next sections, we discuss the implications of our findings on the understanding of the nature of behavioral information embedded in spontaneous connectivity.

3.6.1 Distributed representation of task-specific motor information within intrinsic connectivity

We showed that distributed patterns of spontaneous connectivity in a widespread brain network could predict individual performance in specific motor tasks. In other words, our results reveal that hand action information is represented in a distributed way across the brain even a rest.

We acknowledge, however, that the whole-brain and core models predicting left-hand dexterity were not significant. This weaker performance for left-hand dexterity may be attributable to the characteristics of our sample, which included only right-handed participants. Predictive power for dexterity was lower than for strength even in the dominant (right) hand, suggesting that dexterity may be inherently harder to model from rs-FC and/or that handedness plays a critical role. Future

research should explore how hand dominance affects CPM performance, particularly for fine motor control tasks.

Despite this limitation, our findings are supported - and complementary to - recent fMRI studies (Livne et al., 2022; Zhang et al., 2023, 2025) which directly demonstrated the similarity between patterns of spontaneous brain activity and patterns of task-related activity associated with the performance of hand movements.

Livne et al. (2022) demonstrated that spontaneous activity in the primary motor cortex resembles task-evoked patterns of common, everyday hand actions more than uncommon ones, suggesting the motor cortex encodes frequently used movements even at rest. Extending this evidence, Zhang et al (2023) demonstrated that spontaneous activity patterns in large-scale rs networks (Yeo et al., 2011) also exhibit different similarity with task-related patterns. The DAN aligned with patterns for common hand actions, while the VAN was more attuned to patterns for uncommon ones. This functional dissociation suggests that different rs networks may support distinct aspects of action representation even at rest. More recently, Zhang et al. (2025) showed that dynamic coactivation patterns linking the motor cortex with regions of large-scale rs networks (VAN, DAN, DMN) were preserved across rest and hand movements - even if they underwent a reconfiguration during the task. Taken together, these findings suggest that not only local spontaneous activity patterns (as in Livne et al., 2022; Zhang et al., 2023), but also distributed interactions between brain regions are critical for representing hand action at rest (Zhang et al., 2025), consistent with our data. Task-related information seems to be embedded within the intrinsic organization of these networks even in the absence of any explicit motor output, supporting the idea that these activity patterns code for behaviourally relevant information states.

Building on this evidence, it is tempting to interpret our findings within a framework proposing that resting-state activity and connectivity might be gradually shaped over the lifespan by everyday experience and learning mechanisms, thereby serving as a functional scaffold or priors of task activation patterns (Petersen & Sporns, 2015; Raichle, 2011). Within this view, the specific type of information encoded within the connections of our core CPM is difficult to specify, as different aspects of our tasks might be represented (Gallivan & Culham, 2015). Task-specific predictions may encompass the motor aspects of the actions, the associated visual or somatosensory information, or the sensory feedback generated by the movements. Future studies are therefore needed to disentangle the contributions of different rs-FC patterns to behaviorally relevant information and to clarify their role in supporting distinct components of hand motor control.

3.6.2 Representation of higher-order aspects of hand motor control in intrinsic connectivity

We showed that the core CPM generalized its predictions across tasks, effectors, and even datasets. This aspect of your findings is compelling, as it suggests rs-FC in the core network may encode information about hand behavior at a more abstract level, as indicated by our cross-generalization analyses (see Figure 3.4). We can speculate about the type of higher-order information captured by our CPM by comparing the commonalities between our strength and dexterity tasks. Both tasks require the specification of hand configurations to accomplish task demands. In the strength task, a specific posture of the hand must be maintained throughout the task, whereas in the Nine-Hole Peg test, the hand is continuously reconfigured as pegs are inserted and removed. A plausible interpretation could be that the generalization of prediction of the CPM across these two tasks may imply that the core network encodes common neural principles underlying hand configuration shared across these different motor behaviors.

Our cross-generalization analyses support the idea that, like other cognitive domains, the motor system also relies on domain-general representations that are not exclusively tied to specific task requirements. Nonetheless, while these results demonstrated the presence of such representations within spontaneous connectivity, they do not fully clarify their precise informational content or functional role.

Additional insight comes from the external validation analysis (see Figure 5), which showed that the core CPM generalized primarily to MGA, but not to RTs. This finding supports our proposal that CPM captures general aspects of motor control across tasks. RTs are influenced by task-specific factors such as explicit instructions and attentional demands, whereas MGA reflects an implicit process largely independent of such factors. Indeed, MGA has been associated with visuo-motor transformations required to shape the fingers for performing hand-object interactions (Jeannerod et al., 1995; Rizzolatti et al., 1998; Rizzolatti & Luppino, 2001; Rizzolatti & Matelli, 2003). The representation of the required hand configuration is likely shared across all our motor tasks (strength, dexterity and grasping), a possibility further supported by the cTBS effect on CPM predictive power (see next section).

Following the interpretational framework proposed in the previous section (Petersen & Sporns, 2015; Raichle, 2011), we might view the coding of this task-independent information as embedded not only in task-specific activity but also in the co-activation patterns of resting-state networks. In this sense, spontaneous connectivity may integrate not just task-specific features but also general aspects of motor control that are consistent across tasks.

A more speculative interpretation could be that these representations embedded in spontaneous activity might have a crucial role in prediction (Betti et al., 2021; Dimakou et al., 2025; Pezzulo et al., 2021). It has been proposed that the brain is actively maintaining and updating predictive representations relevant for future interactions with the environment even when "at rest" (Dimakou et al., 2025; Pezzulo et al., 2021). If so, spontaneous connectivity patterns might reflect latent functional architectures that support a more general anticipatory mechanism for predicting task-independent aspects of future actions even in the absence of overt movement.

3.6.3 Specificity of modification of CPM's predictive power following cTBS

To the best of our knowledge, this is the first investigation to demonstrate that TMS can induce changes in the predictive power of a CPM. This finding suggests that informational states related to motor output, embedded in spontaneous activity, can be modified by external perturbation. Specifically, we observed a time-dependent decrease in the core model's ability to predict MGA, consistent with the neurophysiological effects of cTBS on parietal cortex, which unfold gradually to reach their maximum (Romero et al., 2022). The specificity of this effect supports the idea that spontaneous connectivity carries representational content closely related to task-evoked activity.

The stimulated region, hAIP, is known to be an important node involved in the visuo-motor transformation for producing hand motor commands (Jeannerod et al., 1995; Rizzolatti et al., 1998; Rizzolatti & Luppino, 2001; Rizzolatti & Matelli, 2003). Previous studies have shown that TMS over hAIP impairs performance during hand actions (Glover et al., 2005; Gutteling et al., 2013; Rice et al., 2006, 2007; Tunik et al., 2005b, 2008). More recently, a lesion study identified hAIP as causally involved in modifications of hand preshaping, as measured by MGA, during visually guided grasping (Di Caro et al., 2025). This corpus of evidence supports a functional relationship - and possibly an equivalence - between information encoded within the hAIP during hand motor tasks and during rest. By directly demonstrating that transient perturbations of rs-FC can alter CPM predictions, our study supports the functional relevance of spontaneous connectivity patterns, supporting prior reports linking rs modifications to learning (Guerra-Carrillo et al., 2014) and to neurological disorders (Hohenfeld et al., 2018).

3.7 Conclusions

We identified a core hand motor network whose rs-FC predicts individual behavioural performance across distinct motor tasks and generalizes its prediction across effectors, tasks and datasets. Our data converge with growing evidence that spontaneous brain activity has a representational role, embedding behaviorally-relevant information that ranges from local motor features to higher-order task-independent principles of action control. By showing that these representations are distributed, generalizable and sensitive to external perturbation, we provide novel insights into the functional relevance of resting-state connectivity. Our description provides the starting point for investigating how alterations in spontaneous connectivity may also characterise motor impairments in neurological conditions.

4 Chapter 4: General Discussion

4.2 Thesis summary

The present thesis provides converging evidence for the causal and predictive roles of parietal regions in the organization of the human hand motor network. By combining continuous theta-burst stimulation (cTBS), resting-state functional MRI, and connectome-based predictive modeling, we demonstrated that parietal cortex exerts a measurable influence on large-scale motor connectivity and that intrinsic network properties can predict individual differences in motor performance. Together, these findings advance our understanding of how distributed cortical systems support fine motor control and offer a conceptual framework for integrating causal and predictive approaches in systems neuroscience.

4.2.1 Integration of causal and predictive perspectives

A central contribution of this thesis lies in its methodological synthesis. Experiment 1 established a causal link between parietal activity and motor network reconfiguration through the application of cTBS over the anterior intraparietal sulcus (hAIP). Experiment 2 complemented this causal evidence with a predictive framework, showing that interindividual variability in motor behavior can be explained by functional connectivity patterns within the same core network. These two approaches—causal perturbation and predictive modeling—address complementary aspects of the brain–behavior relationship. Whereas TMS-based interventions allow inferences about necessity and directionality, predictive models quantify how well intrinsic network properties can account for behavioral performance. The combination of both provides a richer understanding of motor network dynamics, bridging mechanistic and statistical perspectives on brain function.

4.2.2 Theoretical implications

From a theoretical standpoint, the present results support the view of the hand motor system as a distributed, hierarchically organized network that flexibly integrates parietal, premotor, and cerebellar regions. The modulation of resting-state connectivity following parietal cTBS indicates that hAIP is not merely a sensory or visuomotor node but an active hub capable of shaping the communication within and beyond the dorsal visual stream. This functional integration likely underpins the translation of perceptual information into action planning and motor execution.

Furthermore, the predictive modeling results suggest that resting-state functional connectivity captures meaningful interindividual differences in motor proficiency. These connectivity–behavior associations reflect not only structural constraints but also dynamic, state-dependent properties of the motor network that vary across individuals. This finding aligns with recent theoretical models emphasizing the role of intrinsic brain organization as a substrate for behavioral variability and learning potential.

4.2.3 Methodological contributions

Methodologically, this thesis demonstrates the feasibility and value of integrating non-invasive brain stimulation with advanced multivariate and predictive analyses. The combination of cTBS and rs-fMRI allowed us to track stimulation-induced changes in network topology beyond the stimulated site, revealing system-level reconfigurations that traditional univariate approaches might overlook. The use of connectome-based predictive modeling further enabled us to test whether these network features possess behavioral relevance and generalize across datasets. Importantly, the inclusion of both internal cross-validation and external validation ensured that the identified brain–behavior relationships were not confined to dataset-specific noise or preprocessing artifacts but reflected stable and replicable patterns of neural organization.

This methodological framework contributes to the ongoing shift in cognitive neuroscience from localized activation mapping toward network-based and predictive paradigms. By emphasizing model generalizability and causal manipulation, the present work exemplifies how modern neuroimaging and neuromodulation can be combined to move beyond descriptive correlations toward mechanistic explanations of brain function.

4.3 Methodological considerations and limitations

Several methodological aspects of the present work warrant consideration, as they bear on the interpretation and generalization of the reported findings.

4.3.1 Order of stimulation sessions

In Experiment 1, the order of stimulation sessions was not counterbalanced across participants, as all individuals received the sham stimulation first and the active continuous theta-burst stimulation (cTBS) second. This choice was motivated by well-documented neurophysiological constraints: cTBS-induced effects on cortical excitability can persist for up to one hour (Huang et al., 2005; 2007). Administering the active stimulation first would have resulted in residual neuromodulatory effects contaminating subsequent sham measurements, precluding the acquisition of a valid baseline.

Although the fixed order could, in principle, raise concerns regarding fatigue or time-on-task effects, control analyses revealed no significant within-condition differences between the two resting-state runs, suggesting that these factors did not systematically influence connectivity. Only an uncorrected trend emerged in the second post-TMS run, which did not survive correction for multiple comparisons. The specificity of this isolated effect supports the interpretation that it reflected TMS-related modulation rather than nonspecific influences. Converging evidence from Experiment 2 reinforces this view: the predictive model based on resting-state connectivity successfully predicted motor performance only during the first post-TMS run, in line with the expected temporal evolution of cTBS effects over parietal cortex (Romero et al., 2022). Together, these results suggest that the observed effects were stimulation-specific rather than attributable to session order or fatigue.

4.3.2 Specificity and effectiveness of the TMS stimulation

The spatial and physiological precision of the TMS protocol is another relevant consideration. The stimulation site (mean MNI coordinates: x = –52 ± 6, y = –43 ± 5, z = 57 ± 4) was located in the posterior portion of the inferior parietal lobule, well posterior to the primary motor cortex (M1; typically around y = –20 to –30). Even accounting for individual anatomical variability and magnetic field spread, the induced current is unlikely to have reached the precentral gyrus. This anatomical distinction is consistent with the observed functional results: the searchlight multivariate connectivity analysis revealed a modulation pattern that matched the known connectivity profile of the macaque anterior intraparietal (AIP) area, encompassing ventral premotor, secondary somatosensory, and ventral-stream temporal regions (Borra et al., 2008; 2017). If M1 had been inadvertently stimulated, the resulting network changes would have predominantly involved premotor and descending motor pathways rather than the fronto-parietal and ventral connections identified here. The adopted stimulation intensity (80% of active motor threshold) followed the original and widely validated cTBS protocol (Huang et al., 2005). Although this corresponds to a relatively low absolute intensity (<30% of maximum stimulator output), comparable values have been shown to produce reliable modulatory effects in associative cortices (Chung et al., 2015). The significant changes in resting-state connectivity between post-sham and post-TMS sessions confirm the physiological effectiveness of the stimulation. Nonetheless, as with all non-invasive brain stimulation techniques, some degree of current spread to adjacent tissue cannot be entirely excluded, representing an intrinsic limitation of TMS spatial resolution.

4.3.3 *Cross-validation and external validation of predictive models*

In Experiment 2, we employed connectome-based predictive modeling (CPM) to link resting-state connectivity with individual motor performance. Cross-validation was used to minimize overfitting by testing model performance on unseen data partitions within the same dataset. However, cross-validation cannot fully eliminate overfitting to dataset-specific characteristics, since both training and testing folds originate from the same cohort and share the same acquisition parameters, preprocessing pipeline, and behavioral measures. External validation therefore provides a more stringent test of model generalizability. By applying the model to an entirely independent dataset—including different participants, behavioral variables, and preprocessing procedures—we could confirm that the predictive relationship captured by the model was not driven by sample-specific noise or methodological idiosyncrasies. Thus, while cross-validation effectively mitigates overfitting, external validation serves as an additional safeguard, strengthening the inference that the identified brain–behavior associations reflect stable and generalizable mechanisms.

Taken together, these methodological considerations highlight the robustness of the present findings while acknowledging the inherent constraints of non-invasive neurostimulation and predictive modeling approaches. The converging results across experiments, analyses, and datasets strongly support the conclusion that the observed effects reflect specific and effective modulation of the hand motor network by TMS, as well as behaviorally meaningful brain–behavior relationships captured by resting-state connectivity.

4.4 Answers to the Research Questions

In the introduction, this thesis outlined central yet unresolved research questions in the field of motor control. It began by considering how neural interactions—namely, functional connectivity—are established among brain regions that are well known to participate in motor tasks, but whose patterns of interregional coordination remain poorly understood. The findings from Study 1 directly addressed the first and third questions, demonstrating that stimulation of a key parietal hub (hAIP) modulates connectivity within a broad, distributed network spanning dorsal and ventral streams, frontal motor regions, and the cerebellum. The combination of TMS with resting-state fMRI revealed both local and widespread effects, underscoring the value of integrating causal and correlational methods to map functional architecture.

Since resting-state functional connectivity has been shown to capture the organization of functionally engaged networks, including the motor system, the next question was whether such intrinsic activity

can also be linked to behavioral outputs. More specifically, does resting-state connectivity represent only low-level motor features, or does it also encode more abstract, higher-order aspects of motor control? Study 2 addressed this issue by demonstrating that resting-state connectivity can predict motor behavior across different tasks and effectors, and that a “core hand motor network” supports task-independent, generalizable features of motor function. Importantly, the predictive performance of this network was sensitive to TMS-induced perturbation, thereby linking representational properties observed at rest with causal manipulations of the system.

Taken together, these findings advance the understanding of human motor control by providing converging evidence that intrinsic connectivity patterns not only reflect the distributed organization of the hand motor network but also encode information directly relevant to action planning and execution, thereby fulfilling the conceptual and methodological objectives set out at the outset of this work.

4.5 General conclusions

Hand motor control has captivated scientific inquiry for centuries. The ability to perform thousands of complex, goal-directed actions with apparent ease is a hallmark of human motor function. Interest in this capacity dates back to early philosophical explorations by figures such as Aristotle and Plato. In the modern era, however, systematic scientific investigation—particularly through the advent of neuroimaging and neurostimulation techniques—has substantially deepened our understanding of the neural mechanisms underlying these skilled behaviors.

Across both studies, the results converge on three key conclusions:

- The hand motor system operates as a flexible, distributed network spanning dorsal and ventral pathways, frontal motor areas, and cerebellar regions.
- Intrinsic connectivity patterns encode not only task-specific but also task-independent, higher-order features of motor control.
- Combining rs-fMRI, multivariate analysis, predictive modelling, and TMS provides a powerful framework for mapping both the architecture and the causal relevance of motor networks.

By integrating complementary methods and analytical perspectives, this thesis advances the conceptual understanding of human motor network organization and lays a methodological foundation for future applications in both basic research and clinical translation.

4.5.1 Clinical implications

Beyond its theoretical contributions, the present work has potential translational relevance. First, the identification of a reproducible "core" hand motor network may provide a focused target for clinical investigations. Rather than probing the entire motor system, clinicians could use this reduced set of regions to better characterize specific motor deficits in patient populations, such as after stroke or in degenerative motor disorders. This network-level perspective may allow for more precise diagnosis by highlighting which subnetworks are preserved or disrupted, thereby reducing diagnostic complexity and guiding intervention strategies.

Second, the application of Connectome-Based Predictive Modelling (CPM) to hand motor control offers a promising framework for quantifying individual variability in motor functioning. Our findings that CPM predictions break down following TMS perturbation demonstrate that this approach is sensitive to causal manipulations and could thus serve as a biomarker for pathological disruptions. Similar frameworks have already been used in domains such as attention and ADHD (Wu et al., 2022; Yoo et al., 2022), where predictive models based on resting-state connectivity successfully differentiate between controls and clinical populations. Extending this approach to motor disorders could enable the characterization of latent deficits before they manifest clinically, offering new avenues for early detection and patient stratification.

Finally, the predictive dimension of CPM opens the possibility of forecasting motor recovery trajectories or future decline. In rehabilitation contexts, this could support personalized treatment planning by identifying which patients are most likely to benefit from specific interventions (e.g., neurostimulation, physiotherapy, or combined protocols). In progressive conditions, such as Parkinson's disease, predictive models might be harnessed to anticipate the evolution of motor symptoms and optimize therapeutic timing.

Taken together, the clinical implications of this work suggest that the integration of network-based neuroimaging and predictive modelling may not only deepen our understanding of hand motor control but also provide concrete tools for improving diagnosis, monitoring, and treatment of motor dysfunction in clinical populations.

5 Appendix

5.2 Supplementary materials: chapter 1

5.2.1 List of cited papers: dorsal stream involvement in reaching tasks (direction)

Authors	Label	X	Y	Z	Technique
Ciavarro et al., 2013	L aSPOC	-10	-83	44	TMS
Davare et al., 2012	L mIPS	-32	-49	46	TMS
Davare et al., 2015	L mIPS	-33	-47	48	TMS
	L dPM	-21	-6	68	TMS
Della-Maggiore et al., 2004	L Posterior Parietal	-36	-69	59	TMS
Krasovsky et al., 2014	visual	0	-76	2	MVPA
	L M1	-39	-21	54	MVPA
	L Parietal	-25	-48	67	MVPA
Marigold et al., 2019	L IPS1	-22	-80	41	TMS
	L IPS2	-19	-77	52	TMS
	L hand IPS	-26	-60	61	TMS
Striemer et al., 2011	L aSPL	-31	-47	54	TMS
	L pSPL	-20	-65	54	TMS
Vesia et al., 2010	L SPOC	-9	-79	50	TMS
	L mIPS	-22	-63	49	TMS
	L AG	-42	-66	49	TMS
Busan et al., 2009	No coordinates				TMS
Desmurget et al., 1999	No coordinates				TMS
Barany et al., 2014	No coordinates				MVPA

5.2.2 *List of cited papers: dorsal stream involvement in reaching tasks (effector)*

Authors	Label	X	Y	Z	Technique
Gallivan et al., 2011	L Precentral Gyrus	-45	-13	50	MVPA
	L pIPS	-22	-67	53	MVPA
	L mIPS	-34	-53	51	MVPA
	L dPM	-28	-8	56	MVPA
	L vPM	-59	2	32	MVPA
	L SPOC	-11	-74	40	MVPA
	L dmPFC	-2	-1	61	MVPA
	L dlPFC	-35	35	32	MVPA
Leoné et al., 2014	L mIPS	-21	-63	60	MVPA
	L aIPS	-32	-38	57	MVPA
	L aSPL	-27	-42	63	MVPA
	L aPCu	-15	-45	70	MVPA
	L pIPS	-21	-92	29	MVPA
Lee & Van Donkelaar, 2002	No coordinates				TMS
Lee & Van Donkelaar, 2006	No coordinates				TMS

5.2.3 *List of cited papers: dorsal stream involvement in grasping tasks (planning)*

Authors	Label	X	Y	Z	Technique
Fabbri et al., 2014	L aIPS	-41	-39	37	MVPA
	L anterior SPL	-32	-53	56	MVPA
	L posterior SPL	-17	-60	61	MVPA
	L vPM	-45	-15	49	MVPA
	L dPM1	-33	-26	62	MVPA
	L rostral SPL	-24	-40	69	MVPA
	L SMA	-8	-17	66	MVPA
Fabbri et al., 2016	L aIPS	-40	-40	38	MVPA
	L vPM	-50	-3	34	MVPA
Freud et al., 2018	L aIPS	-36	-47	47	MVPA

Gallivan et al., 2011	L dPM	-23	-2	61	MVPA
	L vPM	-56	9	30	MVPA
	L pIPS	-15	-60	58	MVPA
	L mIPS	-36	-55	49	MVPA
	L post aIPS	-37	-41	52	MVPA
	L aIPS	-51	-30	49	MVPA
	L pre-SMA	-7	10	40	MVPA
	L SMA	-6	4	52	MVPA
	L SPOC	-5	-74	43	MVPA
Gallivan et al., 2013	L dPM	-26	-8	55	MVPA
	L vPM	-55	6	13	MVPA
	L pIPS	-22	-66	53	MVPA
	L mIPS	-33	-53	53	MVPA
	L post-aIPS	-44	-46	49	MVPA
	L aIPS	-44	-37	47	MVPA
	L t-aIPS	-42	-39	52	MVPA
Gallivan et al., 2013	L pIPS	-22	-70	50	MVPA
	L mIPS	-34	-52	49	MVPA
	L post-aIPS	-42	-41	48	MVPA
	L aIPS	-47	-29	51	MVPA
	L aIPS	-45	-33	46	MVPA
	L vPM	-50	3	40	MVPA
	L dPM	-28	-11	55	MVPA
	L dlPFC	-33	34	38	MVPA
	L post-aIPS	-41	-44	43	MVPA
	L pre-SMA	-9	13	36	MVPA
Kadmon Harpaz et al., 2014	L aIPS	-33	-51	56	MVPA
Monaco et al., 2019	L SPOC	-14	-73	39	MVPA
	L dPM	-31	-6	53	MVPA
	L vPM	-47	5	11	MVPA

	L M1/S1	-35	-28	53	MVPA
	L aIPS	-38	-40	49	MVPA
Monaco et al., 2020	L dPM	-28	-12	53	MVPA
	L vPM	-48	9	21	MVPA
	L M1	-36	-26	49	MVPA
	L aIPS	-45	-28	40	MVPA
Schettino et al., 2015	L aIPS	-42	-37	49	TMS
Turella et al., 2020	L pIPS	-21	-70	48	MVPA
	L mIPS	-31	-53	48	MVPA
	L aIPS	-40	-32	46	MVPA
	L dPM	-22	-14	52	MVPA
	L vPM	-54	-6	43	MVPA
Cattaneo et al., 2015	No coordinates				TMS
Davare et al., 2007	No coordinates				TMS
McDowell et al., 2018	No coordinates				TMS
Rice et al., 2006	No coordinates				TMS
Rice et al., 2007	No coordinates				TMS
Schramm et al., 2019	No coordinates				TMS
Tunik et al., 2005	No coordinates				TMS
Tunik et al., 2008	No coordinates				TMS

5.2.4 List of cited papers: dorsal stream involvement in grasping tasks (execution)

Authors	Label	X	Y	Z	Technique
Breveglieri et al., 2023	L phAIP	-40	-43	42	TMS
	L hV6A	-10	-83	44	TMS
Dafotakis et al., 2008	L aIPS	-40	-41	38	TMS
	L vPM	-59	-11	25	TMS
Davare et al., 2006	L vPM	-60	16	23	TMS
	L dPM	-22	-4	71	TMS
	L vPM	-60	16	23	TMS

	L dPM	-22	-4	71	TMS
Davare et al., 2007	L aIPS	-43	-39	46	TMS
Fabbri et al., 2014	L S1	-41	-36	57	MVPA
	L M1	-33	-30	52	MVPA
	L dPM2	-20	-29	70	MVPA
Fabbri et al., 2016	L V1	-5	-85	2	MVPA
	L pSPOC	-12	-80	36	MVPA
	L aSPOC	-13	-81	36	MVPA
Gallivan et al., 2011	L M1	-34	-13	60	MVPA
	L Precentral Gyrus	-40	-5	58	MVPA
	L SMG	-60	-43	29	MVPA
	L aPCu	-13	-73	52	MVPA
Gallivan et al., 2013	L SMG	-59	-33	37	MVPA
	L M1	-39	-25	52	MVPA
	L SPOC	-7	-75	35	MVPA
Gallivan et al., 2013	L M1	-33	-16	58	MVPA
	L SMA	-9	-16	62	MVPA
Glover et al., 2005	L aIPS	-24	-64	68	TMS
Goldenkoff et al., 2023	L PPC	-35	-56	50	TMS
Gutteling et al., 2013	L aIPS	-42	-47	57	TMS
Kadmon Harpaz et al., 2014	L M1	-34	-30	60	MVPA
	L insula	-46	-1	8	MVPA
	L SMA	-3	-11	61	MVPA
Lega et al., 2020	L vPM	-53	-1	50	TMS
	L SMA	-64	18	22	TMS
	L vPM	-8	-1	80	TMS
Monaco et al., 2019	L SPOC	-14	-73	39	MVPA
Parikh et al., 2020	L S1	-42	-25	57	TMS
Potok et al., 2019	L amSMG	-55	-35	39	TMS
Schettino et al., 2015	L vPM	-50	18	3	TMS

	L aIPS	-42	-37	49	TMS
Taubert et al., 2010	L aIPS	-42	-39	44	TMS
Turella et al., 2020	L M1	-31	-28	58	MVPA
	L vPM	-54	-6	43	MVPA
van Polanen et al., 2020	L aIPS	-46	-37	46	TMS
van Polanen et al., 2022	L aIPS	-45	-39	48	TMS
White et al., 2013	L SMA	-7	-6	73	TMS
Dafotakis et al., 2008	No coordinates				TMS
Davare et al., 2007	No coordinates				TMS
McDowell et al., 2018	No coordinates				TMS
Rice et al., 2006	No coordinates				TMS
Rice et al., 2007	No coordinates				TMS
Schramm et al., 2019	No coordinates				TMS
Tunik et al., 2005	No coordinates				TMS
Tunik et al., 2008	No coordinates				TMS

5.2.5 List of cited papers: ventral stream involvement in motor control

Authors	Label	X	Y	Z	Technique
Adam et al., 2016	L LOC	-46	-75	-9	TMS
	L AG	-44	-73	29	TMS
Cohen et al., 2009	L LO	-46	-69	-13	TMS
Freud et al., 2018	L LO	-45	-71	-10	MVPA
Gallivan et al., 2013	L LO	-45	-71	-7	MVPA
	L pFS	-32	-48	-16	MVPA
	L FFA	-40	-42	-23	MVPA
	L PPA	-23	-41	-8	MVPA
	L EBA	-54	-76	12	MVPA
	L FBA	-44	-44	-23	MVPA
Gallivan et al., 2013	L pMTG	-56	-60	-1	MVPA
	L EBA	-52	-75	5	MVPA

Krasovsky et al., 2014	Visual	0	-76	2	MVPA
Monaco et al., 2019	L LO	-39	-1	-7	MVPA
	L LOtv	-45	-65	-10	MVPA
	L EBA	-50	-74	8	MVPA
	L MT	-46	-74	5	MVPA
Monaco et al., 2020	L EVC	-9	-91	8	MVPA
van Polanen et al., 2020	L LO	-47	-61	-16	TMS
Threethipthikoon et al., 2023	No coordinates				MVPA

6 References

Abdelgabar, A. R., Suttrup, J., Broersen, R., Bhandari, R., Picard, S., Keysers, C., De Zeeuw, C. I., & Gazzola, V. (2019). Action perception recruits the cerebellum and is impaired in patients with spinocerebellar ataxia. *Brain*, *142*(12), 3791–3805. https://doi.org/10.1093/brain/awz337

Adam, J. J., Bovend'Eerdt, T. J. H., Schuhmann, T., & Sack, A. T. (2016). Allocentric coding in ventral and dorsal routes during real-time reaching: Evidence from imaging-guided multi-site brain stimulation. *Behavioural Brain Research*, *300*, 143–149. https://doi.org/10.1016/j.bbr.2015.12.018

Andersen, R. A., & Buneo, C. A. (2002). Intentional maps in posterior parietal cortex. *Annual Review of Neuroscience*, *25*, 189–220. https://doi.org/10.1146/annurev.neuro.25.112701.142922

Arfeller, C., Schwarzbach, J., Ubaldi, S., Ferrari, P., Barchiesi, G., & Cattaneo, L. (2013). Whole-brain haemodynamic after-effects of 1-Hz magnetic stimulation of the posterior superior temporal cortex during action observation. *Brain Topography*, *26*(2), 278–291. https://doi.org/10.1007/s10548-012-0239-9

Ariani, G., Pruszynski, J. A., & Diedrichsen, J. (2022). Motor planning brings human primary somatosensory cortex into action-specific preparatory states. *eLife*, *11*, 1–20. https://doi.org/10.7554/eLife.69517

Barany, D. A., Della-Maggiore, V., Viswanathan, S., Cieslak, M., & Grafton, S. T. (2014). Feature interactions enable decoding of sensorimotor transformations for goal-directed movement. *Journal of Neuroscience*, *34*(20), 6860–6873. https://doi.org/10.1523/JNEUROSCI.5173-13.2014

Battaglia-Mayer, A., Ferrari-Toniolo, S., Visco-Comandini, F., Archambault, P. S., Saberi-Moghadam, S., & Caminiti, R. (2013). Impairment of online control of hand and eye movements in a monkey model of optic ataxia. *Cerebral Cortex (New York, N.Y. : 1991)*, *23*(11), 2644–2656. https://doi.org/10.1093/cercor/bhs250

Benjamini, Y., & Hochberg, Y. (1995). Controlling the False Discovery Rate: A Practical and Powerful Approach to Multiple. *Source: Journal of the Royal Statistical Society. Series B (Methodological)*, *57*(1), 289–300.

Bernstein, N. (1966). The co-ordination and regulation of movements. *The Co-Ordination and Regulation of Movements*.

Betti, V., Della Penna, S., De Pasquale, F., & Corbetta, M. (2021). Spontaneous Beta Band Rhythms in the Predictive Coding of Natural Stimuli. *The Neuroscientist*, *27*(2), 184–201. https://doi.org/10.1177/1073858420928988

Binkofski, F., & Buxbaum, L. J. (2013). Two action systems in the human brain. *Brain and Language*, *127*(2), 222–229. https://doi.org/10.1016/j.bandl.2012.07.007

Biswal, B. B., & Uddin, L. Q. (2025). The history and future of resting-state functional magnetic resonance imaging. *Nature*, *641*(8065), 1121–1131. https://doi.org/10.1038/s41586-025-08953-9

Borra, E., Belmalih, A., Calzavara, R., Gerbella, M., Murata, A., Rozzi, S., & Luppino, G. (2008). Cortical connections of the macaque anterior intraparietal (AIP) area. *Cerebral Cortex*, *18*(5), 1094–1111. https://doi.org/10.1093/cercor/bhm146

Borra, E., Gerbella, M., Rozzi, S., & Luppino, G. (2017). The macaque lateral grasping network: A neural substrate for generating purposeful hand actions. *Neuroscience and Biobehavioral Reviews*, *75*, 65–90. https://doi.org/10.1016/j.neubiorev.2017.01.017

Borra, E., Ichinohe, N., Sato, T., Tanifuji, M., & Rockland, K. S. (2010). Cortical connections to area te in monkey: Hybrid modular and distributed organization. *Cerebral Cortex*, *20*(2), 257–270. https://doi.org/10.1093/cercor/bhp096

Borra, E., & Luppino, G. (2017). Functional anatomy of the macaque temporo-parieto-frontal connectivity. *Cortex*, *97*, 306–326. https://doi.org/10.1016/j.cortex.2016.12.007

Borra, E., & Luppino, G. (2019). Large-scale temporo-parieto-frontal networks for motor and cognitive motor functions in the primate brain. *Cortex; a Journal Devoted to the Study of the Nervous System and Behavior*, *118*, 19–37. https://doi.org/10.1016/j.cortex.2018.09.024

Boudrias, M. H., Gonçalves, C. S., Penny, W. D., Park, C. hyun, Rossiter, H. E., Talelli, P., & Ward, N. S. (2012). Age-related changes in causal interactions between cortical motor regions during hand grip. *NeuroImage*, *59*(4), 3398–3405. https://doi.org/10.1016/j.neuroimage.2011.11.025

Bracci, S., Cavina-Pratesi, C., Ietswaart, M., Caramazza, A., & Peelen, M. V. (2012). Closely overlapping responses to tools and hands in left lateral occipitotemporal cortex. *Journal of Neurophysiology*, *107*(5), 1443–1446. https://doi.org/10.1152/jn.00619.2011

Bracci, S., & Peelen, M. V. (2013). Body and object effectors: The organization of object representations in high-level visual cortex reflects body-object interactions. *Journal of Neuroscience*, *33*(46), 18247–18258. https://doi.org/10.1523/JNEUROSCI.1322-13.2013

Breveglieri, R., Borgomaneri, S., Filippini, M., Tessari, A., Galletti, C., Davare, M., & Fattori, P. (2023). Complementary contribution of the medial and lateral human parietal cortex to grasping: A repetitive TMS study. *Cerebral Cortex*, *33*(9), 5122–5134. https://doi.org/10.1093/cercor/bhac404

Breveglieri, R., Bosco, A., Borgomaneri, S., Tessari, A., Galletti, C., Avenanti, A., & Fattori, P. (2020). Transcranial Magnetic Stimulation Over the Human Medial Posterior Parietal Cortex Disrupts Depth Encoding During Reach Planning. *Cerebral Cortex*, *February*, 1–14. https://doi.org/10.1093/cercor/bhaa224

Buckner, R. L. (2013). The cerebellum and cognitive function: 25 years of insight from anatomy and neuroimaging. *Neuron*, *80*(3), 807–815. https://doi.org/10.1016/j.neuron.2013.10.044

Budisavljevic, S., Dell'Acqua, F., Zanatto, D., Begliomini, C., Miotto, D., Motta, R., & Castiello, U. (2016). Asymmetry and Structure of the Fronto-Parietal Networks Underlie Visuomotor Processing in Humans. *Cerebral Cortex*, bhv348. https://doi.org/10.1093/cercor/bhv348

Busan, P., Barbera, C., Semenic, M., Monti, F., Pizzolato, G., Pelamatti, G., & Battaglini, P. P. (2009). Effect of transcranial magnetic stimulation (TMS) on parietal and premotor cortex during planning of reaching movements. *PLoS ONE*, *4*(2). https://doi.org/10.1371/journal.pone.0004621

Cattaneo, L., Maule, F., Tabarelli, D., Brochier, T., & Barchiesi, G. (2015). Online repetitive transcranial magnetic stimulation (TMS) to the parietal operculum disrupts haptic memory for grasping. *Human Brain Mapping*, *36*(11), 4262–4271. https://doi.org/10.1002/hbm.22915

Cavina-Pratesi, C., Monaco, S., Fattori, P., Galletti, C., McAdam, T. D., Quinlan, D. J., Goodale, M. A., & Culham, J. C. (2010). Functional magnetic resonance imaging reveals the neural substrates of arm transport and grip formation in reach-to-grasp actions in humans. *Journal of Neuroscience*, *30*(31), 10306–10323. https://doi.org/10.1523/JNEUROSCI.2023-10.2010

Ciavarro, M., Ambrosini, E., Tosoni, A., Committeri, G., Fattori, P., & Galletti, C. (2013). rTMS of Medial Parieto-occipital Cortex Interferes with Attentional Reorienting during Attention and Reaching Tasks. *Journal of Cognitive Neuroscience*, *25*(9), 1453–1462. https://doi.org/10.1162/jocn_a_00409

Cohen, N. R., Cross, E. S., Tunik, E., Grafton, S. T., & Culham, J. C. (2009). Ventral and dorsal stream contributions to the online control of immediate and delayed grasping: A TMS approach. *Neuropsychologia*, *47*(6), 1553–1562. https://doi.org/10.1016/j.neuropsychologia.2008.12.034

Culham, J. C. (2004). Human brain imaging reveals a parietal area specialized for grasping. *Attention and Perfomance XX. Functional Brain Imeging of Visual Cognition*, 417–438.

Culham, J. C., Cavina-Pratesi, C., & Singhal, A. (2006). The role of parietal cortex in visuomotor control: What have we learned from neuroimaging? *Neuropsychologia*, *44*(13), 2668–2684. https://doi.org/10.1016/j.neuropsychologia.2005.11.003

Culham, J. C., Danckert, S. L., DeSouza, J. F. X., Gati, J. S., Menon, R. S., & Goodale, M. A. (2003). Visually guided grasping produces fMRI activation in dorsal but not ventral stream brain areas. *Experimental Brain Research*, *153*(2), 180–189. https://doi.org/10.1007/s00221-003-1591-5

Culham, J. C., & Valyear, K. F. (2006). Human parietal cortex in action. *Current Opinion in Neurobiology*, *16*(2), 205–212. https://doi.org/10.1016/j.conb.2006.03.005

Dafotakis, M., Sparing, R., Eickhoff, S. B., Fink, G. R., & Nowak, D. A. (2008). On the role of the ventral premotor cortex and anterior intraparietal area for predictive and reactive scaling of grip force. *Brain Research*, *1228*, 73–80. https://doi.org/10.1016/j.brainres.2008.06.027

Davare, M., Andres, M., Clerget, E., Thonnard, J. L., & Olivier, E. (2007). Temporal dissociation between hand shaping and grip force scaling in the anterior intraparietal area. *Journal of Neuroscience*, *27*(15), 3974–3980. https://doi.org/10.1523/JNEUROSCI.0426-07.2007

Davare, M., Andres, M., Cosnard, G., Thonnard, J. L., & Olivier, E. (2006). Dissociating the role of ventral and dorsal premotor cortex in precision grasping. *Journal of Neuroscience*, *26*(8), 2260–2268. https://doi.org/10.1523/JNEUROSCI.3386-05.2006

Davare, M., Duque, J., Vandermeeren, Y., Thonnard, J. L., & Olivier, E. (2007). Role of the ipsilateral primary motor cortex in controlling the timing of hand muscle recruitment. *Cerebral Cortex*, *17*(2), 353–362. https://doi.org/10.1093/cercor/bhj152

Davare, M., Zénon, A., Desmurget, M., & Olivier, E. (2015). Dissociable contribution of the parietal and frontal cortex to coding movement direction and amplitude. *Frontiers in Human Neuroscience*, *9*(MAY), 1–12. https://doi.org/10.3389/fnhum.2015.00241

Davare, M., Zénon, A., Pourtois, G., Desmurget, M., & Olivier, E. (2012). Role of the medial part of the intraparietal sulcus in implementing movement direction. *Cerebral Cortex*, *22*(6), 1382–1394. https://doi.org/10.1093/cercor/bhr210

de Vries, P. M., de Jong, B. M., Bohning, D. E., Walker, J. A., George, M. S., & Leenders, K. L. (2009). Changes in cerebral activations during movement execution and imagery after parietal cortex TMS interleaved with 3T MRI. *Brain Research*, *1285*, 58–68. https://doi.org/10.1016/j.brainres.2009.06.006

Della-Maggiore, V., Malfait, N., Ostry, D. J., & Paus, T. (2004). Stimulation of the Posterior Parietal Cortex Interferes with Arm Trajectory Adjustments during the Learning of New Dynamics. *The Journal of Neuroscience*, *24*(44), 9971–9976. https://doi.org/10.1523/JNEUROSCI.2833-04.2004

Desmurget, M., Epstein, C. M., Turner, R. S., Prablanc, C., Alexander, G. E., & Grafton, S. T. (1999). Role of the posterior parietal cortex in updating reaching movements to a visual target. *Nature Neuroscience*, *2*(6), 563–567. https://doi.org/10.1038/9219

Di Caro, V., Cesari, P., Sala, F., & Cattaneo, L. (2025). The neural bases of the reach–grasp movement in humans: Quantitative evidence from brain lesions. *Proceedings of the National Academy of Sciences*, *122*(10). https://doi.org/10.1073/pnas.2419801122

Diedrichsen, J. (2006). A spatially unbiased atlas template of the human cerebellum. *NeuroImage*, *33*(1), 127–138. https://doi.org/10.1016/j.neuroimage.2006.05.056

Diedrichsen, J., & Zotow, E. (2015). Surface-based display of volume-averaged cerebellar imaging data. *PLoS ONE*, *10*(7), 1–18. https://doi.org/10.1371/journal.pone.0133402

Dimakou, A., Pezzulo, G., Zangrossi, A., & Corbetta, M. (2025). The predictive nature of spontaneous brain activity across scales and species. *Neuron*, 1–23. https://doi.org/10.1016/j.neuron.2025.02.009

Ehrsson, H. H., Fagergren, A., Johansson, R. S., & Forssberg, H. (2003). Evidence for the Involvement of the Posterior Parietal Cortex in Coordination of Fingertip Forces for Grasp Stability in Manipulation. *Journal of Neurophysiology*, *90*(5), 2978–2986. https://doi.org/10.1152/jn.00958.2002

Errante, A., & Fogassi, L. (2020). Activation of cerebellum and basal ganglia during the observation and execution of manipulative actions. *Scientific Reports*, *10*(1), 1–15. https://doi.org/10.1038/s41598-020-68928-w

Errante, A., Ziccarelli, S., Mingolla, G., & Fogassi, L. (2021). Grasping and Manipulation: Neural Bases and Anatomical Circuitry in Humans. *Neuroscience*, *458*, 203–212. https://doi.org/10.1016/j.neuroscience.2021.01.028

Fabbri, S., Strnad, L., Caramazza, A., & Lingnau, A. (2014). Overlapping representations for grip type and reach direction. *NeuroImage*, *94*, 138–146. https://doi.org/10.1016/j.neuroimage.2014.03.017

Fabbri, S., Stubbs, K. M., Cusack, R., & Culham, J. C. (2016). Disentangling representations of object and grasp properties in the human brain. *Journal of Neuroscience*, *36*(29), 7648–7662. https://doi.org/10.1523/JNEUROSCI.0313-16.2016

Fattori, P., Breveglieri, R., Bosco, A., Gamberini, M., & Galletti, C. (2017). Vision for prehension in the medial parietal cortex. *Cerebral Cortex*, *27*(2), 1149–1163. https://doi.org/10.1093/cercor/bhv302

Fattori, P., Breveglieri, R., Raos, V., Bosco, A., & Galletti, C. (2012). Vision for Action in the Macaque Medial Posterior Parietal Cortex. *Journal of Neuroscience*, *32*(9), 3221–3234. https://doi.org/10.1523/JNEUROSCI.5358-11.2012

Fattori, P., Raos, V., Breveglieri, R., Bosco, A., Marzocchi, N., & Galletti, C. (2010). The dorsomedial pathway is not just for reaching: Grasping neurons in the medial parieto-occipital cortex of the macaque monkey. *Journal of Neuroscience*, *30*(1), 342–349. https://doi.org/10.1523/JNEUROSCI.3800-09.2010

Filimon, F. (2010). Human cortical control of hand movements: Parietofrontal networks for reaching, grasping, and pointing. *Neuroscientist*, *16*(4), 388–407. https://doi.org/10.1177/1073858410375468

Filimon, F., Nelson, J. D., Hagler, D. J., & Sereno, M. I. (2007). Human cortical representations for reaching: Mirror neurons for execution, observation, and imagery. *NeuroImage*, *37*(4), 1315–1328. https://doi.org/10.1016/j.neuroimage.2007.06.008

Filimon, F., Nelson, J. D., Huang, R. S., & Sereno, M. I. (2009). Multiple parietal reach regions in humans: Cortical representations for visual and proprioceptive feedback during on-line reaching. *Journal of Neuroscience*, *29*(9), 2961–2971. https://doi.org/10.1523/JNEUROSCI.3211-08.2009

Foltys, H., Meister, I. G., Weidemann, J., Sparing, R., Thron, A., Willmes, K., Töpper, R., Hallett, M., & Boroojerdi, B. (2003). Power grip disinhibits the ipsilateral sensorimotor cortex: A TMS and fMRI study. *NeuroImage*, *19*(2), 332–340. https://doi.org/10.1016/S1053-8119(03)00107-1

Fornia, L., Ferpozzi, V., Montagna, M., Rossi, M., Riva, M., Pessina, F., Boneschi, F. M., Borroni, P., Lemon, R. N., Bello, L., & Cerri, G. (2018). Functional characterization of the left ventrolateral premotor cortex in humans: A direct electrophysiological approach. *Cerebral Cortex*, *28*(1), 167–183. https://doi.org/10.1093/cercor/bhw365

Fornia, L., Rossi, M., Rabuffetti, M., Bellacicca, A., Viganò, L., Simone, L., Howells, H., Puglisi, G., Leonetti, A., Callipo, V., Bello, L., & Cerri, G. (2022). Motor impairment evoked by direct electrical stimulation of human parietal cortex during object manipulation. *NeuroImage*, *248*(December 2021), 118839. https://doi.org/10.1016/j.neuroimage.2021.118839

Freud, E., Macdonald, S. N., Chen, J., Quinlan, D. J., Goodale, M. A., & Culham, J. C. (2018). Getting a grip on reality: Grasping movements directed to real objects and images rely on dissociable neural representations. *Cortex*, *98*, 34–48. https://doi.org/10.1016/j.cortex.2017.02.020

Gale, D. J., Flanagan, J. R., & Gallivan, J. P. (2021). Human somatosensory cortex is modulated during motor planning. *The Journal of Neuroscience*, *41*(27), JN-RM-0342-21. https://doi.org/10.1523/jneurosci.0342-21.2021

Galletti, C., & Fattori, P. (2018). The dorsal visual stream revisited: Stable circuits or dynamic pathways? *Cortex*, *98*, 203–217. https://doi.org/10.1016/j.cortex.2017.01.009

Galletti, C., Gamberini, M., & Fattori, P. (2022). The posterior parietal area V6A: An attentionally-modulated visuomotor region involved in the control of reach-to-grasp action. *Neuroscience & Biobehavioral Reviews*, *141*(May), 104823. https://doi.org/10.1016/j.neubiorev.2022.104823

Gallivan, J. P., Adam McLean, D., Smith, F. W., & Culham, J. C. (2011). Decoding effector-dependent and effector-independent movement intentions from human parieto-frontal brain activity. *Journal of Neuroscience*, *31*(47), 17149–17168. https://doi.org/10.1523/JNEUROSCI.1058-11.2011

Gallivan, J. P., Adam McLean, D., Valyear, K. F., & Culham, J. C. (2013). Decoding the neural mechanisms of human tool use. *eLife*, *2013*(2), 1–29. https://doi.org/10.7554/eLife.00425

Gallivan, J. P., Cant, J. S., Goodale, M. A., & Flanagan, J. R. (2014). Representation of object weight in human ventral visual cortex. *Current Biology*, *24*(16), 1866–1873. https://doi.org/10.1016/j.cub.2014.06.046

Gallivan, J. P., Chapman, C. S., Gale, D. J., Flanagan, J. R., & Culham, J. C. (2019). Selective Modulation of Early Visual Cortical Activity by Movement Intention. *Cerebral Cortex*, *29*(11), 4662–4678. https://doi.org/10.1093/cercor/bhy345

Gallivan, J. P., Chapman, C. S., Mclean, D. A., Flanagan, J. R., & Culham, J. C. (2013). Activity patterns in the category-selective occipitotemporal cortex predict upcoming motor actions. *European Journal of Neuroscience*, *38*(3), 2408–2424. https://doi.org/10.1111/ejn.12215

Gallivan, J. P., & Culham, J. C. (2015). Neural coding within human brain areas involved in actions. *Current Opinion in Neurobiology*, *33*, 141–149. https://doi.org/10.1016/j.conb.2015.03.012

Gallivan, J. P., & Goodale, M. A. (2018). The dorsal "action" pathway. *Handbook of Clinical Neurology*, *151*, 449–466. https://doi.org/10.1016/B978-0-444-63622-5.00023-1

Gallivan, J. P., McLean, A., & Culham, J. C. (2011). Neuroimaging reveals enhanced activation in a reach-selective brain area for objects located within participants' typical hand workspaces. *Neuropsychologia*, *49*(13), 3710–3721. https://doi.org/10.1016/j.neuropsychologia.2011.09.027

Gallivan, J. P., McLean, D. A., Flanagan, J. R., & Culham, J. C. (2013). Where one hand meets the other: Limb-specific and action-dependent movement plans decoded from preparatory signals in single human frontoparietal brain areas. *Journal of Neuroscience*, *33*(5), 1991–2008. https://doi.org/10.1523/JNEUROSCI.0541-12.2013

Gallivan, J. P., McLean, D. A., Valyear, K. F., Pettypiece, C. E., & Culham, J. C. (2011). Decoding action intentions from preparatory brain activity in human parieto-frontal networks. *Journal of Neuroscience*, *31*(26), 9599–9610. https://doi.org/10.1523/JNEUROSCI.0080-11.2011

Gamberini, M., Passarelli, L., Fattori, P., Zucchelli, M., Bakola, S., Luppino, G., & Galletti, C. (2009). Cortical connections of the visuomotor parietooccipital area V6Ad of the macaque monkey. *The Journal of Comparative Neurology*, *513*(6), 622–642. https://doi.org/10.1002/cne.21980

Gharbawie, O. a, Stepniewska, I., Qi, H., & Kaas, J. H. (2011). Multiple parietal-frontal pathways mediate grasping in macaque monkeys. *The Journal of Neuroscience : The Official Journal of the Society for Neuroscience*, *31*(32), 11660–11677. https://doi.org/10.1523/JNEUROSCI.1777-11.2011

Giampiccolo, D., Basaldella, F., Badari, A., Squintani, G. M., Cattaneo, L., & Sala, F. (2021). Feasibility of cerebello-cortical stimulation for intraoperative neurophysiological monitoring of cerebellar mutism. *Child's Nervous System*, *37*(5), 1505–1514. https://doi.org/10.1007/s00381-021-05126-7

Glasser, M. F., Coalson, T. S., Robinson, E. C., Hacker, C. D., Harwell, J., Yacoub, E., Ugurbil, K., Andersson, J., Beckmann, C. F., Jenkinson, M., Smith, S. M., & Van Essen, D. C. (2016). A multi-modal parcellation of human cerebral cortex. *Nature*, *536*(7615), 171–178. https://doi.org/10.1038/nature18933

Glasser, M. F., Sotiropoulos, S. N., Wilson, J. A., Coalson, T. S., Fischl, B., Andersson, J. L., Xu, J., Jbabdi, S., Webster, M., Polimeni, J. R., Van Essen, D. C., & Jenkinson, M. (2013). The minimal preprocessing pipelines for the Human Connectome Project. *NeuroImage*, *80*, 105–124. https://doi.org/10.1016/j.neuroimage.2013.04.127

Glover, S., Miall, R. C., & Rushworth, M. F. S. (2005). Parietal rTMS disrupts the initiation but not the execution of on-line adjustments to a perturbation of object size. *Journal of Cognitive Neuroscience*, *17*(1), 124–136. https://doi.org/10.1162/0898929052880066

Goldenkoff, E. R., Deluisi, J. A., Destiny, D. P., Lee, T. G., Michon, K. J., Brissenden, J. A., Taylor, S. F., Polk, T. A., & Vesia, M. (2023). The behavioral and neural effects of parietal theta burst stimulation on the grasp network are stronger during a grasping task than at rest. *Frontiers in Neuroscience*, *17*, 1198222. https://doi.org/10.3389/fnins.2023.1198222

Goodale, M. A. (2005). Action insight: The role of the dorsal stream in the perception of grasping. *Neuron*, *47*(3), 328–329. https://doi.org/10.1016/j.neuron.2005.07.010

Goodale, M. A., Króliczak, G., & Westwood, D. A. (2005). Dual routes to action: Contributions of the dorsal and ventral streams to adaptive behavior. *Progress in Brain Research*, *149*, 269–283. https://doi.org/10.1016/S0079-6123(05)49019-6

Goodale, M. A., & Milner, A. D. (1992). Separate visual pathways for perception and action. *Trends Neurosci*, *15*, 20–25.

Goodman, J. M., Tabot, G. A., Lee, A. S., Suresh, A. K., Rajan, A. T., Hatsopoulos, N. G., & Bensmaia, S. (2019). Postural Representations of the Hand in the Primate Sensorimotor Cortex. *Neuron*, *104*(5), 1000-1009.e7. https://doi.org/10.1016/j.neuron.2019.09.004

Gordon, E. M., Laumann, T. O., Adeyemo, B., Huckins, J. F., Kelley, W. M., & Petersen, S. E. (2016). Generation and Evaluation of a Cortical Area Parcellation from Resting-State Correlations. *Cerebral Cortex*, *26*(1), 288–303. https://doi.org/10.1093/cercor/bhu239

Grafton, S. T. (2010). The cognitive neuroscience of prehension: Recent developments. *Experimental Brain Research*, *204*(4), 475–491. https://doi.org/10.1007/s00221-010-2315-2

Grefkes, C., & Fink, G. R. (2005). The functional organization of the intraparietal sulcus in humans and monkeys. *Journal of Anatomy*, *207*(1), 3–17. https://doi.org/10.1111/j.1469-7580.2005.00426.x

Grefkes, C., Nowak, D. A., Wang, L. E., Dafotakis, M., Eickhoff, S. B., & Fink, G. R. (2010). Modulating cortical connectivity in stroke patients by rTMS assessed with fMRI and dynamic causal modeling. *NeuroImage*, *50*(1), 233–242. https://doi.org/10.1016/j.neuroimage.2009.12.029

Greulich, R. S., Adam, R., Everling, S., & Scherberger, H. (2020). Shared functional connectivity between the dorso-medial and dorso-ventral streams in macaques. *Scientific Reports*, *10*(1), 1–17. https://doi.org/10.1038/s41598-020-75219-x

Griffanti, L., Salimi-Khorshidi, G., Beckmann, C. F., Auerbach, E. J., Douaud, G., Sexton, C. E., Zsoldos, E., Ebmeier, K. P., Filippini, N., Mackay, C. E., Moeller, S., Xu, J., Yacoub, E., Baselli, G., Ugurbil, K., Miller, K. L., & Smith, S. M. (2014). ICA-based artefact removal and accelerated fMRI acquisition for improved resting state network imaging. *NeuroImage*, *95*, 232–247. https://doi.org/10.1016/j.neuroimage.2014.03.034

Grill-Spector, K., & Malach, R. (2004). The human visual cortex. *Annual Review of Neuroscience*, *27*, 649–677. https://doi.org/10.1146/annurev.neuro.27.070203.144220

Guerra-Carrillo, B., Mackey, A. P., & Bunge, S. A. (2014). Resting-State fMRI: A Window into Human Brain Plasticity. *The Neuroscientist*, *20*(5), 522–533. https://doi.org/10.1177/1073858414524442

Gutteling, T. P., Park, S. Y., Kenemans, J. L., & Neggers, S. F. W. (2013). TMS of the anterior intraparietal area selectively modulates orientation change detection during action preparation. *Journal of Neurophysiology*, *110*(1), 33–41. https://doi.org/10.1152/jn.00622.2012

Gutteling, T. P., Petridou, N., Dumoulin, S. O., Harvey, B. M., Aarnoutse, E. J., Leon Kenemans, J., & Neggers, S. F. W. (2015). Action preparation shapes processing in early visual cortex. *Journal of Neuroscience*, *35*(16), 6472–6480. https://doi.org/10.1523/JNEUROSCI.1358-14.2015

Handwerker, D. A., Ianni, G., Gutierrez, B., Roopchansingh, V., Gonzalez-Castillo, J., Chen, G., Bandettini, P. A., Ungerleider, L. G., & Pitcher, D. (2020). Theta-burst TMS to the posterior superior temporal sulcus decreases resting-state fMRI connectivity across the face processing network. *Network Neuroscience*, *4*(3), 746–760. https://doi.org/10.1162/netn_a_00145

Haufe, S., Meinecke, F., Görgen, K., Dähne, S., Haynes, J. D., Blankertz, B., & Bießmann, F. (2014). On the interpretation of weight vectors of linear models in multivariate neuroimaging. *NeuroImage*, *87*, 96–110. https://doi.org/10.1016/j.neuroimage.2013.10.067

Hikosaka, O., Tanaka, M., Sakamoto, M., & Iwamura, Y. (1985). Deficits in manipulative behaviors induced by local injections of muscimol in the first somatosensory cortex of the conscious monkey. *Brain Research*, *325*(1–2), 375–380. https://doi.org/10.1016/0006-8993(85)90344-0

Hohenfeld, C., Werner, C. J., & Reetz, K. (2018). Resting-state connectivity in neurodegenerative disorders: Is there potential for an imaging biomarker? *NeuroImage: Clinical*, *18*, 849–870. https://doi.org/10.1016/j.nicl.2018.03.013

Howells, H., Simone, L., Borra, E., Fornia, L., Cerri, G., & Luppino, G. (2020). Reproducing macaque lateral grasping and oculomotor networks using resting state functional connectivity and diffusion tractography. *Brain Structure and Function*, *225*(8), 2533–2551. https://doi.org/10.1007/s00429-020-02142-2

Huang, Y. Z., Chen, R. S., Rothwell, J. C., & Wen, H. Y. (2007). The after-effect of human theta burst stimulation is NMDA receptor dependent. *Clinical Neurophysiology*, *118*(5), 1028–1032. https://doi.org/10.1016/j.clinph.2007.01.021

Huang, Y. Z., Edwards, M. J., Rounis, E., Bhatia, K. P., & Rothwell, J. C. (2005). Theta burst stimulation of the human motor cortex. *Neuron*, *45*(2), 201–206. https://doi.org/10.1016/j.neuron.2004.12.033

Huang, Y.-Z., Edwards, M. J., Rounis, E., Bhatia, K. P., & Rothwell, J. C. (2005). Theta burst stimulation of the human motor cortex. *Neuron*, *45*(2), 201–206. https://doi.org/10.1016/j.neuron.2004.12.033

Hutchison, R. M., Culham, J. C., Everling, S., Flanagan, J. R., & Gallivan, J. P. (2014). Distinct and distributed functional connectivity patterns across cortex reflect the domain-specific constraints of object, face, scene, body, and tool category-selective modules in the ventral visual pathway. *NeuroImage*, *96*, 216–236. https://doi.org/10.1016/j.neuroimage.2014.03.068

Hutchison, R. M., & Gallivan, J. P. (2018). Functional coupling between frontoparietal and occipitotemporal pathways during action and perception. *Cortex*, *98*, 8–27. https://doi.org/10.1016/j.cortex.2016.10.020

Ishida, H., Fornia, L., Grandi, L. C., Umiltà, M. A., & Gallese, V. (2013). Somato-Motor Haptic Processing in Posterior Inner Perisylvian Region (SII/pIC) of the Macaque Monkey. *PLoS ONE*, *8*(7). https://doi.org/10.1371/journal.pone.0069931

Ishida, H., Grandi, L. C., & Fornia, L. (2024). Secondary somatosensory and posterior insular cortices: A somatomotor hub for object prehension and manipulation movements. *Frontiers in Integrative Neuroscience*, *18*(April). https://doi.org/10.3389/fnint.2024.1346968

Jeannerod, M., Arbib, M. A., Rizzolatti, G., & Sakata, H. (1995). Grasping objects: The cortical mechanisms of visuomotor transformation. *Trends in Neurosciences*, *18*(7), 314–320. https://doi.org/10.1016/0166-2236(95)93921-J

Johnen, V. M., Neubert, F. X., Buch, E. R., Verhagen, L. M., O'Reilly, J., Mars, R. B., & Rushworth, M. F. S. (2015). Causal manipulation of functional connectivity in a specific neural pathway during behaviour and at rest. *eLife*, *2015*(4), 1–23. https://doi.org/10.7554/eLife.04585

Kadmon Harpaz, N., Flash, T., & Dinstein, I. (2014). Scale-invariant movement encoding in the human motor system. *Neuron*, *81*(2), 452–462. https://doi.org/10.1016/j.neuron.2013.10.058

Kastner, S., & Ungerleider, L. G. (2000). Mechanisms of Visual attention in the human cortex. *Annual Review of Neuroscience*, *23*, 315–341.

Kim, J., Andrews-Hanna, J. R., Eisenbarth, H., Lux, B. K., Kim, H. J., Lee, E., Lindquist, M. A., Losin, E. A. R., Wager, T. D., & Woo, C. W. (2023). A dorsomedial prefrontal cortex-based dynamic functional connectivity model of rumination. *Nature Communications*, *14*(1), 1–14. https://doi.org/10.1038/s41467-023-39142-9

Kim, L. H., Heck, D. H., & Sillitoe, R. V. (2024). Cerebellar Functions Beyond Movement and Learning. *Annual Review of Neuroscience*, *47*(1), 145–166. https://doi.org/10.1146/annurev-neuro-100423-104943

King, M., Hernandez-Castillo, C. R., Poldrack, R. A., Ivry, R. B., & Diedrichsen, J. (2019). Functional boundaries in the human cerebellum revealed by a multi-domain task battery. *Nature Neuroscience*, *22*(8), 1371–1378. https://doi.org/10.1038/s41593-019-0436-x

Krasovsky, A., Gilron, R., Yeshurun, Y., & Mukamel, R. (2014). Differentiating intended sensory outcome from underlying motor actions in the human brain. *Journal of Neuroscience*, *34*(46), 15446–15454. https://doi.org/10.1523/JNEUROSCI.5435-13.2014

Kriegeskorte, N., & Bandettini, P. (2007). Analyzing for information, not activation, to exploit high-resolution fMRI. *NeuroImage*, *38*(4), 649–662. https://doi.org/10.1016/j.neuroimage.2007.02.022

Kristo, G., Rutten, G. J., Raemaekers, M., de Gelder, B., Rombouts, S. A. R. B., & Ramsey, N. F. (2014). Task and task-free FMRI reproducibility comparison for motor network identification. *Human Brain Mapping*, *35*(1), 340–352. https://doi.org/10.1002/hbm.22180

Lake, E. M. R., Finn, E. S., Noble, S. M., Vanderwal, T., Shen, X., Rosenberg, M. D., Spann, M. N., Chun, M. M., Scheinost, D., & Constable, R. T. (2019). The Functional Brain Organization of an Individual Allows Prediction of Measures of Social Abilities Transdiagnostically in Autism and Attention-Deficit/Hyperactivity Disorder. *Biological Psychiatry*, *86*(4), 315–326. https://doi.org/10.1016/j.biopsych.2019.02.019

Lanzilotto, M., Ferroni, C. G., Livi, A., Gerbella, M., Maranesi, M., Borra, E., Passarelli, L., Gamberini, M., Fogassi, L., Bonini, L., & Orban, G. A. (2019). Anterior intraparietal area: A hub in the observed manipulative action network. *Cerebral Cortex*, *29*(4), 1816–1833. https://doi.org/10.1093/cercor/bhz011

Lee, J. H., & Van Donkelaar, P. (2006). The human dorsal premotor cortex generates on-line error corrections during sensorimotor adaptation. *Journal of Neuroscience*, *26*(12), 3330–3334. https://doi.org/10.1523/JNEUROSCI.3898-05.2006

Lee, J.-H., & Van Donkelaar, P. (2002). Dorsal and ventral visual stream contributions to perception-action interactions during pointing. *Experimental Brain Research*, *143*(4), 440–446. https://doi.org/10.1007/s00221-002-1011-2

Lega, C., Pirruccio, M., Bicego, M., Parmigiani, L., Chelazzi, L., & Cattaneo, L. (2020). The Topography of Visually Guided Grasping in the Premotor Cortex: A Dense-Transcranial Magnetic Stimulation (TMS) Mapping Study. *Journal of Neuroscience*, *40*(35), 6790–6800. https://doi.org/10.1523/JNEUROSCI.0560-20.2020

Leoné, F. T. M., Heed, T., Toni, I., & Pieter Medendorp, W. (2014). Understanding effector selectivity in human posterior parietal cortex by combining information patterns and activation measures. *Journal of Neuroscience*, *34*(21), 7102–7112. https://doi.org/10.1523/JNEUROSCI.5242-13.2014

Livne, T., Kim, D., Metcalf, N. V., Zhang, L., Pini, L., Shulman, G. L., & Corbetta, M. (2022). Spontaneous activity patterns in human motor cortex replay evoked activity patterns for hand movements. *Scientific Reports*, *12*(1). https://doi.org/10.1038/s41598-022-20866-5

Luppino, G., Matelli, M., Camarda, R., & Rizzolatti, G. (1993). Corticocortical connections of area F3 (SMA-proper) and area F6 (pre-SMA) in the macaque monkey. *The Journal of Comparative Neurology*, *338*(1), 114–140. https://doi.org/10.1002/cne.903380109

Malfatti, G., & Turella, L. (2021). Neural encoding and functional interactions underlying pantomimed movements. *Brain Structure and Function*, *226*(7), 2321–2337. https://doi.org/10.1007/s00429-021-02332-6

Manni, E., & Petrosini, L. (2004). A century of cerebellar somatotopy: A debated representation. *Nature Reviews. Neuroscience*, *5*(3), 241–249. https://doi.org/10.1038/nrn1347

Marigold, D. S., Lajoie, K., & Heed, T. (2019). No effect of triple-pulse TMS medial to intraparietal sulcus on online correction for target perturbations during goal-directed hand and foot reaches. *PLOS ONE*, *14*(10), e0223986. https://doi.org/10.1371/journal.pone.0223986

Maule, F., Barchiesi, G., Brochier, T., & Cattaneo, L. (2015). Haptic Working Memory for Grasping: The Role of the Parietal Operculum. *Cerebral Cortex*, *25*(2), 528–537. https://doi.org/10.1093/cercor/bht252

McDowell, T., Holmes, N. P., Sunderland, A., & Schürmann, M. (2018). TMS over the supramarginal gyrus delays selection of appropriate grasp orientation during reaching and grasping tools for use. *Cortex*, *103*, 117–129. https://doi.org/10.1016/j.cortex.2018.03.002

Medendorp, W. P., Goltz, H. C., Crawford, J. D., & Vilis, T. (2005). Integration of target and effector information in human posterior parietal cortex for the planning of action. *Journal of Neurophysiology*, *93*(2), 954–962. https://doi.org/10.1152/jn.00725.2004

Monaco, S., Cavina-Pratesi, C., Sedda, A., Fattori, P., Galletti, C., & Culhaml, J. C. (2011). Functional magnetic resonance adaptation reveals the involvement of the dorsomedial stream in hand orientation for grasping. *Journal of Neurophysiology*, *106*(5), 2248–2263. https://doi.org/10.1152/jn.01069.2010

Monaco, S., Chen, Y., Medendorp, W. P., Crawford, J. D., Fiehler, K., & Henriques, D. Y. P. (2014). Functional magnetic resonance imaging adaptation reveals the cortical networks for processing grasp-relevant object properties. *Cerebral Cortex*, *24*(6), 1540–1554. https://doi.org/10.1093/cercor/bht006

Monaco, S., Gallivan, J. P., Figley, T. D., Singhal, A., & Culham, J. C. (2017). Recruitment of foveal retinotopic cortex during haptic exploration of shapes and actions in the dark. *Journal of Neuroscience*, *37*(48), 11572–11591. https://doi.org/10.1523/JNEUROSCI.2428-16.2017

Monaco, S., Malfatti, G., Culham, J. C., Cattaneo, L., & Turella, L. (2020). Decoding motor imagery and action planning in the early visual cortex: Overlapping but distinct neural mechanisms. *NeuroImage*, *218*(December 2019), 116981. https://doi.org/10.1016/j.neuroimage.2020.116981

Monaco, S., Malfatti, G., Zendron, A., Pellencin, E., & Turella, L. (2019). Predictive coding of action intentions in dorsal and ventral visual stream is based on visual anticipations, memory-based information and motor preparation. *Brain Structure and Function*, *224*(9), 3291–3308. https://doi.org/10.1007/s00429-019-01970-1

Murata, A., Gallese, V., Luppino, G., Kaseda, M., & Sakata, H. (2000). Selectivity for the shape, size, and orientation of objects for grasping in neurons of monkey parietal area AIP. *Journal of Neurophysiology*, *83*(5), 2580–2601. https://doi.org/10.1152/jn.2000.83.5.2580

Nettekoven, C., Zhi, D., Shahshahani, L., Pinho, A. L., Saadon-grosman, N., & Diedrichsen, J. (2023). A hierarchical atlas of the human cerebellum for functional precision mapping. *bioRxiv*, 1–27. https://doi.org/10.1101/2023.09.14.557689

Oosterhof, N. N., Connolly, A. C., & Haxby, J. V. (2016). CoSMoMVPA: Multi-Modal Multivariate Pattern Analysis of Neuroimaging Data in Matlab/GNU Octave. *Frontiers in Neuroinformatics*, *10*, 27. https://doi.org/10.3389/fninf.2016.00027

Orban, G. A., & Caruana, F. (2014). The neural basis of human tool use. *Frontiers in Psychology*, *5*(APR), 1–12. https://doi.org/10.3389/fpsyg.2014.00310

Orlov, T., Makin, T. R., Zohary, E., Peelen, M. V., Downing, P. E., Astafiev, S. V., Stanley, C. M., Shulman, G. L., & Corbetta, M. (2010). Topographic Representation of the Human Body in the Occipitotemporal Cortex. *Neuron*, *68*(3), 586–600. https://doi.org/10.1016/j.neuron.2010.09.032

Parikh, P. J., Fine, J. M., & Santello, M. (2020). Dexterous Object Manipulation Requires Context-Dependent Sensorimotor Cortical Interactions in Humans. *Cerebral Cortex*, *30*(5), 3087–3101. https://doi.org/10.1093/cercor/bhz296

Paus, T. (2005). Inferring causality in brain images: A perturbation approach. *Philosophical Transactions of the Royal Society B: Biological Sciences*, *360*(1457), 1109–1114. https://doi.org/10.1098/rstb.2005.1652

Pesaran, B., Nelson, M. J., & Andersen, R. A. (2010). A relative position code for saccades in dorsal premotor cortex. *Journal of Neuroscience*, *30*(19), 6527–6537. https://doi.org/10.1523/JNEUROSCI.1625-09.2010

Petersen, S. E., & Sporns, O. (2015). Brain Networks and Cognitive Architectures. *Neuron*, *88*(1), 207–219. https://doi.org/10.1016/j.neuron.2015.09.027

Pezzulo, G., Zorzi, M., & Corbetta, M. (2021). The secret life of predictive brains: What's spontaneous activity for? *Trends in Cognitive Sciences*, *25*(9), 730–743. https://doi.org/10.1016/j.tics.2021.05.007

Pierotti, E., Speranza, C., Cattaneo, L., & Turella, L. (2025). Investigating resting-state functional connectivity of the human hand motor system: An offline TMS-fMRI study. *NeuroImage*, *314*, 121254. https://doi.org/10.1016/j.neuroimage.2025.121254

Pitzalis, S., Sereno, M. I., Committeri, G., Fattori, P., Galati, G., Tosoni, A., & Galletti, C. (2013). The human homologue of macaque area V6A. *NeuroImage*, *82*, 517–530. https://doi.org/10.1016/j.neuroimage.2013.06.026

Potok, W., Maskiewicz, A., Króliczak, G., & Marangon, M. (2019). The temporal involvement of the left supramarginal gyrus in planning functional grasps: A neuronavigated TMS study. *Cortex*, *111*, 16–34. https://doi.org/10.1016/j.cortex.2018.10.010

Prado, J., Clavagnier, S., Otzenberger, H., Scheiber, C., Kennedy, H., & Perenin, M. T. (2005). Two cortical systems for reaching in central and peripheral vision. *Neuron*, *48*(5), 849–858. https://doi.org/10.1016/j.neuron.2005.10.010

Premereur, E., Van Dromme, I. C., Romero, M. C., Vanduffel, W., & Janssen, P. (2015). Effective connectivity of depth-structure-selective patches in the lateral bank of the macaque intraparietal sulcus. *PLoS Biology*, *13*(2), e1002072. https://doi.org/10.1371/journal.pbio.1002072

Rabini, G., Pierotti, E., Meli, C., Dodich, A., Papagno, C., & Turella, L. (2023). Connectome-based fingerprint of motor impairment is stable along the course of Parkinson's disease. *Cerebral Cortex*, *33*(17), 9896–9907. https://doi.org/10.1093/cercor/bhad252

Raichle, M. E. (2011). The Restless Brain. *Brain Connectivity*, *1*(1), 3–12. https://doi.org/10.1089/brain.2011.0019

Ranzini, M., Scarpazza, C., Radua, J., Cutini, S., Semenza, C., & Zorzi, M. (2022). A common neural substrate for number comparison, hand reaching and grasping: A SDM-PSI meta-analysis of neuroimaging studies. *Cortex*, *148*, 31–67. https://doi.org/10.1016/j.cortex.2021.12.007

Reichenbach, A., Bresciani, J. P., Peer, A., Bülthoff, H. H., & Thielscher, A. (2011). Contributions of the PPC to online control of visually guided reaching movements assessed with fMRI-Guided TMS. *Cerebral Cortex*, *21*(7), 1602–1612. https://doi.org/10.1093/cercor/bhq225

Rens, G., Figley, T. D., Gallivan, J. P., Liu, Y., & Culham, J. C. (2023). Grasping with a twist: Dissociating action goals from motor actions in human frontoparietal circuits. *Journal of Neuroscience (Revision Requested); BioRxiv*, *215131*.

Rice, N. J., Tunik, E., Cross, E. S., & Grafton, S. T. (2007). On-line grasp control is mediated by the contralateral hemisphere. *Brain Research*, *1175*(1), 76–84. https://doi.org/10.1016/j.brainres.2007.08.009

Rice, N. J., Tunik, E., & Grafton, S. T. (2006). The anterior intraparietal sulcus mediates grasp execution, independent of requirement to update: New insights from transcranial magnetic stimulation. *Journal of Neuroscience*, *26*(31), 8176–8182. https://doi.org/10.1523/JNEUROSCI.1641-06.2006

Rizzolatti, G., Cattaneo, L., Fabbri-Destro, M., & Rozzi, S. (2014). Cortical mechanisms underlying the organization of goal-directed actions and mirror neuron-based action understanding. *Physiological Reviews*, *94*(2), 655–706. https://doi.org/10.1152/physrev.00009.2013

Rizzolatti, G., & Luppino, G. (2001). The cortical motor system. *Neuron*, *31*, 889–901.

Rizzolatti, G., Luppino, G., & Matelli, M. (1998). The organization of the cortical motor system: New concepts. *Electroencephalography and Clinical Neurophysiology*, *106*, 283–296. https://doi.org/10.3892/ijmm.16.5.911

Rizzolatti, G., & Matelli, M. (2003). Two different streams form the dorsal visual system: Anatomy and functions. *Experimental Brain Research*, *153*(2), 146–157. https://doi.org/10.1007/s00221-003-1588-0

Romero, M. C., Merken, L., Janssen, P., & Davare, M. (2022). Neural effects of continuous theta-burst stimulation in macaque parietal neurons. *eLife*, *11*, 1–19. https://doi.org/10.7554/eLife.65536

Rosenberg, M. D., Zhang, S., Hsu, W. T., Scheinost, D., Finn, E. S., Shen, X., Constable, R. T., Li, C. S. R., & Chun, M. M. (2016). Methylphenidate modulates functional network connectivity to enhance attention. *Journal of Neuroscience*, *36*(37), 9547–9557. https://doi.org/10.1523/JNEUROSCI.1746-16.2016

Rossi, S., Hallett, M., Rossini, P. M., & Pascual-Leone, A. (2011). Screening questionnaire before TMS: An update. *Clinical Neurophysiology*, *122*(8), 1686. https://doi.org/10.1016/j.clinph.2010.12.037

Rossi, S., Hallett, M., Rossini, P. M., Pascual-Leone, A., Avanzini, G., Bestmann, S., Berardelli, A., Brewer, C., Canli, T., Cantello, R., Chen, R., Classen, J., Demitrack, M., Di Lazzaro, V., Epstein, C. M., George, M. S., Fregni, F., Ilmoniemi, R., Jalinous, R., … Ziemann, U. (2009). Safety, ethical considerations, and application guidelines for the use of transcranial magnetic stimulation in clinical practice and research. *Clinical Neurophysiology*, *120*(12), 2008–2039. https://doi.org/10.1016/j.clinph.2009.08.016

Rozzi, S., Calzavara, R., Belmalih, A., Borra, E., Gregoriou, G. G., Matelli, M., & Luppino, G. (2006). Cortical connections of the inferior parietal cortical convexity of the macaque monkey. *Cerebral Cortex*, *16*(10), 1389–1417. https://doi.org/10.1093/cercor/bhj076

Sakreida, K., Effnert, I., Thill, S., Menz, M. M., Jirak, D., Eickhoff, C. R., Ziemke, T., Eickhoff, S. B., Borghi, A. M., & Binkofski, F. (2016). Affordance processing in segregated parieto-frontal dorsal stream sub-pathways. *Neuroscience & Biobehavioral Reviews*, *69*(August), 89–112. https://doi.org/10.1016/j.neubiorev.2016.07.032

Salimi-Khorshidi, G., Douaud, G., Beckmann, C. F., Glasser, M. F., Griffanti, L., & Smith, S. M. (2014). Automatic denoising of functional MRI data: Combining independent component analysis and hierarchical fusion of classifiers. *NeuroImage*, *90*, 449–468. https://doi.org/10.1016/j.neuroimage.2013.11.046

Sartin, S., Ranzini, M., Scarpazza, C., & Monaco, S. (2023). Cortical areas involved in grasping and reaching actions with and without visual information: An ALE meta-analysis of neuroimaging studies. *Current Research in Neurobiology*, *4*(December 2022), 100070. https://doi.org/10.1016/j.crneur.2022.100070

Schaefer, A., Kong, R., Gordon, E. M., Laumann, T. O., Zuo, X.-N., Holmes, A. J., Eickhoff, S. B., & Yeo, B. T. T. (2018). Local-Global Parcellation of the Human Cerebral Cortex from Intrinsic Functional Connectivity MRI. *Cerebral Cortex*, *28*(9), 3095–3114. https://doi.org/10.1093/cercor/bhx179

Scheinost, D., Noble, S., Horien, C., Greene, A. S., Lake, E. M., Salehi, M., Gao, S., Shen, X., O'Connor, D., Barron, D. S., Yip, S. W., Rosenberg, M. D., & Constable, R. T. (2019). Ten simple rules for predictive modeling of individual differences in neuroimaging. *NeuroImage*, *193*, 35–45. https://doi.org/10.1016/j.neuroimage.2019.02.057

Schettino, L. F., Adamovich, S. V., Bagce, H., Yarossi, M., & Tunik, E. (2015). Disruption of activity in the ventral premotor but not the anterior intraparietal area interferes with on-line correction to a haptic perturbation during grasping. *Journal of Neuroscience*, *35*(5), 2112–2117. https://doi.org/10.1523/JNEUROSCI.3000-14.2015

Schmahmann, J. D., Guell, X., Stoodley, C. J., & Halko, M. A. (2019). The Theory and Neuroscience of Cerebellar Cognition. *Annual Review of Neuroscience*, *42*, 337–364. https://doi.org/10.1146/annurev-neuro-070918-050258

Schramm, S., Albers, L., Ille, S., Schröder, A., Meyer, B., Sollmann, N., & Krieg, S. M. (2019). Navigated transcranial magnetic stimulation of the supplementary motor cortex disrupts fine motor skills in healthy adults. *Scientific Reports*, *9*(1), 1–16. https://doi.org/10.1038/s41598-019-54302-y

Shen, X., Finn, E. S., Scheinost, D., Rosenberg, M. D., Chun, M. M., Papademetris, X., & Constable, R. T. (2017). Using connectome-based predictive modeling to predict individual behavior from brain connectivity. *Nature Protocols*, *12*(3), 506–518. https://doi.org/10.1038/nprot.2016.178

Shitara, H., Shinozaki, T., Takagishi, K., Honda, M., & Hanakawa, T. (2011). Time course and spatial distribution of fMRI signal changes during single-pulse transcranial magnetic stimulation to the primary motor cortex. *NeuroImage*, *56*(3), 1469–1479. https://doi.org/10.1016/j.neuroimage.2011.03.011

Siebner, H. R., Bergmann, T. O., Bestmann, S., Massimini, M., Johansen-Berg, H., Mochizuki, H., Bohning, D. E., Boorman, E. D., Groppa, S., Miniussi, C., Pascual-Leone, A., Huber, R., Taylor, P. C. J., Ilmoniemi, R. J., De Gennaro, L., Strafella, A. P., K??hk??nen, S., Kl??ppel, S., Frisoni, G. B., … Rossini, P. M. (2009). Consensus paper: Combining transcranial stimulation with neuroimaging. *Brain Stimulation*, *2*(2), 58–80. https://doi.org/10.1016/j.brs.2008.11.002

Sim, E.-J., Helbig, H. B., Graf, M., & Kiefer, M. (2015). When Action Observation Facilitates Visual Perception: Activation in Visuo-Motor Areas Contributes to Object Recognition. *Cerebral Cortex*, *25*(9), 2907–2918. https://doi.org/10.1093/cercor/bhu087

Simone, L., Rozzi, S., Bimbi, M., & Fogassi, L. (2015). Movement-related activity during goal-directed hand actions in the monkey ventrolateral prefrontal cortex. *European Journal of Neuroscience*, *42*(11), 2882–2894. https://doi.org/10.1111/ejn.13040

Smith, S. M., Beckmann, C. F., Andersson, J., Auerbach, E. J., Bijsterbosch, J., Douaud, G., Duff, E., Feinberg, D. A., Griffanti, L., Harms, M. P., Kelly, M., Laumann, T., Miller, K. L., Moeller, S., Petersen, S., Power, J., Salimi-Khorshidi, G., Snyder, A. Z., Vu, A. T., … Glasser, M. F. (2013). Resting-state fMRI in the Human Connectome Project. *NeuroImage*, *80*, 144–168. https://doi.org/10.1016/j.neuroimage.2013.05.039

Strick, P. L., Dum, R. P., & Fiez, J. a. (2009). Cerebellum and nonmotor function. *Annual Review of Neuroscience*, *32*, 413–434. https://doi.org/10.1146/annurev.neuro.31.060407.125606

Striemer, C. L., Chouinard, P. A., & Goodale, M. A. (2011). Programs for action in superior parietal cortex: A triple-pulse TMS investigation. *Neuropsychologia*, *49*(9), 2391–2399. https://doi.org/10.1016/j.neuropsychologia.2011.04.015

Tanné-Gariépy, J., Rouiller, E. M., & Boussaoud, D. (2002). Parietal inputs to dorsal versus ventral premotor areas in the macaque monkey: Evidence for largely segregated visuomotor pathways. *Experimental Brain Research*, *145*(1), 91–103. https://doi.org/10.1007/s00221-002-1078-9

Taubert, M., Dafotakis, M., Sparing, R., Eickhoff, S., Leuchte, S., Fink, G. R., & Nowak, D. A. (2010). Inhibition of the anterior intraparietal area and the dorsal premotor cortex interfere with arbitrary visuo-motor mapping. *Clinical Neurophysiology*, *121*(3), 408–413. https://doi.org/10.1016/j.clinph.2009.11.011

Thomas Yeo, B. T., Krienen, F. M., Sepulcre, J., Sabuncu, M. R., Lashkari, D., Hollinshead, M., Roffman, J. L., Smoller, J. W., Zöllei, L., Polimeni, J. R., Fischl, B., Liu, H., & Buckner, R. L. (2011). The organization of the human cerebral cortex estimated by intrinsic functional connectivity. *Journal of Neurophysiology*, *106*(3), 1125–1165. https://doi.org/10.1152/jn.00338.2011

Threethipthikoon, T., Li, Z., & Shigemasu, H. (2023). Orientation representation in human visual cortices: Contributions of non-visual information and action-related process. *Frontiers in Psychology*, *14*, 1231109. https://doi.org/10.3389/fpsyg.2023.1231109

Tunik, E., Frey, S. H., & Grafton, S. T. (2005a). Virtual lesions of the anterior intraparietal area disrupt goal-dependent on-line adjustments of grasp. *Nature Neuroscience*, *8*(4), 505–511. https://doi.org/10.1038/nn1430

Tunik, E., Frey, S. H., & Grafton, S. T. (2005b). Virtual lesions of the anterior intraparietal area disrupt goal-dependent on-line adjustments of grasp. *Nature Neuroscience*, *8*(4), 505–511. https://doi.org/10.1038/nn1430

Tunik, E., Lo, O. Y., & Adamovich, S. V. (2008). Transcranial magnetic stimulation to the frontal operculum and supramarginal gyrus disrupts planning of outcome-based hand-object interactions. *Journal of Neuroscience*, *28*(53), 14422–14427. https://doi.org/10.1523/JNEUROSCI.4734-08.2008

Turella, L., & Lingnau, A. (2014). Neural correlates of grasping. *Frontiers in Human Neuroscience*, *8*(SEP), 1–8. https://doi.org/10.3389/fnhum.2014.00686

Turella, L., Rumiati, R., & Lingnau, A. (2020). Hierarchical Action Encoding Within the Human Brain. *Cerebral Cortex*, *30*(5), 2924–2938. https://doi.org/10.1093/cercor/bhz284

Valyear, K. F., Cavina-Pratesi, C., Stiglick, A. J., & Culham, J. C. (2007). Does tool-related fMRI activity within the intraparietal sulcus reflect the plan to grasp? *NeuroImage*, *36*(SUPPL. 2), T94–T108. https://doi.org/10.1016/j.neuroimage.2007.03.031

van Polanen, V., Buckingham, G., & Davare, M. (2022). The effects of TMS over the anterior intraparietal area on anticipatory fingertip force scaling and the size-weight illusion. *Journal of Neurophysiology*, *128*(2), 290–301. https://doi.org/10.1152/jn.00265.2021

van Polanen, V., & Davare, M. (2015). Interactions between dorsal and ventral streams for controlling skilled grasp. *Neuropsychologia*, *79*, 186–191. https://doi.org/10.1016/j.neuropsychologia.2015.07.010

van Polanen, V., Rens, G., & Davare, M. (2020). The role of the anterior intraparietal sulcus and the lateral occipital cortex in fingertip force scaling and weight perception during object lifting. *Journal of Neurophysiology*, *124*(2), 557–573. https://doi.org/10.1152/JN.00771.2019

Vesia, M., & Crawford, J. D. (2012). Specialization of reach function in human posterior parietal cortex. *Experimental Brain Research*, *221*(1), 1–18. https://doi.org/10.1007/s00221-012-3158-9

Vesia, M., Prime, S. L., Yan, X., Sergio, L. E., & Crawford, J. D. (2010). Specificity of human parietal saccade and reach regions during transcranial magnetic stimulation. *Journal of Neuroscience*, *30*(39), 13053–13065. https://doi.org/10.1523/JNEUROSCI.1644-10.2010

Vingerhoets, G. (2014). Contribution of the posterior parietal cortex in reaching, grasping, and using objects and tools. *Frontiers in Psychology*, *5*(MAR), 1–17. https://doi.org/10.3389/fpsyg.2014.00151

Volz, L. J., Eickhoff, S. B., Pool, E. M., Fink, G. R., & Grefkes, C. (2015). Differential modulation of motor network connectivity during movements of the upper and lower limbs. *NeuroImage*, *119*, 44–53. https://doi.org/10.1016/j.neuroimage.2015.05.101

White, O., Davare, M., Andres, M., & Olivier, E. (2013). The role of left supplementary motor area in grip force scaling. *PLoS ONE*, *8*(12), 4–12. https://doi.org/10.1371/journal.pone.0083812

Whitfield-Gabrieli, S., & Nieto-Castanon, A. (2012). Conn: A Functional Connectivity Toolbox for Correlated and Anticorrelated Brain Networks. *Brain Connectivity*, *2*(3), 125–141. https://doi.org/10.1089/brain.2012.0073

Wu, J., Eickhoff, S. B., Hoffstaedter, F., Patil, K. R., Schwender, H., Thomas Yeo, B. T., & Genon, S. (2021). A Connectivity-Based Psychometric Prediction Framework for Brain-Behavior Relationship Studies. *Cerebral Cortex*, *31*(8), 3732–3751. https://doi.org/10.1093/cercor/bhab044

Wu, J., Li, J., Eickhoff, S. B., Hoffstaedter, F., Hanke, M., Yeo, B. T. T., & Genon, S. (2022). Cross-cohort replicability and generalizability of connectivity-based psychometric prediction patterns. *NeuroImage*, *262*(March), 119569. https://doi.org/10.1016/j.neuroimage.2022.119569

Wu, J., Li, J., Eickhoff, S. B., Scheinost, D., & Genon, S. (2023). The challenges and prospects of brain-based prediction of behaviour. *Nature Human Behaviour*, *7*(8), 1255–1264. https://doi.org/10.1038/s41562-023-01670-1

Xia, M., Wang, J., & He, Y. (2013). BrainNet Viewer: A Network Visualization Tool for Human Brain Connectomics. *PLoS ONE*, *8*(7), e68910. https://doi.org/10.1371/journal.pone.0068910

Yoo, K., Rosenberg, M. D., Kwon, Y. H., Lin, Q., Avery, E. W., Sheinost, D., Constable, R. T., & Chun, M. M. (2022). A brain-based general measure of attention. *Nature Human Behaviour*, *6*(6), 782–795. https://doi.org/10.1038/s41562-022-01301-1

Zalesky, A., Fornito, A., & Bullmore, E. T. (2010). Network-based statistic: Identifying differences in brain networks. *NeuroImage*, *53*(4), 1197–1207. https://doi.org/10.1016/j.neuroimage.2010.06.041

Zhang, L., Pini, L., Kim, D., Shulman, G. L., & Corbetta, M. (2023). Spontaneous Activity Patterns in Human Attention Networks Code for Hand Movements. *The Journal of Neuroscience*, *43*(11), 1976–1986. https://doi.org/10.1523/jneurosci.1601-22.2023

Zhang, L., Pini, L., Shulman, G. L., & Corbetta, M. (2025). Brain-wide dynamic coactivation states code for hand movements in the resting state. *Proceedings of the National Academy of Sciences*, *122*(11), 2017. https://doi.org/10.1073/pnas.2415508122

Zlatkina, V., & Petrides, M. (2010). Morphological patterns of the postcentral sulcus in the human brain. *Journal of Comparative Neurology*, *518*(18), 3701–3724. https://doi.org/10.1002/cne.22418